4A

PNL-3320
UC-88

INTERIM REPORT

Wire Rope Improvement Program Fiscal Years 1979-1980

M. H. Morgenstern
J. M. Alzheimer
W. E. Anderson
G. H. Beeman
R. C. Rice
L. A. Strope
E. V. Werry

August 1980

Prepared for the U.S. Department of Energy
under Contract DE-AC06-76RLO 1830

Pacific Northwest Laboratory
Operated for the U.S. Department of Energy
by Battelle Memorial Institute

Battelle

PNL-3320

PACIFIC NORTHWEST LABORATORY
operated by
BATTELLE
for the
UNITED STATES DEPARTMENT OF ENERGY
Under Contract DE-AC06-76RLO 1830

Printed in the United States of America
Available from
National Technical Information Service
United States Department of Commerce
5285 Port Royal Road
Springfield, Virginia 22151

Price: Printed Copy $_____*; Microfiche $3.00

*Pages	NTIS Selling Price
001-025	$4.00
026-050	$4.50
051-075	$5.25
076-100	$6.00
101-125	$6.50
126-150	$7.25
151-175	$8.00
176-200	$9.00
201-225	$9.25
226-250	$9.50
251-275	$10.75
276-300	$11.00

PNL-3320
UC-88

INTERIM REPORT

WIRE ROPE IMPROVEMENT PROGRAM
FISCAL YEARS 1979-1980

M. H. Morgenstern(a)
J. M. Alzheimer
W. E. Anderson
G. H. Beeman
R. C. Rice(b)
L. A. Strope
E. V. Werry

August 1980

Prepared for the
U.S. Department of Energy
under Contract DE-AC06-76RLO 1830

Pacific Northwest Laboratory
Richland, Washington 99352

(a) Project Manager
(b) Battelle Columbus Laboratories, Columbus, Ohio

DOE-Richland, WA

SUMMARY

This report describes the work performed by the Pacific Northwest Laboratory (PNL) and its subcontractor Battelle Columbus Laboratories (BCL) on the Wire Rope Improvement Program during FY-1979 and the first half of FY80. The program, begun in 1975 by the U.S. Bureau of Mines, was transferred to the U.S. Department of Energy (DOE) on October 1, 1978. Since that time, the DOE's Division of Solid Fuels Mining and Preparation has sponsored the program.

To address identified problems and provide information from which behavior of large-diameter wire rope could be better understood, efforts in the following areas were undertaken during FY79 and continued in FY80:

- large-diameter rope testing
- small-diameter rope testing
- data analysis and evaluation
- wear and failure analysis
- load sensor development
- technology transfer.

Wire ropes 3/4 in., 1-1/2 in., and 3 in. in diameter were tested in bend-over-sheave fatigue. Attempts were made to correlate fatigue life of these ropes. Limited field rope data were available to compare with test results. The modes of failure and wear in laboratory ropes were compared with those seen previously in field ropes.

A load sensor was designed and ordered in FY79. It will be connected to the drag rope and jewelry of working draglines during the summer of FY80.

Technology transfer was achieved through disseminating written materials, conducting seminars, holding a national symposium, and filming of selected field operations.

ACKNOWLEDGMENTS

The authors gratefully acknowledge the contributions of PNL senior technician Leonard Shotwell. He has kept the fatigue machine running, changed ropes, disassembled and examined failed rope, and offered many valuable suggestions that contributed substantially to a smooth operation. The authors wish to thank Jim Merrill, PNL statistician, whose comments and suggestions added much to the research approach and this report. The authors also acknowledge the invaluable contribution of PNL editor/writer Andrea Currie. She not only edited the text to make it more readable, but also coordinated the word processing, graphics and photography production, and final printing.

The authors wish to also acknowledge the inputs and participation of program consultants Dr. Sam Gambrell of the University of Alabama and Len Hansson of the Bucyrus-Erie Company.

CONTENTS

FIGURES

TABLES

INTERIM REPORT
WIRE ROPE IMPROVEMENT PROGRAM
FISCAL YEARS 1979-1980

1.0 INTRODUCTION

The work described herein was performed by the Pacific Northwest Laboratory under the continuation of a program begun by the U.S. Bureau of Mines in 1975. On October 1, 1978, the program was transferred to the Division of Solid Fuels Mining and Preparation, U.S. Department of Energy.

Initial results of the program showed that large-diameter wire rope having an independent wire rope core behaved quite differently when tested under bend-over-sheave (BOS) fatigue than did small-diameter wire rope having a fiber core (see Figure 1.1). It was not known if this was due to a size effect, the difference in core materials, or a breakdown in the Drucker-Tachau bearing pressure ratio (Drucker and Tachau 1944).

Another interesting result was the extremely short fatigue life exhibited by large-diameter wire rope when tested in BOS fatigue at design factors greater than 2.5.[(a)] This result, coupled with an extensive examination of failed ropes from the field, leads to the conclusion that field ropes may see greater service loads than previously expected.

It was also confirmed that there was no standardization of techniques for care or removal of wire rope from service. In some instances, there was a lack of understanding of how wire rope behaves and how it should be cared for.

To address the identified problems and provide information from which behavior of large-diameter wire rope could be better understood, the following program was undertaken during FY79:

(a) Design Factor = $\frac{\text{Rated Breaking Strength}}{\text{Test Load}}$

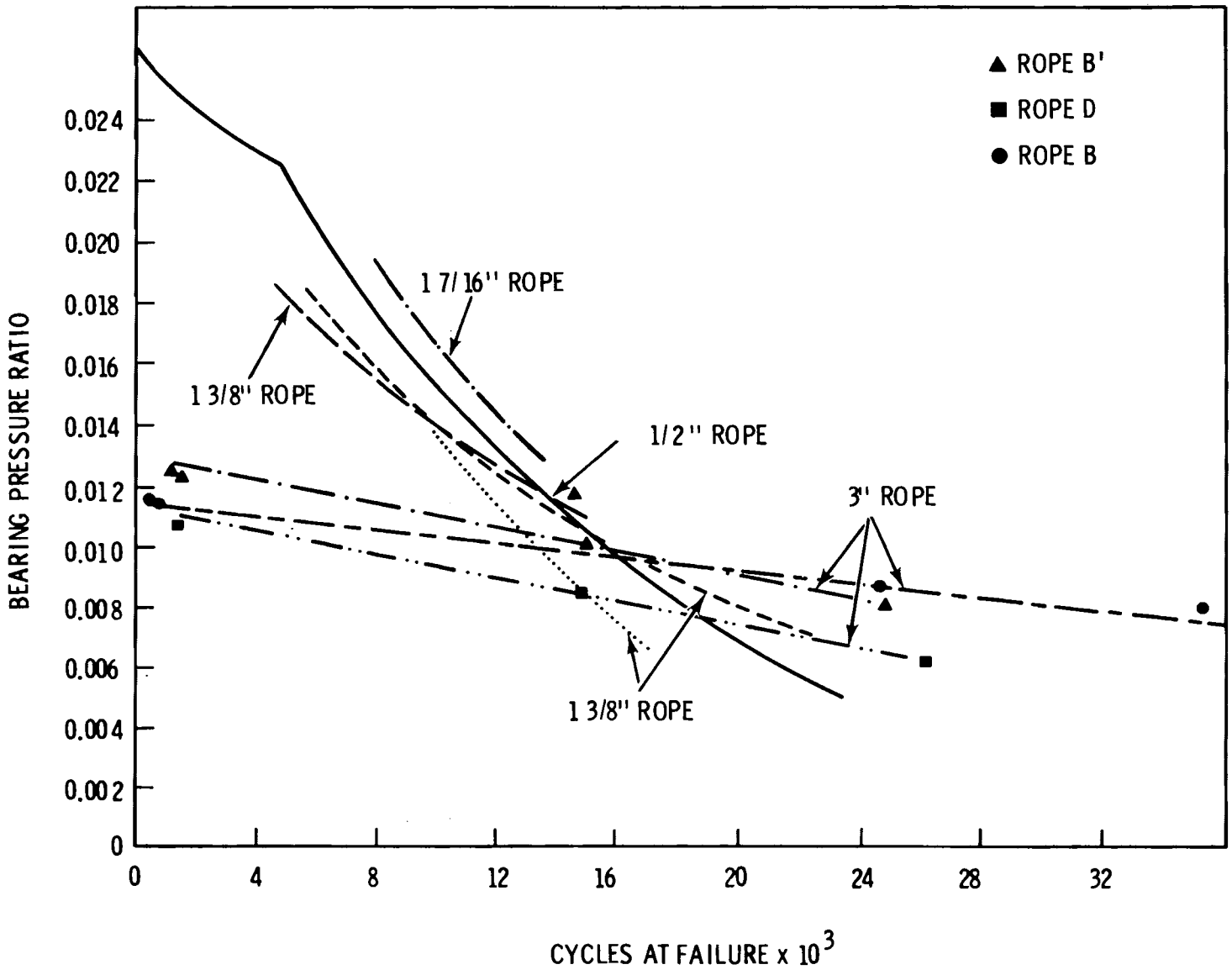

FIGURE 1.1. Large- and Small-Diameter Rope Data Compared Using the Drucker-Tachau Ratio

- Large-Diameter Rope Testing
- Small-Diameter Rope Testing
- Data Analysis and Evaluation
- Wear and Failure Analysis
- Load Sensor Development
- Technology Transfer Seminars.

One obvious approach to the program is through simulation; that is, through performing scaled-down experiments on smaller-diameter wire ropes. If a correlation could be found with similar tests performed on large-diameter ropes, the results of the small rope tests could be used to identify trends expected to occur in the large-diameter ropes. Such an approach, if successful, would offer tremendous savings in cost and time.

Another approach is to determine actual causes of rope failure in the field. Using this knowledge, appropriate remedial actions could be taken.

A third approach is to communicate wire rope research findings directly to rope users--the mine operators and supervisors. Providing basic education in the most current technology could lead to altered field handling procedures that would extend wire rope life.

Each of these three approaches was employed. The primary objectives in the FY79 and FY80 Wire Rope Improvement Program were:

- to conduct large- and small-diameter rope tests for similar rope constructions
- to develop analytical means by which large-diameter wire rope bending fatigue behavior could be accurately projected from small-diameter wire rope tests and single-wire tests on wire samples taken from rope of both size ranges
- to develop, through wear and failure analyses, a more complete understanding of how drag and hoist ropes fail in service. In FY80, the wear study was expanded to include the evaluation of certain nondestructive techniques, to monitor the progressive failure of the test ropes and to assess the possible use of these techniques in the field.

- to develop a load sensor capable of measuring both steady and dynamic loads on an operating dragline, to provide data necessary to evaluate hoist and drag rope performance
- to provide mine operators and supervisors with more direct guidance concerning the basic reasons for shortened wire rope life.

This report describes the work performed toward these objectives. Some of the information presented here appeared in an earlier project report (Beeman 1978). The conclusions are presented first in Section 2.0. Section 3.0 documents the experimental research on largeand small-diameter wire ropes.[a] The analytical work is presented in Section 4.0. Wear and failure analyses conducted to determine causes of test rope failure are described in Section 5.0. In Section 6.0, the development of the load sensor is discussed. Section 7.0 describes the technology transfer activities completed. Recommendations stemming from the program efforts are presented in Section 8.0.

(a) Small-diameter rope tests were performed at Battelle Columbus Laboratories.

2.0 CONCLUSIONS

Conclusions based on previous program work and the contract activities completed in FY79 and FY80 are described in the following paragraphs for each research area.

2.1 EXPERIMENTAL WORK

The experimental work led to three conclusions:

- Similar modes of failure occurred during BOS fatigue tests of large- and small-diameter wire rope.
- Fatigue life of large-diameter wire rope at design factors of 4 and 5 fell within expected trends.
- Differences in BOS fatigue life for small-diameter wire ropes were observed for different rope constructions.

2.2 ANALYTICAL WORK

Three conclusions emerged from the analysis of bending stresses in wire ropes and the correlation of bend-over-sheave fatigue data for Lang-lay IWRC construction:

- A modified bearing pressure ratio generally consolidates bending fatigue data on ropes of different constructions somewhat better than the standard Drucker-Tachau bearing pressure ratio.
- Tensile and bending stresses in the exterior wires of all three rope diameters studied (from 3/4 in. to 3 in.), each having 16 outer wires per strand, are approximately equal for D/d ratios of 30 and larger, but differ markedly for D/d ratios of 15 and less.
- Long-life laboratory data on small wire ropes are comparable with field data on large dragline hoist ropes, when consistent retirement criteria are used.

2.3 WEAR AND FAILURE ANALYSIS

The wear and failure analysis led to five conclusions:

- Wear patterns on test ropes and field ropes were similar, except for less crown wear on the laboratory ropes.
- Cracked but unfailed wires are more prevalent in retired laboratory ropes tested at the highest design factors (lowest test loads).
- Wire strength and bending fatigue resistance appear to be directly related at low design factors (high loads) and inversely related at high design factors (low loads).
- Both ac and dc electromagnetic techniques may be useful for the inspection of large-diameter wire rope in the field.
- A radiographic technique developed at Battelle, Pacific Northwest Laboratories, and adapted to large-diameter wire rope was identified as a candidate for monitoring the failure progression of wire rope and for use in the field examination of selected regions. This technique can easily resolve a 1/8-in. diameter hole in the IWRC of a 3-in. wire rope.

2.4 LOAD SENSOR DEVELOPMENT

Two conclusions were drawn from the load sensor studies in FY79:

- Drag rope dynamic loads should be considered before hoist rope loads because of the high uncertainty and severity of drag rope loads.
- A load link of convenient size and shape inserted into the drag string was selected as the prime concept over an instrumented replacement part or strain gaging of existing hardware.

2.5 TECHNOLOGY TRANSFER

The technology transfer activities of the Wire Rope Improvement Program have been rewarding and interesting. Mine operators, engineers, and others are generally responsive to suggestions for improved use of wire rope; their responsiveness is expected to lead to reduced operating costs and improved

production. PNL has observed little need to "push" wire rope technology transfer, because strong technological interest continues to come from the wire rope community. Technology transfer is an effective and practical method to provide basic information and research developments to ultimate users and is, therefore, scheduled to continue as a viable component of the Wire Rope Improvement Program.

3.0 EXPERIMENTAL RESEARCH

The parameters for large- and small-diameter wire rope bend-over-sheave (BOS) fatigue tests are shown in matrix form in Table 3.1. Large-diameter wire rope came from one manufacturer and was of filler-wire Seale construction. Small-diameter wire ropes were purchased from two comparable manufacturers for both the 3/4- and 1-1/2-in. diameter ropes. One manufacturer supplied filler-wire Seale ropes while the other supplied Warrington Seale ropes. Thus, it was possible to examine the potential effects of modest differences in construction on bending fatigue resistance. Two sheave-to-rope diameter (D/d) ratios and four design factors were considered so that the traditionally-used bearing pressure ratio value could be examined for a range of test conditions.

TABLE 3.1. Bend-Over-Sheave Fatigue Test Parameter Matrix

Rope Diameter, in.	Rope Manufacturer	D/d 20 Design Factor 2	D/d 20 Design Factor 3	D/d 20 Design Factor 4	D/d 30 Design Factor 2	D/d 30 Design Factor 3	D/d 30 Design Factor 4	D/d 30 Design Factor 5	Rope Construction	Number of Outside Wires per Strand
3/4	M		X	X		X	X		6 x 36 WS[a]	14
	H	X	X	X		X	X		6 x 41 FWS[b]	16
1-1/2	M		X	X		X	X		6 x 41 FWS	16
	H		X	X		X	X		6 x 41 FWS	16
3	B'				X	X	X	X	6 x 57 FWS	16
	B				X	X			6 x 57 FWS	16
	D				X	X			6 x 41 FWS	

(a) Warrington Seale.
(b) Filler-Wire Seale.

The bearing pressure ratio value (Drucker and Tachau 1944) was first proposed as an empirical factor or design criterion that could be used to correlate wire rope bending fatigue data (for a particular construction) generated at different combinations of wire strength, rope diameter, sheave diameter, and rope tension. This bearing pressure ratio (B) is expressed as

$$B = \frac{2T}{UDd} \quad , \tag{3.1}$$

where

T = rope tension, lb

U = wire ultimate strength, psi

D = sheave diameter, in.

d = rope diameter, in.

The usefulness and limitations of this parameter will be discussed in more detail in Section 4.0.

The experimental research completed at BCL involved BOS fatigue tests on small-diameter wire ropes and tensile tests on rope wires. The experimental studies completed by PNL were bend-over-sheave tests on large-diameter wire ropes. These companion studies are described in this section. The test results were used to determine if a correlation exists between large- and small-diameter IWRC wire rope when tested under BOS fatigue. The extent of correlation is discussed in Section 4.0 of this report.

3.1 LARGE-DIAMETER WIRE ROPE TESTS

During FY79 and the first half of FY80, fourteen ropes were tested. Of these, eleven were tested to failure on the large-diameter bend-over-sheave (BOS) fatigue machine. The test methods and results are documented in the next two subsections.

3.1.1 Test Methods

Ropes tested were of the 6 x 37 class, 3 in. in diameter with an IWRC. Ropes were of Right Lang-lay construction. Design factors of 4 and 5 were used for test loads. Rope failure was defined as damage severe enough to preclude further field service.

The large-diameter fatigue testing machine is shown in Figure 3.1 This machine is designed to test two 3-in. diameter wire ropes simultaneously under tensile loads up to 425,000 lb each. The tensile load is provided by a 24-in.

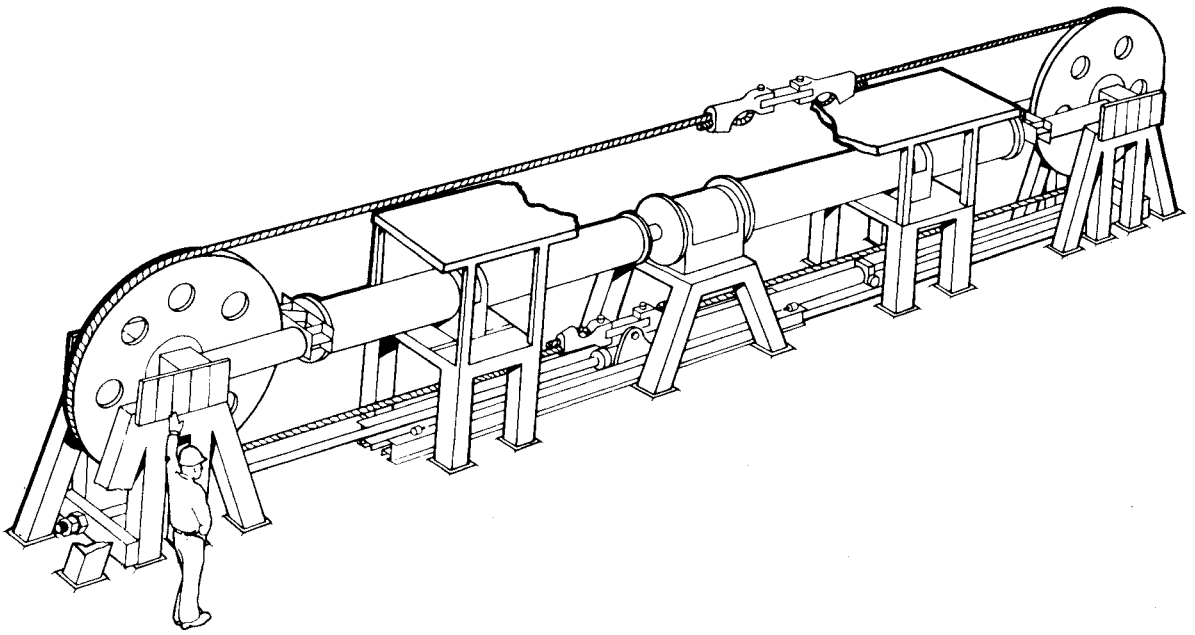

FIGURE 3.1. Large-Diameter Wire Rope Fatigue Test Machine

diameter hydraulic cylinder. The ropes are cycled over a 90-in. diameter sheave for a sheave-to-rope diameter (D/d) ratio of 30:1. Translation of the ropes is accomplished by a double-acting hydraulic cylinder with up to 20-ft stroke. This arrangement subjects each rope to three different strain areas. The no-bend region is never cycled over the sheave; the single-bend region undergoes one bending cycle per machine cycle; and the double-bend region experiences two bending cycles per machine cycle. Approximately 17 rope diameters (approximately two lay lengths) were subjected to double-bend fatigue.

Data obtained during fatigue testing included:

- bending cycles to failure of one strand for a given load history
- change in rope diameter with cycles
- rope elongation with cycles
- numbers and location of broken wires.

After fatigue testing, ropes were disassembled and examined for mode of failure.

3.1.2 Test Results

By the end of FY79, 27 large-diameter wire ropes had been tested in BOS fatigue. Testing to failure was carried out on 21 of the 27 ropes.

Fatigue test data are summarized in Table 3.2. Both total and adjusted cycles to failure are noted. The total cycles include "start-up" cycles at a reduced non-test load. The adjusted cycles represent the cycles at the actual test load. Table 3.3 shows the test results for those ropes tested at two different test loads. Load 1 was applied first. After some number of cycles, Load 1 was changed to Load 2 and ropes were cycled to failure, where failure was defined as that which would have surely caused its retirement in the field. In most cases, this was the failure of at least one strand. Multiple load tests were a result of the test procedures used in large-diameter rope testing. Initially, two ropes were placed on the machine. When a rope failed, it was replaced and testing continued.

Ropes tested at two load levels were cycled initially for periods ranging from 33% to 75% of their expected life at the first load. The load was then changed and the test continued until failure. Figure 3.2 is a schematic representation of the ropes' load history. Failure data are summarized in Table 3.4 along with comparisons of expected and actual life. Expected cycles were obtained by estimating life on the basis of final loading conditions only, and on the average number of cycles from previously obtained data.

Figure 3.3 is a plot of load versus cycles (S-N curve) for all large-diameter ropes tested. This shows that, even at design factors as low as 5, large-diameter wire rope has a finite BOS fatigue life (for a D/d ratio of 30). Tests are being conducted at a design factor of 6. It appears that, for these test conditions, the endurance limit of the rope (10^6 cycles) will not be reached at any reasonable design factor.

Figure 3.4 represents elongation of a typical rope as a function of test cycles. Regardless of test load, ropes generally exhibited this type of elongation behavior. The only variation was a shortening of all three stages with increasing load. The steep slope of the curve seen during Stage 1 comes from early "wearing in" of the rope. A 6 x 37 class, 3-in. diameter IWRC wire rope

TABLE 3.2. Large-Diameter Rope Fatigue Test Data Summary

Rope No.	Load, lb	Design Factor	Manufacturer	Bending Cycles to Failure		$B \times 10^{-3}$
				Total	Adjusted	
1	249,000	3.4	D	61,610	51,070	7.1
1a	249,000	3.4	D	61,610	51,070[a]	7.1
2	249,000	2.9	B	152,004	84,712	8.0
2a	249,000	2.9	B	152,004	84,712[a]	8.0
3	330,000	2.6	D	20,816	29,346	9.4
3a	330,000	2.6	D	30,816	29,346[a]	9.4
4	330,000	2.2	B	43,866	43,760	10.6
4a	330,000	2.2	B	42,866	43,760[a]	10.6
5	413,000	2.1	D	2,774	2,682	118.0
5a	413,000	2.1	D	2,774	2,682[a]	118.0
6	413,000	1.7	B	614	508	133.0
7	413,000	1.7	B	1,568	1,218	133.0
8	348,300	2.3	B'	30,318	29,464	108.0
9	348,300	2.3	B'	26,666	26,208	108.0
10			See Table 3.3			
11			See Table 3.3			
12	424,100	1.9	B'	28,880	28,158	131.0
13	424,100	1.9	B'	3,180	2,924	131.0
14	424,100	1.9	B'	2,608	2,554	131.0
15			See Table 3.3			
16	278,200	2.9	B'	44,232	44,086	8.6
17	278,200	2.9	B'	49,878	49,678	8.6
18	278,200	2.9	B'	43,290	43,114[a]	8.6
19	199,000	4.0	B'	103,190	103,112	6.1
20	199,000	4.0	B'	156,120	156,026	6.1
21			See Table 3.3			
22	159,200	5.0	B'	219,480	219,424	4.9

(a) Did not fail.

TABLE 3.3. Mixed Load Failure Data

Rope No.	Load 1, lb	Load 2, lb	Bending Cycles at Load 1		Bending Cycles at Load 2		Bending Cycles at Failure	
			Total	Adjusted	Total	Adjusted	Total	Adjusted
10	413,000 (1.9)[a]	348,300 (2.3)	954	816	66,370	65,150	67,324	65,876
11	348,300 (2.3)	424,100 (1.9)	9,386	9,340	24,716	24,256	34,102	33,596
15	424,100 (1.9)	278,200 (2.9)	1,578	1,554	50,820	50,650	52,398	52,204
21	199,000 (4.0)	159,200 (5.0)	52,950	52,918	132,808	132,776	185,758	185,694

(a) Numbers in parentheses are design factors.

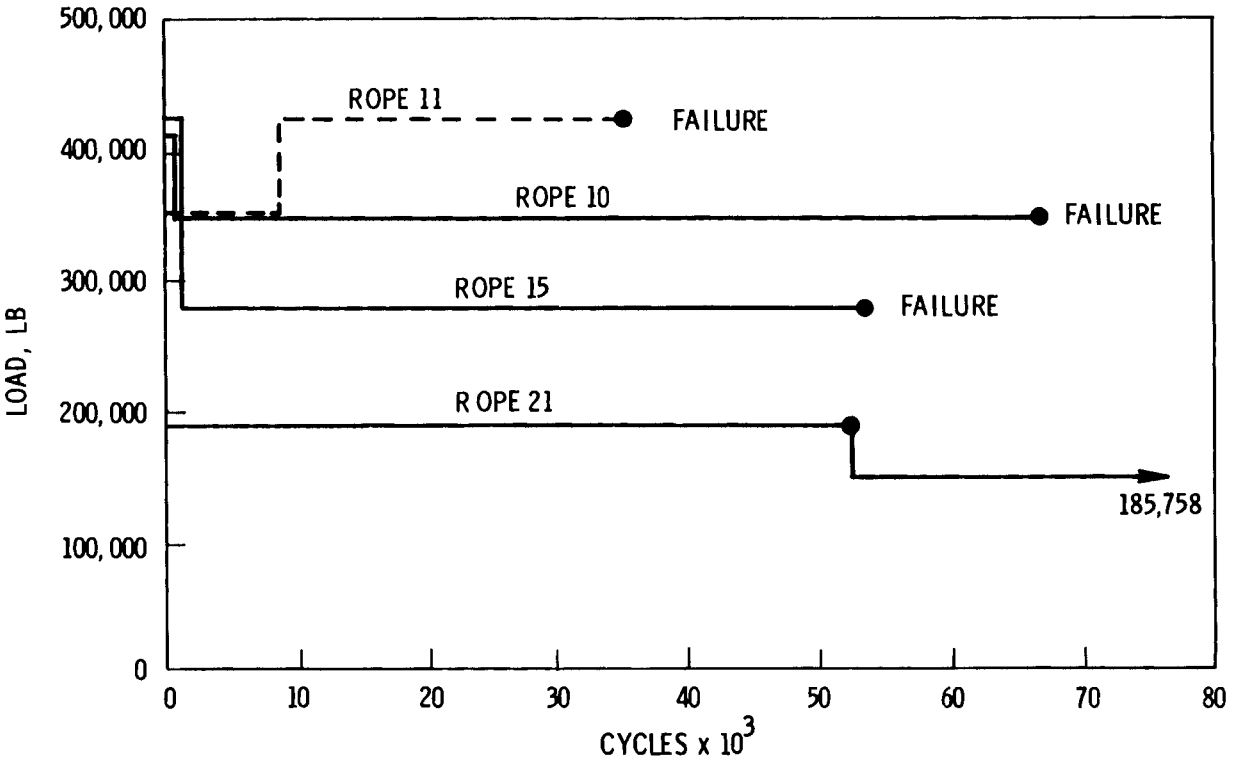

FIGURE 3.2. Mixed Load Testing

TABLE 3.4. Mixed Load Life Data

Rope No.	Final Load, lb	Expected Cycles	Actual Cycles	Percent Increase in Life
10	348,300	28,500	65,966	131
11	424,100	2,880	33,596	1,067
15	278,200	47,100	52,204	11
21	159,200	219,480	185,694	-15

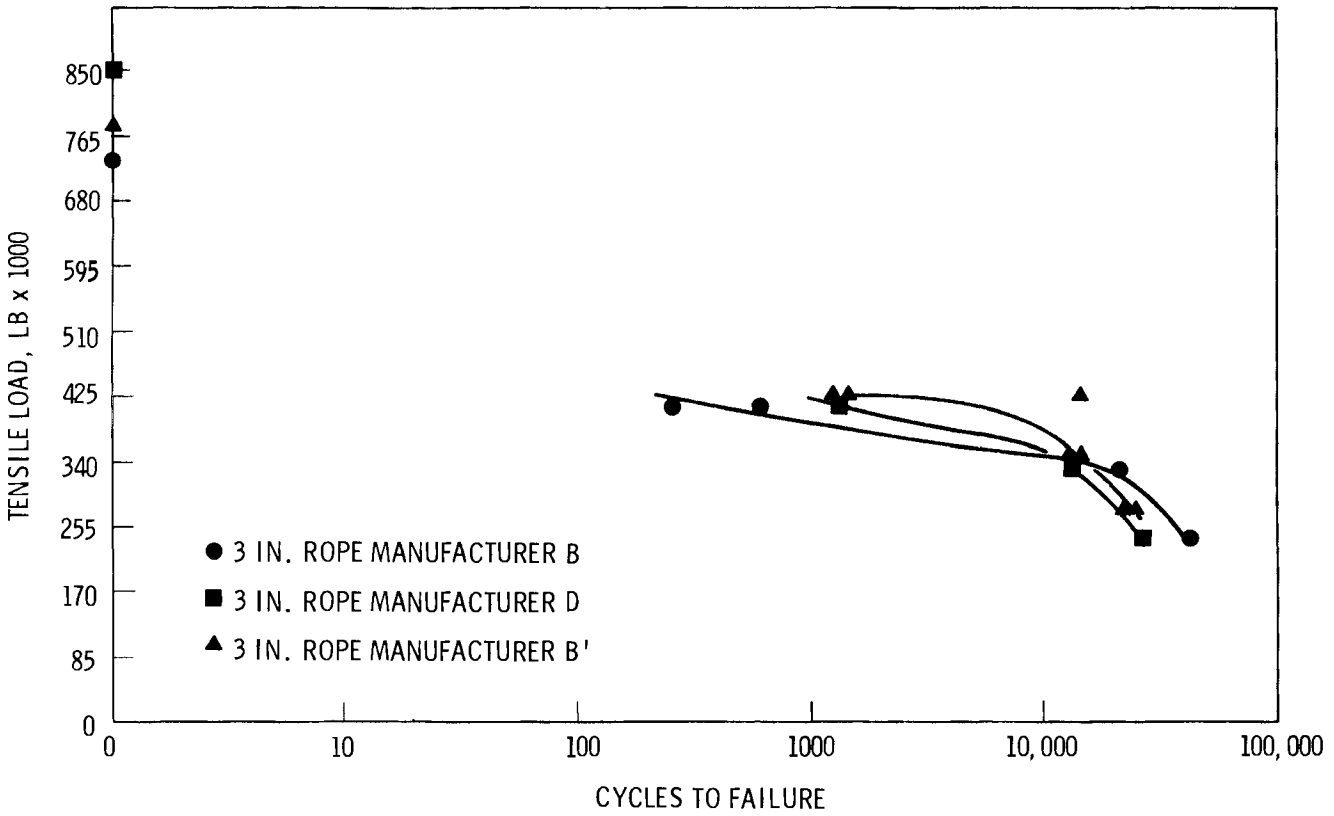

FIGURE 3.3. Fatigue Curve for Large-Diameter Rope

has more than 250 individual wires of varying sizes. The composite nature of rope accounts for the initial elongation segment, due to relative movement of wires as they become more tightly packed, and contributes to the early reduction in rope diameter.

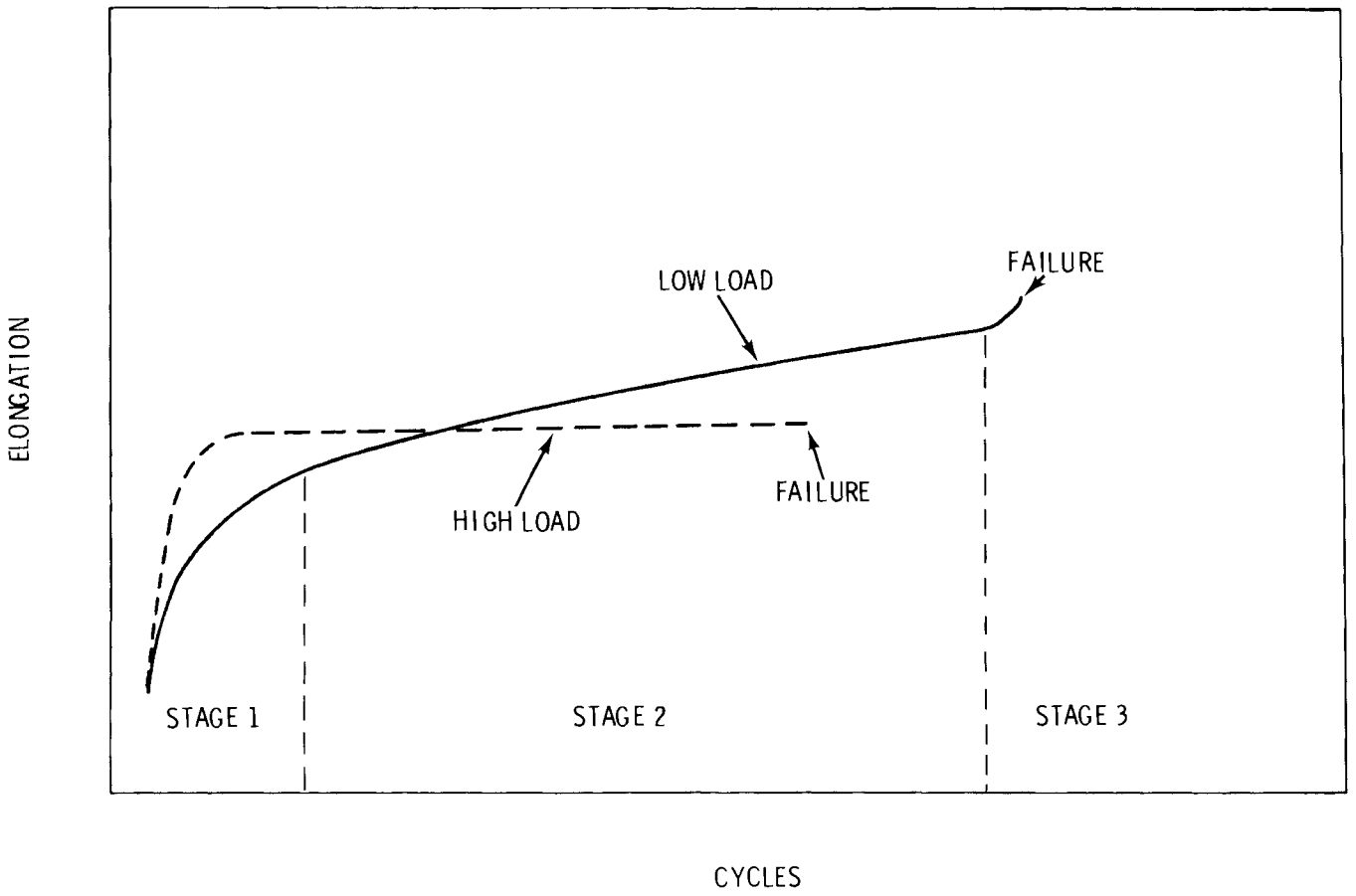

FIGURE 3.4. Typical Rope Elongation with Test Cycles

Change in rope diameter as a function of cycles is shown in Figure 3.5. Typical reduction in rope diameter was <5%. Diameter change is more pronounced in the double-bend region and much less obvious in those areas of rope that are never cycled over a sheave. However, at high loads the initial compaction was not as obvious as expected. High loads may lock the wires in place and prevent them from moving, causing more severe notching and a different failure sequence than at lower loads.

The second stage of the elongation curve is the longest of the three stages. During this stage, elongation increases at a fairly constant rate. Most individual wire wear occurs during this stage. Depending on rope construction and, to some extent, on wire ultimate tensile strength (UTS), broken

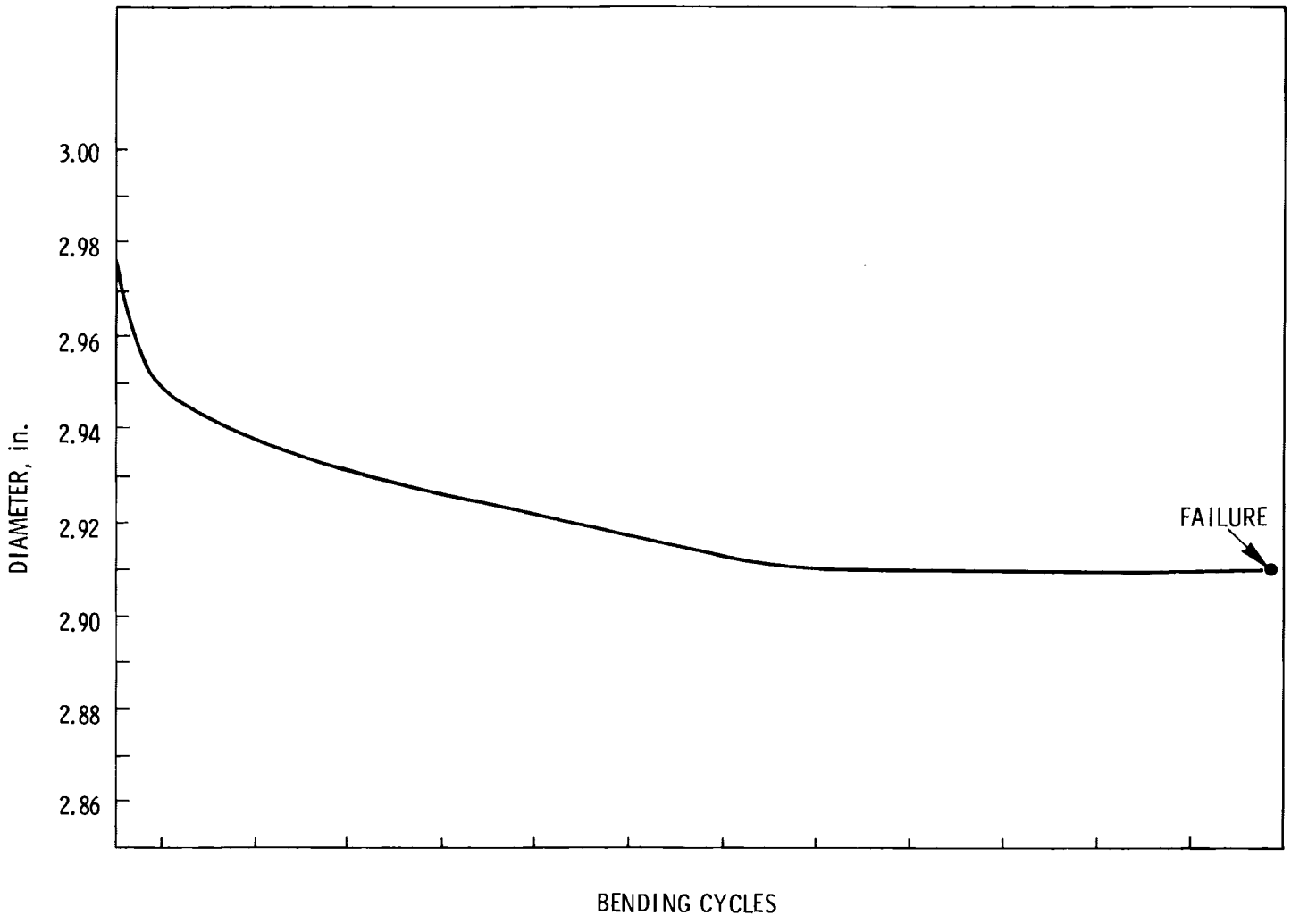

FIGURE 3.5. Typical Rope Diameter Change with Test Cycles

wires begin to appear during this stage. Wires usually break at some internal contact point and work out to the surface. In some tests, more than 20 broken wires were found before failure. At the highest loads, no broken wires were observed before failure.

The third and final stage has a steep slope and is of short duration. It may be from 10 to 100 cycles long, depending on the load, with the fewest number of cycles occurring at the highest loads. In some cases, particularly at the higher loads, this final stage was not clearly defined.(a) More wires break during this stage; sometimes, however, they may not become externally visible because of the short exposure in this stage. Such wire breakage reduces the load-carrying capacity, and failure of one or more strands quickly develops. At lower loads, the majority of failed wires had the appearance of brittle failure. At loads above approximately 40% of the catalog UTS for the rope, the majority of wires in the failed region failed in a ductile manner.

3.2 SMALL-DIAMETER WIRE ROPE AND WIRE TESTS

Bend-over-sheave fatigue tests and tensile tests on single rope wires conducted at BCL are documented in the following two subsections.

3.2.1 Bend-Over-Sheave Fatigue Tests

Two bend-over-sheave fatigue machines were used for the small-diameter wire rope experiments. Each machine had two sheaves, one rigidly positioned on its axle and the other mounted on a movable rigid frame through which tension was applied to a pair of rope specimens, as shown schematically in Figure 3.6. Sheave spacing and stroke length were chosen so that, for all conditions tested, a critical section of each rope would pass on and off its sheave during each machine cycle. In other words, this primary test section received two bending cycles per machine cycle. The length of this critical section was always maintained at no less than four rope lay lengths, or approximately 26 rope diameters. Secondary test sections located to each side of the critical or primary test section of each rope sample were subjected to

(a) Failure of wire rope usually occurs in a localized area. For this reason, any change in length at failure is small when compared to the overall length of the rope; the effect may obscure measurement and observation of the third stage.

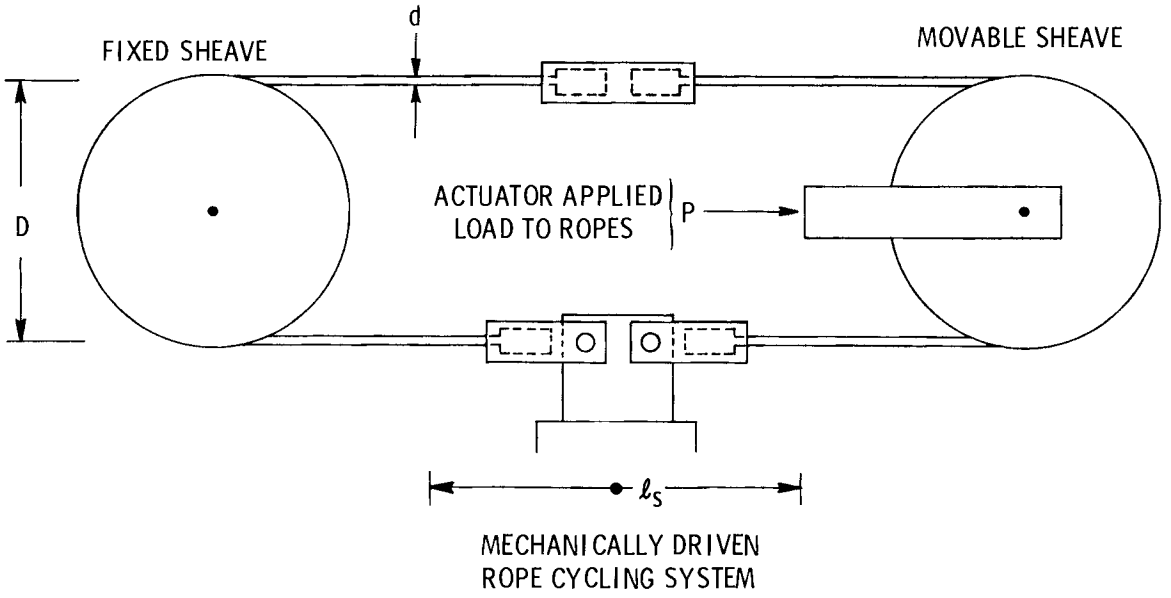

D = SHEAVE PITCH DIAMETER, in.

d = ROPE DIAMETER, in

ℓ_s = STROKE LENGTH, in.

P = ACTUATOR LOAD = 2 x ROPE TENSION (T)

FIGURE 3.6. Small-Diameter Wire Rope Test Machine Schematic

a single bending cycle during each machine cycle. As shown in Figure 3.7, the length of these secondary test sections was dictated by the sheave diameter.

Sheaves manufactured from 1045 steel plate were 3 in. thick for the 1-1/2-in. diameter rope and 1-1/2 in. thick for the 3/4-in. diameter rope. Sheave grooves were machined to 7% oversize in accordance with new ANSI standards for mining ropes. Throat angles of 30^{o} were used on all sheave grooves; groove depths were set at the nominal rope diameter. After machining, all sheave grooves were flame-hardened to R_C = 55 to 60, so that no significant changes in sheave groove contour would occur during testing.

Selected rope tension was achieved and maintained through constant hydraulic pressure on the sheave load actuator. Load-pressure calibration of this actuator was determined before testing with a precision load cell traceable to the National Bureau of Standards. Linearity and stability of this calibration were within 2%.

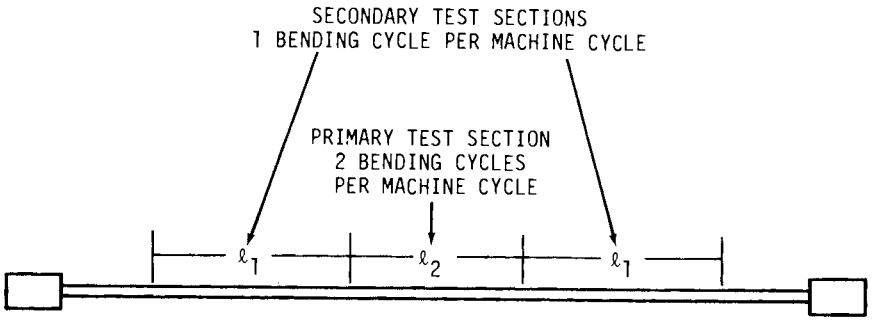

ℓ_2 >4 ROPE LAY LENGTHS; $\sim$ 26 x ROPE DIAMETER

$\ell_1 = \frac{\pi D}{2}$; D = SHEAVE DIAMETER

FIGURE 3.7. Test Sections Within Each Small-Diameter Rope Sample

As mentioned previously, two specimens were cycled simultaneously. A given test was continued until one rope specimen failed, at which time a "dummy" rope of the same construction was mounted in place of the failed rope. The test was then restarted and continued until the second rope failed. Rope failure was defined as the failure of one complete strand. Failure of a strand always occurred in the primary test section, although some broken wires were observed in the secondary test sections of long-life rope samples.

The resulting wire rope bend-over-sheave fatigue data are listed in Table 3.5 and shown in Figure 3.8. Generally, linear patterns of bearing pressure ratio versus life were evident in each rope construction when plotted on log-log paper. Overall, the 6 x 41 FWS, 3/4-in. diameter ropes had the longest lives, while the 6 x 36 WS, 3/4-in. diameter wire ropes experienced the shortest lives. The 1-1/2-in. diameter rope data for both 6 x 41 constructions fell between the two 3/4-in. diameter rope data sets. These small rope data trends are compared in Section 4.0 with the 3-in. rope data. The probable reasons for the moderate layering in fatigue life of the data generated for different constructions and manufacturers are also discussed in Section 4.0.

3.2.2 Single-Wire Experiments

Tensile tests were performed on wires taken from the 3/4-in., 1-1/2-in., and 3-in. diameter wire ropes to compare static tensile properties of the wire

TABLE 3.5. Bend-Over-Sheave Fatigue Test Results for 3/4-in. and 1-1/2-in. Lang-Lay IWRC Rope

Rope Diameter in.	Sheave-to-Rope Diameter Ratio, D/d	Design Factor, d.f.(a)	Manufacturer(b)			Manufacturer(c)			Bearing Pressure Ratio x 10^{-3}
			Specimen Identif.	Bending Cycles to Failure	Average Cycles to Failure	Specimen Identif.	Bending Cycles to Failure	Average Cycles to Failure	
3/4	20	2.11				10N202B1	45,786	44,897	15.8
						10S202B1	44,008		
		3.00	7N203A1	33,756	33,276	9N203B1	78,520	75,665	11.1
			7S203A1	32,796		9S203B1	72,810		
		4.00	6N204A1	50,944	52,897	8N204B1	109,534	101,985	8.35
			6S204A1	54,850		8S204B1	94,436		
	30	3.00	2N303A1	80,118	74,670	4N303B1	120,358	123,200	7.42
			2S303A1	69,226		4S303B1	125,954		
		4.00	1N304A1	106,906	107,700	3N304B1	179,642	183,200	5.57
			1S304A1	108,544		3S304B1	186,762		
1-1/2	20	3.05	2N203A2	47,598	45,340				10.9
			2S203A2	43,090					
		3.63				4N203B2	59,354	58,671	9.16
						4S203B2	57,988		
		4.00	1N204A2	69,360	63,450	3N204B2	66,498	65,737	8.33
			1S204A2	57,542		3S204B2	64,976		
	30	3.05				6N303B2	99,082	95,511	7.29
						6S303B2	91,940		
		4.00				5N304B2	137,030	131,339	5.56
						5S304B2	125,648		

(a) d.f. = rated rope strength/rope tension.
(b) Construction in 3/4-in. rope was 6 x 36 WS; 1-1/2-in. rope was 6 x 41 WS construction.
(c) Construction in 3/4-in. rope was 6 x 41 FWS; 1-1/2-in. rope was 6 x 41 FWS construction.

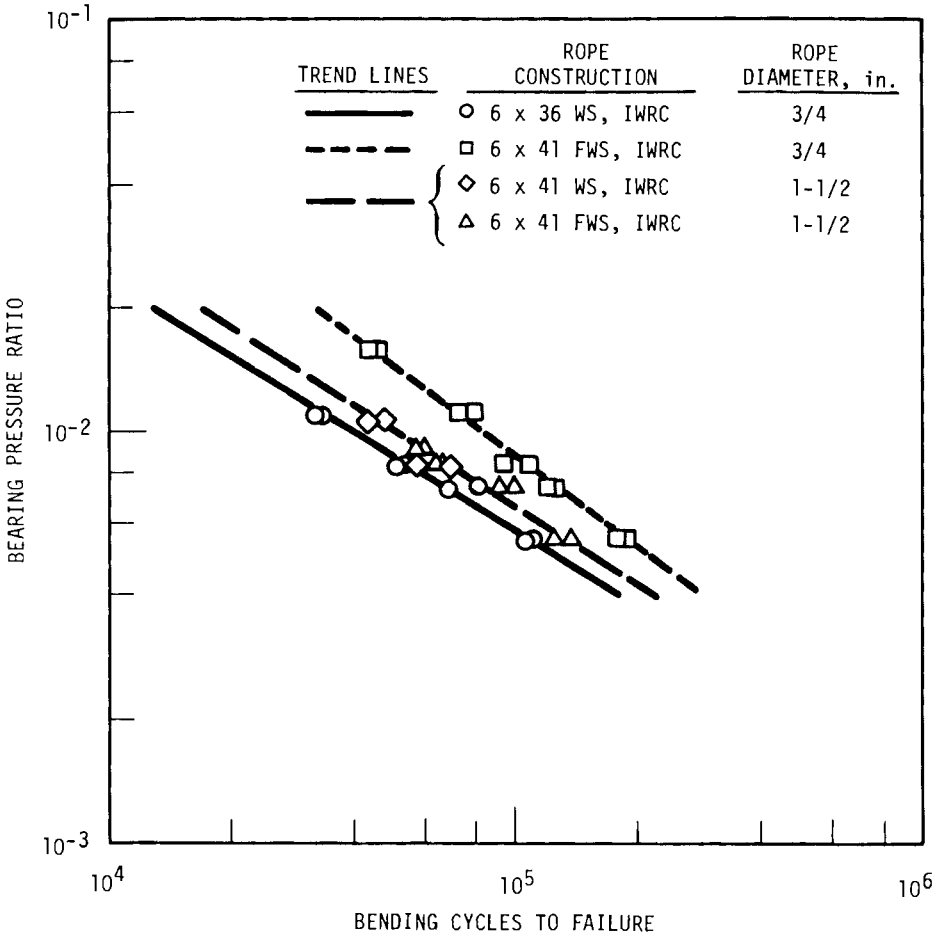

FIGURE 3.8. Small-Diameter Wire Rope Bend-Over-Sheave Fatigue Data

materials. Only the outer wires in each rope construction were tested. Wires were tested under displacement control in an electrohydraulic test system. At minimum, a 10-in. gage length was used in each experiment. The resulting data are given in Table 3.6. This table includes information on the rope construction and diameter from which the wires were taken, as well as a range of experimental measurements and computations.(a) These data are based on an average of two tensile tests per wire size for each rope size/construction.

(a) Experimental measurements and computations include proportional limit stress, yield strength, ultimate tensile strength, apparent elastic modulus, reduction in area, a shape parameter (Ramberg and Osgood 1943), and plastic strain coefficient (see Appendix A) for each wire.

TABLE 3.6. Single Wire Tensile Properties[a]

Rope Diameter in.	Rope Construction	Wire Diameter, d_w, in.	Proportional Limit[b] $\sigma_{p.L.}$, ksi	Strength[c] σ_y, ksi	Tensile Strength σ_u, ksi	Apparent Elastic Modulus,[d] $E_{app.}$, 10^3 ksi	Reduction in Area, R.A., %	Ramberg-Osgood Value, n	Plastic Strain Coefficient, K
3/4	6 x 36 WS	0.042	138.0	235.0	295.0	32.0	38.0	5.60	1.05×10^{-14}
3/4	6 x 41 FWS	0.039	111.0	213.0	285.0	30.8	52.0	4.53	5.75×10^{-12}
1-1/2	6 x 41 WS	0.76	95.0	212.0	288.0	27.5	51.0	3.71	4.65×10^{-16}
1-1/2	6 x 41 FWS	0.077	137.0	230.0	286.0	26.5	49.0	5.83	3.41×10^{-15}
3	6 x 57 FWS	0.149	129.0	190.0	221.0	25.6	55.0	7.75	4.52×10^{-19}

(a) Based on an average of two tensile tests per wire size for each rope size/construction.
(b) Based on plastic strain level of 0.01%.
(c) Based on plastic strain level of 0.20%.
(d) Listed as "apparent" because not established from precision modulus experiment; a likely value for these wire materials would be 29×10^3 ksi.

Table 3.7 shows an example of the stress and strain data calculated from each pair of load-displacement records for each wire size and rope construction. The resultant stress-strain curves for the five wire conditions tested are shown in Appendix A.

In summary, the 3/4- and 1-1/2-in. diameter rope wires exhibited little difference in tensile strength or area reduction. The values found corresponded favorably with wire rope industry standards for extra-improved plow steel wire. The 3-in. rope wire material was substantially lower in strength and corresponded more closely to improved plow steel strength standards. Yield strengths and proportional limit stresses were quite variable because of differences in strain hardening behavior. This variability is reflected in the substantial difference in shape parameters.

TABLE 3.7. Sample Stress-Strain Data for Single Wire from Small-Diameter Wire Rope[a]

Stress, σ, ksi	Specimen No. 1 Total Strain, ε_t, %	Specimen No. 2 Total Strain, ε_t, %	Elastic Strain[b] ε_e, %	Plastic Strain[c] ε_{pavg}, %
20	0.64	0.58	0.062	--
40	0.132	0.120	0.125	--
60	0.196	0.177	0.187	--
80	0.263	0.238	0.250	--
100	0.328	0.297	0.312	--
120	0.400	0.359	0.375	0.0045
140	0.469	0.423	0.437	0.009
160	0.555	0.499	0.500	0.027
180	0.643	0.577	0.562	0.048
200	0.749	0.674	0.625	0.086
220	0.871	0.791	0.687	0.144
240	1.03	0.934	0.750	0.232
260	1.24	1.13	0.812	0.373
280	1.47	1.36	0.875	0.540
290	1.66	1.54	0.906	0.694

(a) Rope diameter = 3/4 in.; 6 x 36 WS; wire diameter = 0.042 in.

(b) Based on a value of $E = \sigma/\varepsilon_{pavg}$ at $\sigma = 80$ ksi.

(c) $\varepsilon_{pavg} = \frac{\varepsilon_{t1} + \varepsilon_{t2}}{2} - \varepsilon_e$, $\varepsilon_e > 0.0$

4.0 ANALYTICAL RESEARCH

More than 35 years ago, Drucker and Tachau (1944) demonstrated that a bearing pressure ratio was useful in correlating wire rope bend-over-sheave fatigue data generated over a range of test conditions and rope diameters. The formulation was presented earlier as Equation (3.1), but it will be repeated here for continuity.

$$B = \frac{2T}{UDd} \quad , \tag{4.1}$$

where

T = rope tension, lb
U = wire ultimate strength, ksi
D = sheave diameter, in.
d = rope diameter, in.

Equation (4.1) has been used extensively in the wire rope industry, and has been proven useful in accounting for rope size effects for ropes of a given construction, 1/2 in. to 1-7/16 in. in diameter.[a] Experimental work (Gibson 1974) on two regular-lay IWRC rope constructions showed that the Drucker-Tachau ratio could be used to correlate BOS fatigue data from IWRC ropes. These data are shown in Figures 4.1 and 4.2 for 6 x 36 and 6 x 26 construction, respectively; no definite layering with rope diameter is evident. Until recently, however, no laboratory bend-over-sheave fatigue data have been available on ropes of any construction exceeding 1-1/2 in. in diameter, so it was not possible to check adequacy of the formulation in correlating data trends for large-diameter ropes comparable to those used in the surface mining industry.

4.1 SMALL-DIAMETER ROPE DATA CORRELATION

A primary objective of this program was to generate bending fatigue data on wire ropes of similar constructions over a wide range of rope diameters, so

(a) It should be noted that these ropes had fiber cores.

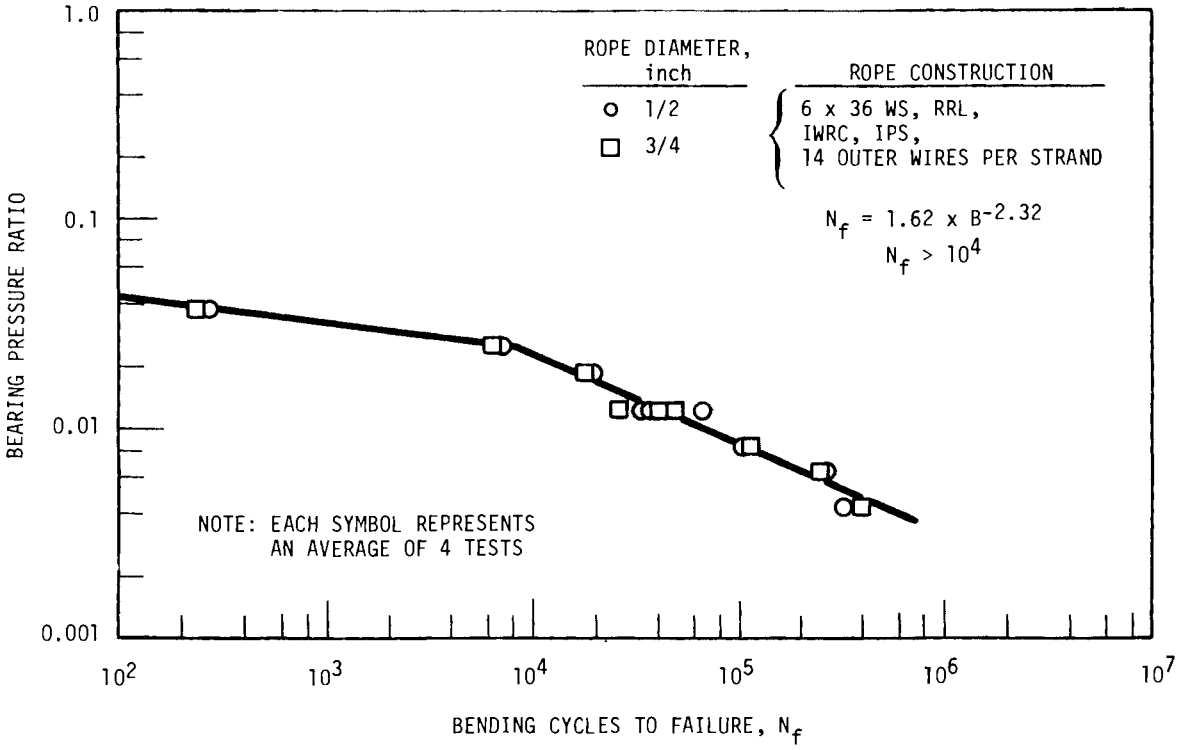

FIGURE 4.1. Bend-Over-Sheave Fatigue Data for Small-Diameter Rope, 6 x 36 Construction

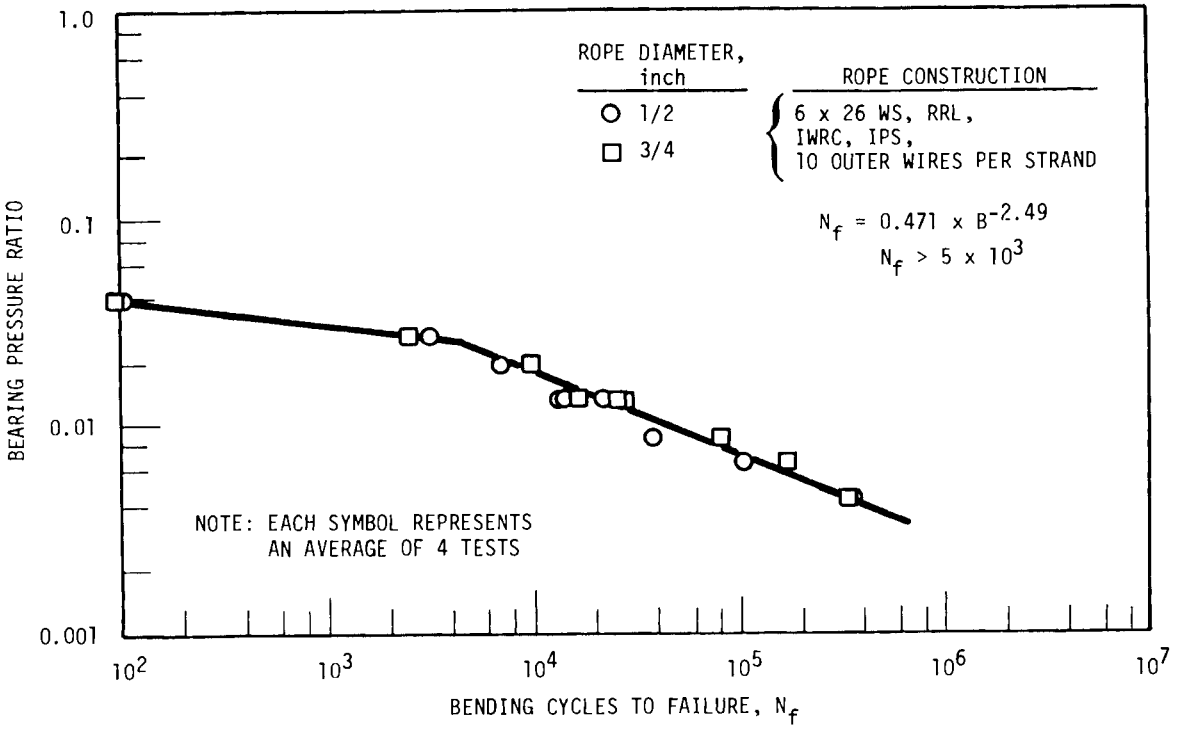

FIGURE 4.2. Bend-Over-Sheave Fatigue Data for Small-Diameter Rope, 6 x 26 Construction

that adequacy of the bearing pressure ratio as a vehicle for correlation could be fully evaluated. Some limitations of the bearing pressure ratio correlation are, of course, expected at extreme rope loads or relatively small sheave diameters. These limiting conditions are discussed in Appendix B; discussion here focuses on intermediate rope loads and sheave diameters typical of surface mining usage.

Small rope data generated in this program were presented earlier in Figure 3.8. Some layering of those data was evident, especially between the two 3/4-in. diameter rope constructions. The 1-1/2-in. diameter rope data were nearly indistinguishable. One obvious explanation for these trends lies in the construction differences for the 3/4-in. ropes. The 6 x 36 WS rope has only 14 outer wires per strand; the smaller number of outer wires per strand leads to lower flexibility and decreased bending fatigue resistance.

In an attempt to account for differences in rope constructions used to generate the small rope data, the bearing pressure ratio was modified. The originalformulation was changed by multiplying by the ratio of the outer wire diameter to the rope diameter $\left(\frac{d_w}{d}\right)$. In all other respects, the formula remained the same, so that it was expressed as

$$B' = \frac{2\,T\,d_w}{UDd^2} \quad , \tag{4.2}$$

where

d_w = outer wire diameter in a rope strand, in.
d = rope diameter, in.

The small rope data were replotted in Figure 4.3 as a function of B', the modified bearing pressure ratio. A more compact grouping of the data is evident, as compared to Figure 3.8. Some layering of the data remains; however, the effect is likely the result of variations in fatigue resistance of the wires in the individual rope constructions. Because no data on the fatigue resistance of individual wires were obtained, this issue could not be addressed further.

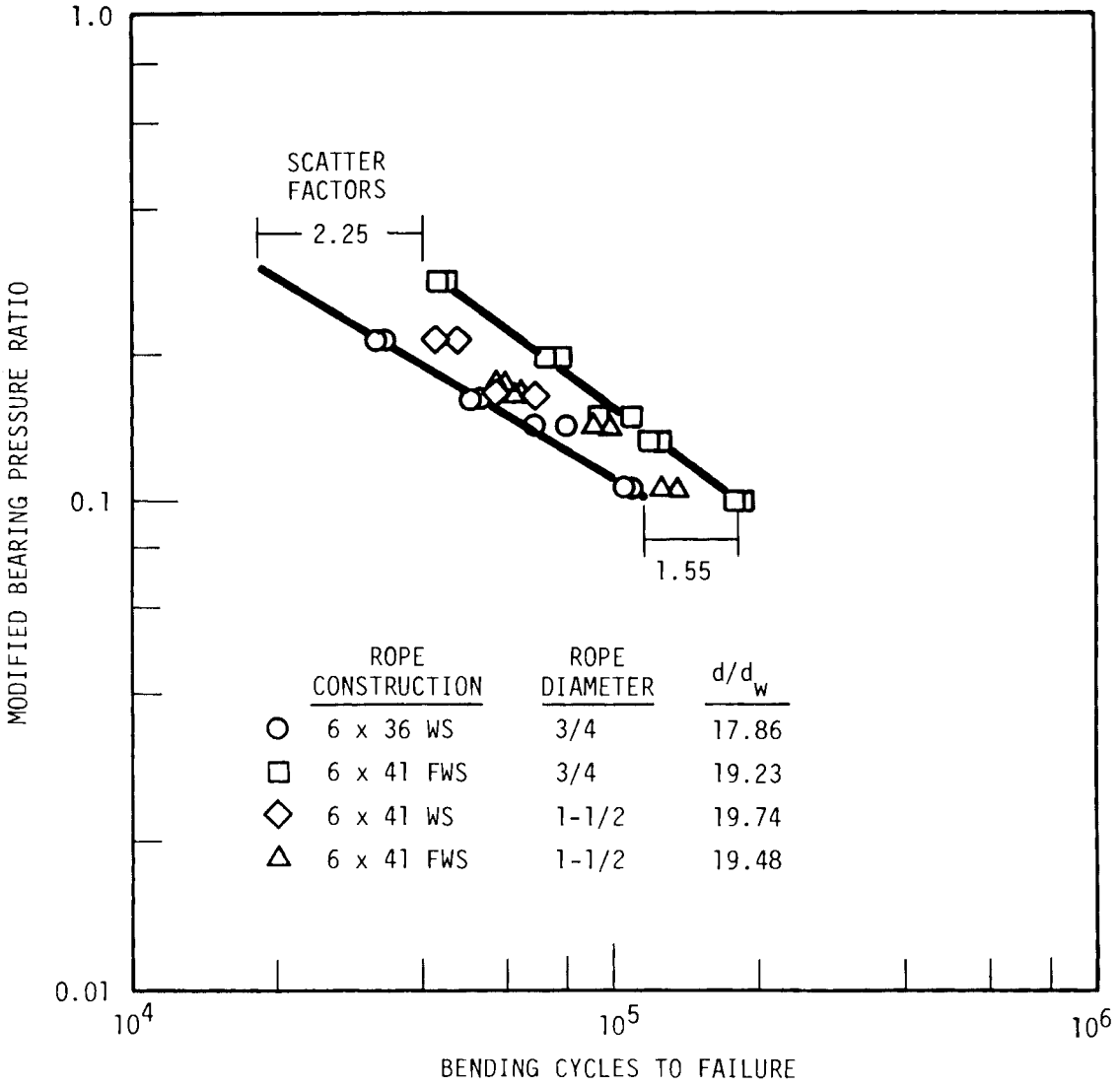

FIGURE 4.3. Small-Diameter Rope Bending Fatigue Data Plotted as a Function of Modified Bearing Pressure Ratio

The scatter in Figure 4.3 is quantified in terms of ratio of maximum to minimum fatigue life at the high and low ends of the fatigue-life range. This scatter factor is only 2.25 at the low fatigue life end of the data collection. The scatter is even lower at the high end, with a scatter factor of 1.55. Scatter factors of 2.0 or higher are not uncommon with simple coupon fatigue

data; therefore, the amount of scatter observed in this study would have to be considered "normal." In comparison, the scatter factors computed in Figure 3.8 for the data plotted according to the standard bearing pressure ratio model were 2.55 and 1.75 for the low and high fatigue lives, respectively. These values were about 13% higher than those found using the modified bearing pressure ratio (MBPR). This finding supports the decision to use the modified bearing pressure ratio in place of the traditional expression.

In Figures 4.1 and 4.2, data were presented for two different regular-lay (IWRC) rope constructions, 6 x 36 and 6 x 26. The 6 x 36 construction had 14 outer wires while the 6 x 26 had only 10 outer wires. As expected, the 6 x 36 construction displayed higher fatigue lives for all bearing pressure ratios. Looking at specific fatigue lives, the 6 x 36 construction endured a bearing pressure ratio of 0.023 for 10^4 bending cycles to failure and a value of 0.0086 for 10^5 cycles to failure. In comparison, the 6 x 26 construction endured a bearing pressure ratio of 0.018 for 10^4 cycles to failure and a value of 0.0072 for 10^5 cycles to failure. The values of bearing pressure ratio for the 6 x 26 construction are 20% to 40% below those for the 6 x 36 construction. Interestingly, the outer wire diameters in these two constructions are different by about the same ratio [(0.55-0.043) 0.043 = 28%]. In effect, this result suggests that the two curves shown in Figures 4.1 and 4.2 would very nearly be superimposed if plotted according to the modified bearing pressure ratio. This comparison is made in Figures 4.4 and 4.5. In Figure 4.4 the two mean lines are plotted according to bearing pressure ratio. The average scatter factor between the means is 1.63; i.e., the 6 x 36 construction has a 63% higher fatigue life for a given B value. However, when plotted according to the modified bearing pressure ratio as in Figure 4.5, the scatter factor between the mean curves drops to only 1.19, a 19% difference in fatigue life.

For the reasons just cited, the modified bearing pressure ratio (MBPR) will be used in all subsequent comparisons within this report.

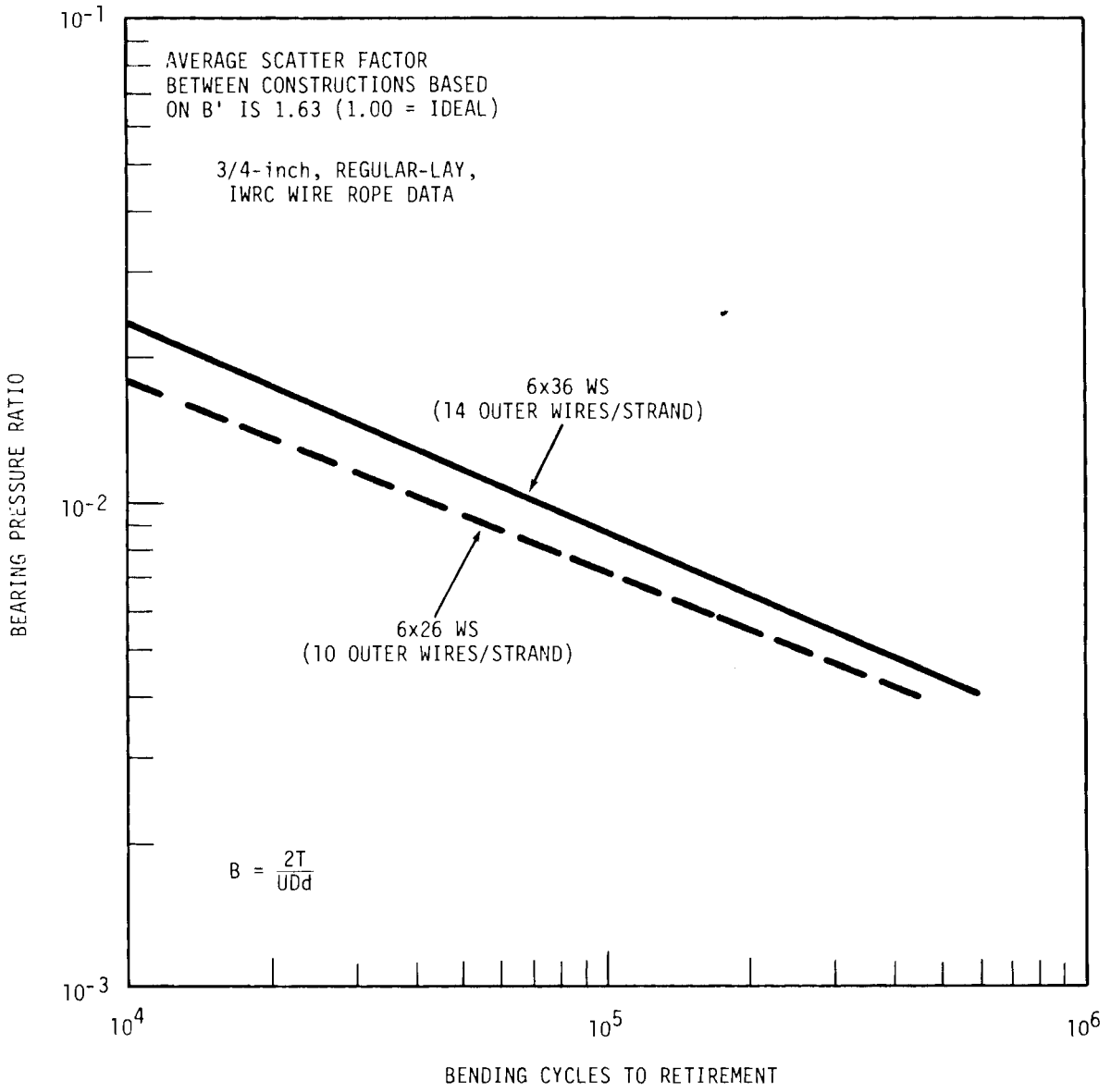

FIGURE 4.4. Scatter Between Rope Constructions with Different Numbers of Outer Wires, Based on the Bearing Pressure Ratio

4.2 LARGE- AND SMALL-DIAMETER ROPE DATA COMPARISON

A comparison of bend-over-sheave fatigue results for the large- and small-diameter wire ropes tested in this program is given in Figure 4.6. The bounds of the 3/4-in. and 1-1/2-in. diameter rope data are shown in comparison to the 3-in. diameter rope data.

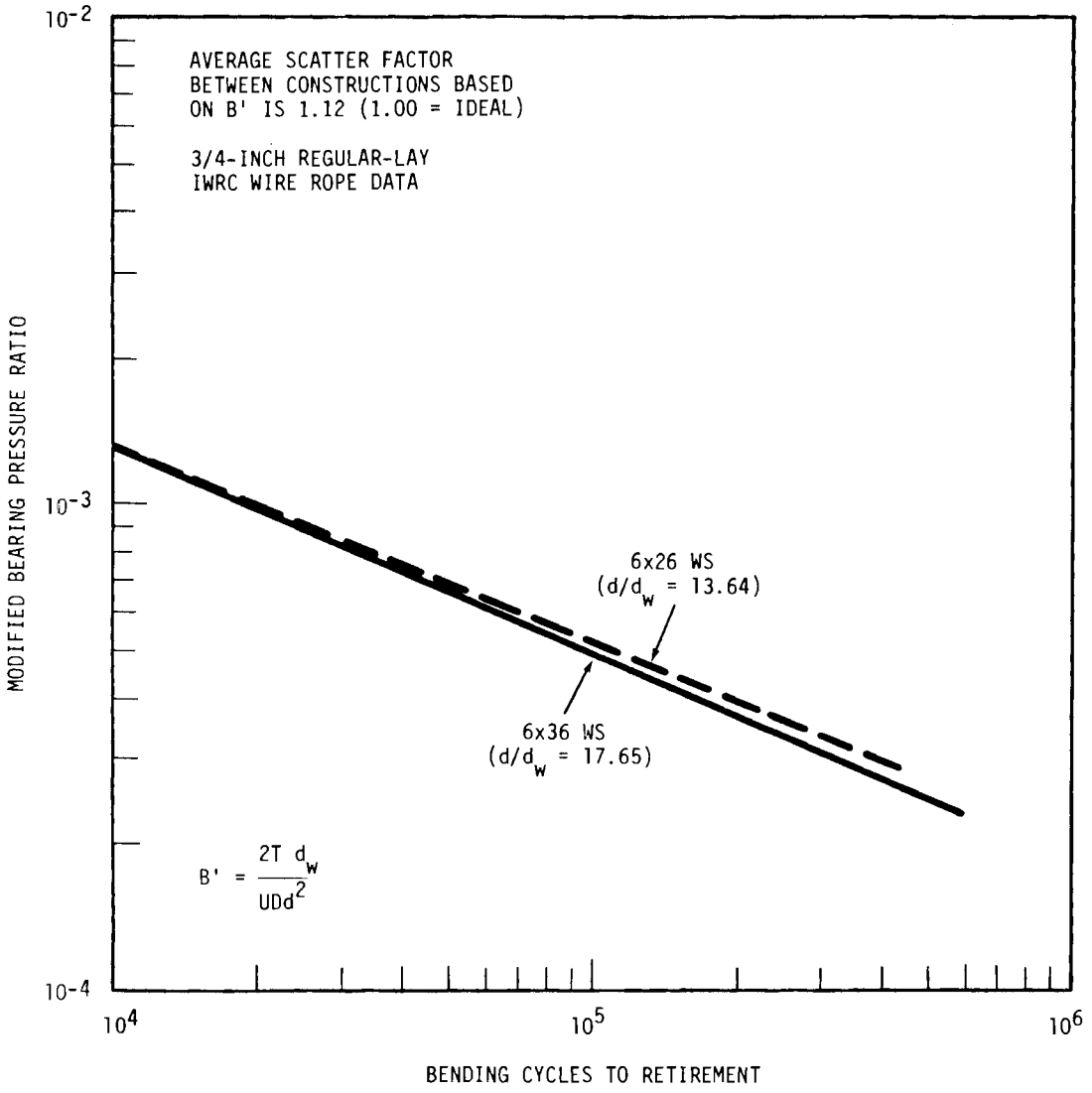

FIGURE 4.5. Scatter Between Rope Constructions with Different Numbers of Outer Wires, Based on the Modified Bearing Pressure Ratio

The large-diameter rope data generally do not follow the same trends as do the small-diameter rope data. However, all of the large rope data (with the exception of extremely early failures at high loads) fall within (or close to) the small rope data bounds.

Actually, two different trends seem to be evident for the large-diameter rope data. In the long-life region (above about 100,000 cycles), the slope

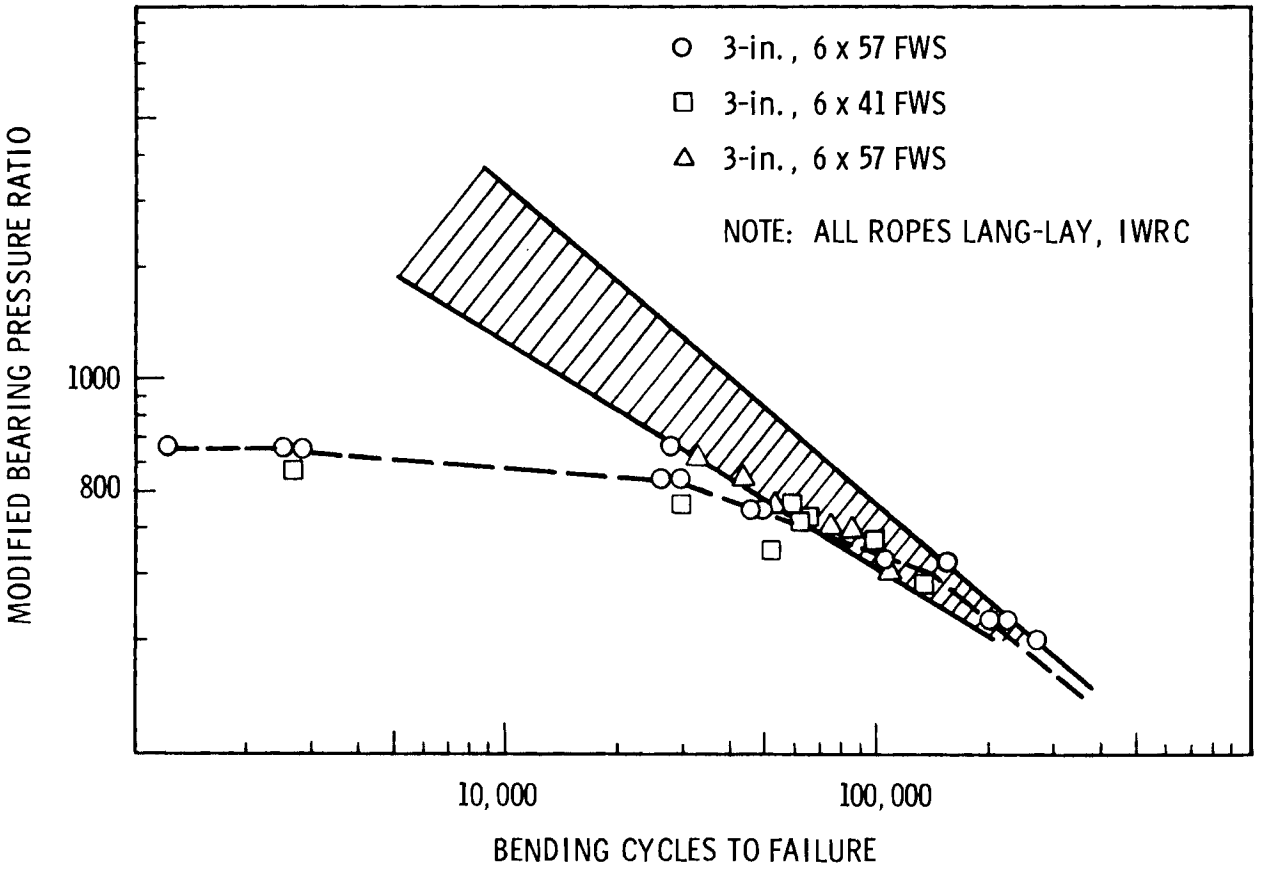

FIGURE 4.6. Comparison of Large- and Small-Diameter Wire Rope Bending Fatigue Data

for the large rope data curve compares reasonably well with that for the small rope data. The mean of the large rope trend line is closely approximated by the upper bound of the small rope data. In other words, the relationship between B' and cycles to failure in the long-life region seems to be similar for the large and small ropes. Below 100,000 cycles to failure, the trends are definitely different, with the fatigue lives of the large ropes dropping substantially faster for increasing B' values than those for the smaller ropes.

The difference in fatigue life trends may be a result of differences in sheave groove oversize and sheave hardness that exist in the machines used to test the large (3-in.) and small (3/4-in. and 1-1/2-in.) ropes. The small rope tests were completed on flame-hardened sheave grooves machined to 7% oversize based on nominal rope diameter. The large rope tests were completed on unhardened sheaves designed to the nominal rope diameter (nonoversized). The effect of sheave hardness, independent of sheave groove geometry, is disputed in the literature. One experimental program (Gambrell 1969) on various soft sheaves (in comparison to tool-steel sheaves) showed increased fatigue life with the harder sheaves; the increase was greatest at the highest rope loads. However, in a similar study (Gibson 1971) comparing aluminum and hardened-steel sheaves, little difference in life was observed. The original work by Drucker and Tachau (1944) cites several investigators who report that soft sheaves increase rope life.

The effect of sheave groove size and shape on fatigue life is somewhat more clearly established. A round sheave groove about 5% to 7% oversize with a 30 to 60^{o} throat angle has been reported to provide near optimal bending fatigue resistance (VDI 1968). This same European source indicates that groove radii below, and substantially above, this level decrease fatigue lives. No similar U.S. data are publicly available, although these trends are generally supported by the recommendations of the Wire Rope Technical Board (1979).

There is some probability that the effects of sheave groove geometry may be lost in the noise in high cycle (low load) fatigue. Current and previous tests at design factors of 3 or more on large-diameter rope are probably affected very little by nonoversized sheave grooves. The decrease in rope diameter that occurs during testing allows the rope to accommodate to the sheave groove after several thousand cycles.

The break in the large-diameter rope fatigue data at a design factor of 2.5 may be attributed to the onset of gross plastic deformation in the rope due to the combination of tensile, bending, and contact streses. At low loads, even with the increased contact force due to the sheave groove, a semi-elastic stress mode may still be in effect. Some plastic deformation

does occur but it probably is not enough to cause significant damage. The size of the plastic zone created by the contact between wires is probably small when compared to the wire diameter. At high test loads the size of the plastic zone created by the increased contact force between wires, as a result of a nonoversized sheave groove, may be a significant portion of the wire diameter. This, coupled with the bending and tensile stresses, leads to failure at fewer cycles than would be expected with an oversized sheave groove.

To study this effect in greater detail, BOS fatigue tests are being conducted on small-diameter wire rope using nonoversized unhardened sheaves. Results from these tests will be used to help determine the effect of a nonoversized unhardened sheave groove on the large-diameter ropes tested at high loads. Initial test results indicate that the differences between small- and large-diameter ropes' fatigue lives cannot be explained wholly by differences in sheave hardness and sheave groove hardness.

4.3 LABORATORY AND FIELD ROPE FATIGUE LIFE COMPARISON

An obvious and very important consideration in this program is the relationship between laboratory test results and actual field rope service performance. Fortunately, a limited number of documented field data on hoist ropes were obtained for review. These data are presented in Table 4.1. The raw data include the bucket size and weight, point sheave diameter, rope diameter, and average yardage of overburden removed before rope retirement. With a few reasonable assumptions, it was possible to convert these data into a form that was comparable to the laboratory-developed data. The results of the analysis of the field data are presented in Table 4.2.

First, a D/d ratio was computed to identify the severity of bending over the point sheave. Second, the number of bending cycles before retirement was computed as the yardage removed before retirement divided by the bucket size multiplied by two bending cycles per machine cycle. Rehandle was not considered in the computation of machine cycles, because exact values were unknown. It is not unlikely that 10% to 20% rehandle did occur in some cases, which, of course, would have increased actual rope bending cycles beyond those

TABLE 4.1. Field Data on Hoist Rope Fatigue Performance

Mine	Bucket Size, yd^3	Bucket Weight, lb	Point Sheave Diameter, in.	Hoist Rope Diameter, in.	Overburden Removed Before Rope Retirement, yd^3
11	58	116,000	120	3	4,094,000[a]
3	60	140,000	120	3	4,876,000[a]
8	100	200,000	144	4-1/2	3,258,000[a]
6	41	80,000	85-1/4	2-7/8	3,598,000[b]
5	70	140,000	110	3-1/2	4,424,000[b]

(a) An average value based on a series of ropes over a period of time.
(b) A single rope retirement yardage.

computed. This factor is probably at least partially compensated for, however, by the fact that the bucket is not always full during every dump cycle. Third, the full bucket weight was estimated based on an overburden density of 2700 lb/yd^3. This overburden density would correspond to dry clay and gravel. Densities as low as 2050 lb/yd^3 are found for loose, dry earth; densities as high as 3400 lb/yd^3 are found for wet sand and gravel. Acknowledging this potential spread in overburden density, a density of 2700 lb/yd^3 was chosen as a reasonable average. Fourth, the approximate design factors for the bucket, both full and empty, were computed based on a pair of 6 x 61 class, IWRC, Lang-lay wire ropes of improved plow steel grade. The design factors were computed based on a bucket position factor (or load magnification factor) of 1.20. This factor is required to account for the angle from vertical in which the bucket is held during a dumping cycle. This consideration is discussed more completely in Appendix C. Fifth, the outer wire diameters of each pair of ropes were computed based on 16 outer wires per strand (common in 6 x 61-class ropes). Finally, different MBPR values were computed based on a full bucket, an empty bucket, and an equivalent bucket weight. The first two MBPR calculations are straightforward, after a wire strength level is assumed. An ultimate strength value of 220 ksi was chosen as typical of IPS grade wire rope in the 3- to 5-in. diameter range. The

TABLE 4.2. Field Rope Data Analysis

Mine	Sheave to Rope Ratio, D/d	Rope Bending Cycles[a]	Estimated Bucked Load When Full,[b] lb	Approximate Design Factor[c]		Outer Wire Diameter, in.	Approximate Modified Bearing Pressure Ratio x 10^{-4}[d]		Equivalent Value[e]
				Bucket Full	Bucket Empty		Bucket Full	Bucket Empty	
11	40	141,200	272,600	4.40	10.3	0.153	2.11	0.89	1.37
3	40	162,500	302,000	3.97	8.57	0.153	2.33	1.09	1.49
8	32	65,150	470,000	5.48	12.9	0.230	2.02	0.87	1.33
6	29.6	175,510	190,700	4.82	13.9	0.147	2.17	0.92	1.40
5	31.4	126,410	329,000	4.90	11.5	0.178	2.37	1.01	1.54

(a) Bending Cycles = $\frac{\text{Yardage Removed}}{\text{Bucket Size}}$ x 2 (2 bending cycles/operating cycles).

(b) Based on overburden weight of 2700 lb/yd^3; could actually vary from about 2100 lb/yd^3 to 3200 lb/yd^3 depending on type of overburden.

(c) Based on 6 x 61, IWRC, Lang-lay, IPS Wire Rope, and Bucket suspended at 20° from vertical with drag rope at 15° below horizontal (i.e., load magnification factor of 1.20).

(d) $B' = \frac{2 \times \text{Individual Rope Tension} \times \text{Rope Wire Diameter}}{\text{UTS} \times \text{Sheave Diameter} \times (\text{Rope Diameter})^2}$.

(e) Based on assumption that $N_f = A\ B^{-2}$.

third calculation for an MBPR is less straightforward, however, and requires some explanation. It essentially represents the MBPR that would have caused rope replacement in the observed number of cycles to rope retirement, assuming the bucket load always remained constant--never full and never empty, but constantly partially full. Field service lives at this equivalent MBPR should most nearly compare to the laboratory test data that were developed under constant load conditions.

To compute this equivalent MBPR, it is necessary to assume a relationship between cycles to failure and MBPR. The laboratory test data suggest that the following relationship is approximately correct:

$$N_f = A\ B'^{-n} \quad , \tag{4.3}$$

where

B' = modified bearing pressure ratio (MBPR)
A = constant
N_f = bending cycles to failure.
n = a constant of approximately 2.0.

Equation (4.3) says that a twofold decrease in B' should cause a four-fold increase (2^2) in cycles to failure. This approximate trend was observed experimentally. As will be noted later, the criterion for rope failure is crucial in establishing a particular relationship between MBPR and bending cycles to failure. In the discussion here, laboratory ropes were considered to have failed when one complete strand had separated.

One other elementary factor must also be established before an equivalent MBPR can be computed: half of the total bending cycles to failure were made with a full bucket and half were made with an empty bucket. In other words,

$$N_1 = N_2 \quad , \tag{4.4}$$

where

$$N_f = N_1 + N_2$$

and

N_1 = full bucket cycles

N_2 = empty bucket cycles

N_f = total bending cycles to rope retirement.

Then, using Equation (4.3), it is possible to state that

$$N_1^* = A\ B'_1{}^{-n} \quad ,$$

and (4.5)

$$N_2^* = A\ B'_2{}^{-n} \quad ,$$

where N_1^* and N_2^* represent the number of cycles to failure of a rope tested at B' values of B'_1 and B'_2, respectively. Because half the cycles seen by the rope were at B'_1 and half at B'_2, it is safe to say that N_f should lie between N_1^* and N_2^*. One of the important factors to determine is the relationship between N_1 and N_1^* and between N_2 and N_2^*. In that regard, it can be said that

$$N_1 = X\ N_1^* \quad , \tag{4.6}$$

$$N_2 = (1 - X)N_2^* \quad , \tag{4.7}$$

where

X = a number between 0 and 1 that represents the fraction of damage caused by the loaded bucket cycles.(a)

If nearly all damage were caused by the loaded bucket cycles, then X would be close to 1.

(a) This relationship is based on the assumption that Miner's Rule for cumulative fatigue damage applies to wire rope.

Equating Equations (4.6) and (4.7), it is apparent that

$$X = \frac{N_2^*}{N_1^* + N_2^*} \quad . \tag{4.8}$$

Combining Equations (4.5), (4.6), and (4.8), X is defined as

$$X = \frac{A\ B_1'^{-n}}{A\ B_1'^{-n} + A\ B_2'^{-n}} \quad ,$$

or

$$X = \frac{B_1'^{-n}}{B_1'^{-n} + B_2'^{-n}} \quad . \tag{4.9}$$

Now that X is defined in terms of known parameters, it only remains to compute an equivalent B' from X and other known quantities. This can be done by first considering that

$$N_f = A\ B_{eq}'^{-n} \quad , \tag{4.10}$$

where B_{eq}' = the equivalent modified bearing pressure ratio.

Then, from Equation (4.10),

$$B_{eq}' = \left(\frac{A}{N_f}\right)^{-1/n} ,$$

or

$$B_{eq}' = \left(\frac{A}{X\ N_1^* + (1-X)N_2^*}\right)^{-1/n} , \tag{4.11}$$

which leads to

$$B'_{eq} = \left(\frac{A}{X\ A\ B_1'^{-n} + (1-X)\ A\ B_2'^{-n}} \right)^{-1/n}$$

or

$$B'_{eq} = \left(\frac{1}{X\ B_1'^{-n} - B_2'^{-n} + B_2'^{-n}} \right)^{-n} \qquad (4.12)$$

The values for B'_{eq} are tabulated in the last column of Table 4.1. Interestingly, values for X from Equation (4.9), assuming n = 2.0, were all between 0.82 and 0.85 for the five field ropes examined. In other words, 82% to 85% of the damage would be expected to be caused by the full bucket bending cycles and only 15% to 18% of the damage by the unloaded bucket cycles.

The field rope results from Table 4.2 are compared in Figure 4.7 with the laboratory results. All of the field rope data fall well below the laboratory data when compared on the basis of B'_{eq}. Four of the field rope retirement lives fall about a factor of two below the small-diameter laboratory wire rope fatigue life trends, while a fifth rope was retired at only about one-fourth of the small rope fatigue life trends. If predictions of field rope service life were made based on the small rope fatigue life trends as shown in Figure 4.5, it is obvious that very unconservative life estimates (i.e., dangerously high estimates) would result. Where does the correlation of field and laboratory rope fatigue performance break down?

Several factors can significantly influence the correlation of field and laboratory wire rope fatigue lives. All revolve around the assumptions in the analysis. Material rehandle could increase the actual number of bending cycles by 20% over the apparent cycles in some cases. Heavy overburden could also bias the results, as could consistently high or low bucket position factors (see Appendix C).

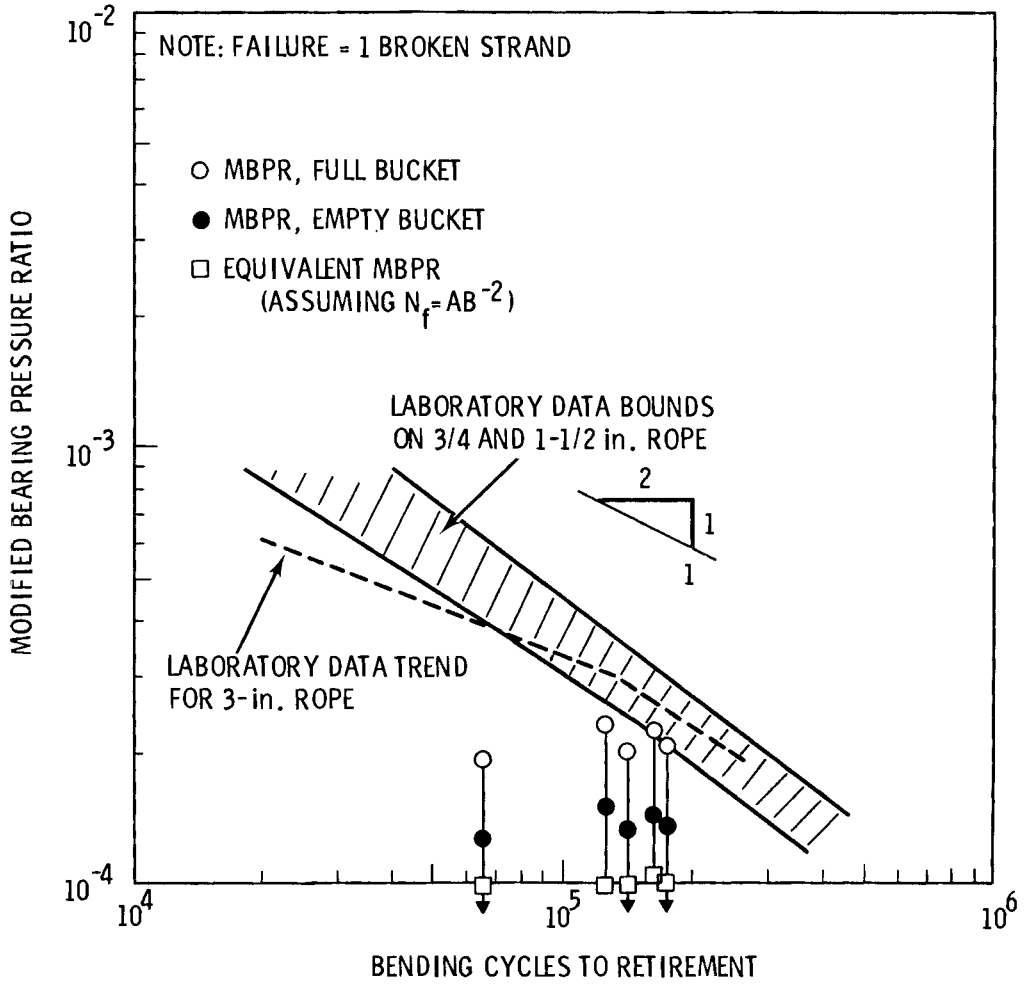

FIGURE 4.7. Laboratory and Field Rope Bend-Over-Sheave Fatigue Data Comparison Using the One-Strand Failure Criterion

On the average, however, it does appear likely that hoist ropes in the field do fail primarily by bending fatigue in a manner similar to small-diameter wire ropes of a similar construction tested in the laboratory. This conclusion, of course, is not obvious from Figure 4.7. Field and laboratory fatigue lives appear to be different in Figure 4.7 because of a difference in failure criteria. In the laboratory tests on small-diameter ropes, a rope was not considered failed until one complete strand had failed. Hoist ropes in the field are never purposely left in service this long. Failure of one complete strand in a hoist rope could be catastrophic, leading potentially to

failure of the complete rope and high risks in loss of life and/or substantial unnecessary (and expensive) downtime. Most large hoist ropes are retired in compliance with the guidelines of ANSI M11.1, which indicate rope retirement according to the "6 and 2" rule, i.e., six total broken wires in one lay or two broken wires in a single strand of one lay.

Through a review of laboratory records it was possible to ascertain approximately the point at which most of the laboratory-tested wire ropes exceeded the "6 and 2" rule. A plot of MBPR versus cycles to retirement is shown in Figure 4.8. Scatter is noticeable in the results but a generally log-linear pattern in the laboratory data is evident. Most significantly, the slope of the laboratory data band in Figure 4.8 is much steeper than that shown in Figure 4.7. This trend holds because fewer wire breaks can be sustained in a wire rope before strand failure at high loads and/or small sheaves. At lower loads on large sheaves, numerous wire breaks can be sustained before a complete strand fails. This, in turn, means that a large number of bending cycles can be endured at low load levels between attainment of the "6 and 2" rule and retirement by the one-strand failure rule. This trend was evident in the data. In fact, at MBPR values less than about 3×10^{-4}, from 40% to 60% of the total cycles to strand failure were sustained after experiencing from two to five wire breaks in the critical test section.

The difference in failure criteria changed the slope of the fatigue data trends from about -2 in Figure 4.7 to about -1 in Figure 4.8. The change in slope affected the basic relationship between B'_{eq} and N_f given in Equation (4.3), i.e., the exponent n changed from 2 to 1. Taking this factor into account, new values of B'_{eq} were computed for the field data and these values were plotted in Figure 4.8 along with the laboratory data. Incidentally, the change in slope of the fatigue curve significantly changed the values of X computed in Equation (4.8). Values ranging from 0.68 to 0.70 were obtained in the final analysis, which indicated that a higher percentage of the damage (wire breaks) could be ascribed to the empty bucket cycles than had previously been suspected.

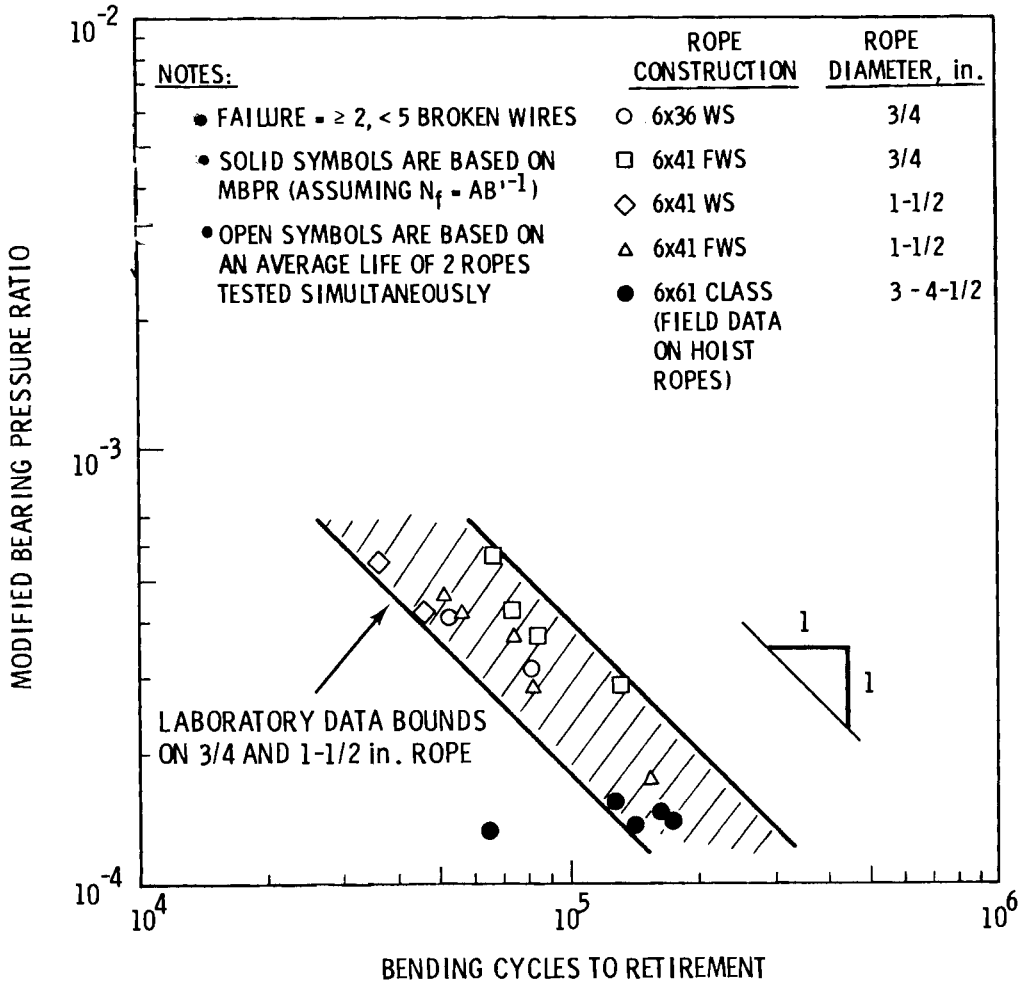

FIGURE 4.8. Laboratory and Field Rope Bend-Over-Sheave Fatigue Data Comparison Using the Two- to Five-Strand Failure Criterion

Figure 4.8 shows a remarkably good correlation of laboratory and field fatigue life data. If it is assumed that the cluster of four field failures represents good operating practice under normal operating conditions, and that the outlier on the low side represents either bad operating practice (i.e., poor sheaves, unnecessary dynamic loading) or poor operating conditions (i.e., very heavy overburden, very deep overburden layers), it is easy to conclude that the correlation between laboratory and field data is quite good. If such

a correlation is accepted, this figure has a variety of interesting implications. First, it implies that hoist rope fatigue lives may be reasonably estimated from laboratory tests on small ropes (if the appropriate assumptions are made, of course). Second, it implies that most hoist rope failures are relatively long-life failures, corresponding to laboratory failures that one might see on D/d = 30 sheaves at design factors between 4 and 6. Third, it implies that, at least for hoist ropes, the especially severe loading conditions (design factors below 3) are uncommon and probably not of great concern.

4.4 TENSILE AND BENDING STRESSES IN WIRE ROPE

In addition to the analytical efforts to correlate wire rope fatigue trends for different size ropes, a companion effort was undertaken to evaluate the tensile and bending stresses experienced by the wire ropes in this study for different test conditions.

Tensile stresses for the wires in a strand of 3-in. rope were evaluated (Hruska 1951). The stresses due to tension-only loading for the outer wires are shown in Table 4.3.

TABLE 4.3. Tensile Stesses in the Outer Wires of 3-in. Diameter Test Ropes

Design Factor	psi
10.0	19,777
5.0	39,554
3.3	59,330
2.5	79,107
2.0	98,884
1.7	118,661

Bending stresses were also calculated, using a computer program developed previously (Gibson et al. 1971). This program was then modified to calculate the tensile stresses and combine them with the bending stresses. Combined tensile and bending stresses for the outer wires are shown in Table 4.4.

TABLE 4.4. Maximum and Minimum Combined Tensile and Bending Stresses in Outer Wires of 3-in. Diameter Test Ropes (D/d of 30)

Design Factor	Maximum Stress (psi)	Minimum Stress (psi)
10.0	71,859	-26,646
5.0	91,445	-7,060
3.3	110,030	12,525
2.5	117,867	32,110
2.0	150,201	51,696
1.7	169,786	71,281

For combined bending and tensile stress, the yield point of some outer wires is reached at loads of 30% to 40% of the UTS of the rope.

Bending stresses were also calculated for the 3/4-in. and 1-1/2-in. diameter test ropes. The bending stresses are comparable for the different rope diameters at D/d ratios of 30 and greater. Bending stresses as a function of D/d ratio for some test ropes are shown in Figure 4.9.

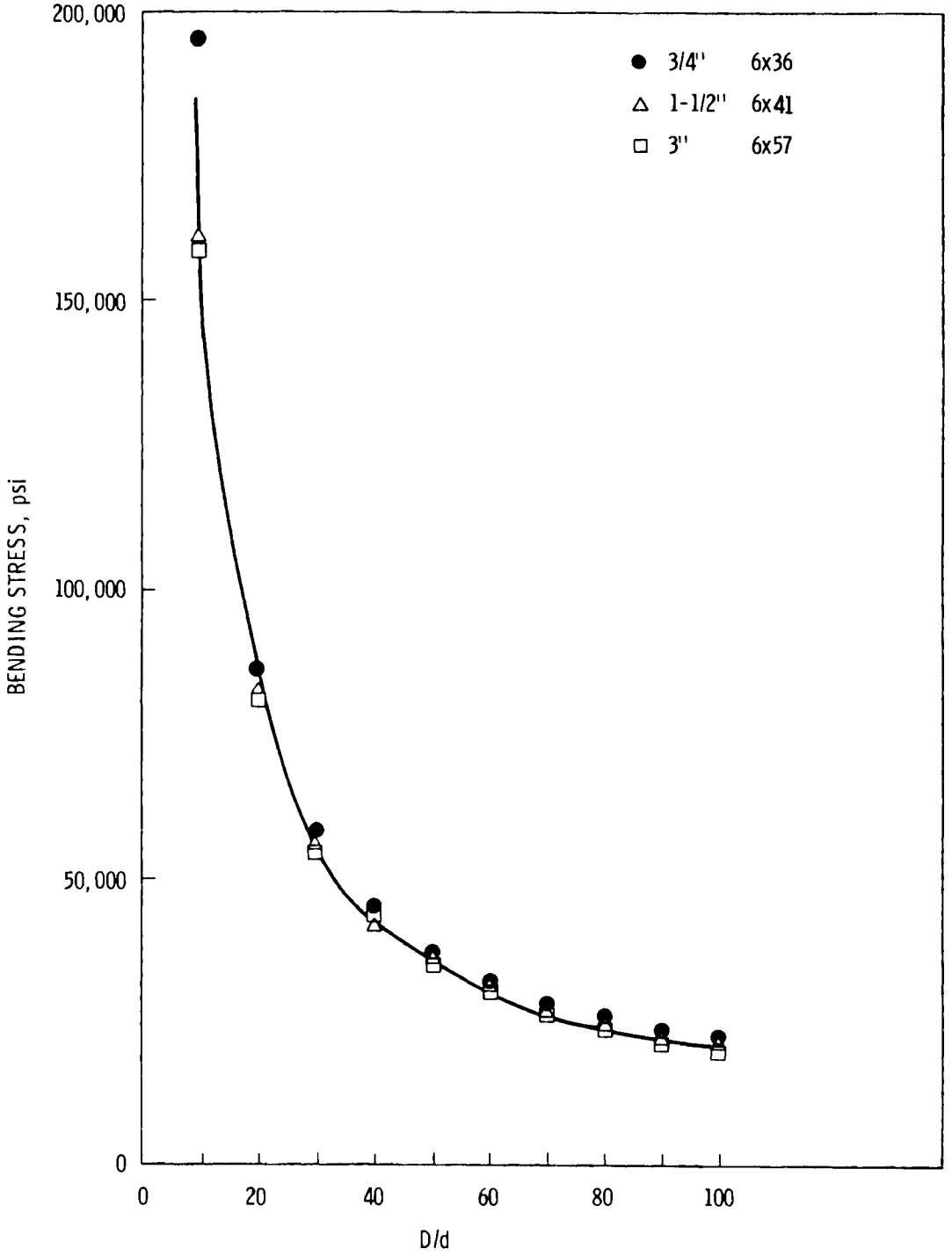

FIGURE 4.9. Bending Stresses as a Function of D/d Ratio

5.0 LABORATORY ROPE WEAR AND FAILURE ANALYSIS

The test ropes were examined to compare damage with that found previously in field ropes. An attempt was made to correlate damage with the test load. A total of 67 rope specimens from fatigue-tested ropes were examined for cracks, broken wires, and other visible damage.

5.1 WIRE WEAR

Wear patterns on the test ropes, illustrated in Figure 5.1, were very similar to those found in the field ropes (Beeman 1978), with only one difference. The outer wear of the test ropes was somewhat less than that of the field ropes, for two reasons. First, the sheaves on the test machine are made of mild steel, which causes little wear of the rope outer wires. Second, test methods and machine design prevent gross relative motion (sliding) between the rope and the sheave.

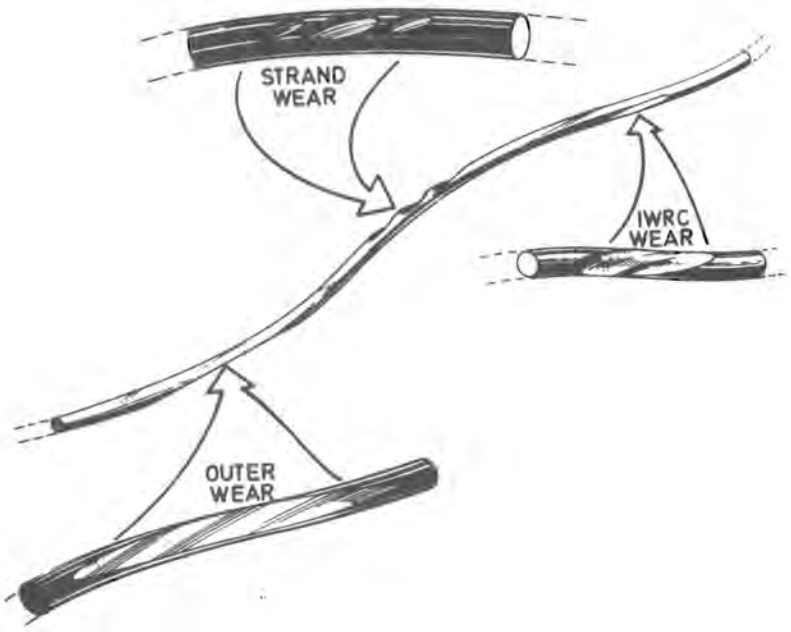

FIGURE 5.1. Wire Wear Patterns

Wear of outer wires for the test ropes from contact with the sheave was from 5% to 15% of the original diameter, depending on the number of cycles. Wear and deformation at points of contact with the IWRC ranged from 4% to 16% as the number of cycles increased. Interstrand contact wear and deformation varied from 1% to 5% as loads decreased and cycles increased.

5.2 WIRE CRACKING

Magnetic particle detection was used to examine individual wires for cracks. During previous testing at design factors of 3 and less, over 3000 wires were examined and only 7 cracks were found. During the testing phase at design factors of 4 and 5, more than 200 wires were examined and more than 40 cracks were found. The majority of these occurred in ropes tested at a design factor of 5.

A 6 x 37 class IWRC wire rope has over 250 individual wires of varying diameter, tensile strength, and carbon content. The wires are made from plain carbon steel in the range of AISI 1030 to 1080. The wires are severely cold-worked during drawing and have an ultimate tensile strength in the range of 220 to 280 ksi. In general, the higher strengths are associated with the greater carbon content; however, this may vary with different amounts of cold working. Core and filler wires are usually made from the lower carbon steel and are, therefore, softer and more ductile. The core and filler wires wear sacrificially with respect to the wires of the strand. Strand wires are made from the higher carbon steels and will fail in a ductile manner under normal conditions; however, if a crack is present, the wire fails in a brittle fashion. When a crack is present, very little energy is required to propagate the crack through the wire.

Examination of broken wires from the wire rope tests provided little evidence of progressive fatigue failures. It is felt that this is due to the high notch sensitivity of the wires. Any cracks that form propagate to failure in relatively few cycles. This is particularly true at the higher test loads. At the lower test loads the number of cycles to failure would be greater. This hypothesis is borne out by the fact that substantially more cracks were found in the wire of the ropes tested at low loads.

These cracks were observed to form at points of wire-to-wire contact. At these contact points, stresses are very high; the stress concentration promotes crack initiation.

Another cause of wire damage on exterior wires is rapid frictional heating. The involved areas can be raised to the austenization temperature in 10^{-3} to 10^{-4} seconds (Quinn 1962) and then quenched very rapidly. This process leads to the formation of a white layer, sometimes identified as an amorphous martensite. This white layer has been found on the outer wires of field ropes. The wire shown in Figure 5.2 had received severe surface wear due to scrubbing across the fairlead sheaves. Under these conditions, the formation of a white layer is quite common. To date, this layer has not been found in other wear areas of field or test ropes. Additional photomicrographs of wear on field and test ropes are shown in Figure 5.3. The white layer is extremely hard and brittle. Cracks form in this layer or at the interface with the metal matrix. Once the crack has formed, it commonly will grow through the wire in the next few cycles.

If the cracks are below the size at which they grow rapidly, they might be arrested or completely destroyed by the next cycle. This might come about by welding the crack shut or completely removing it through the adhesion wear process. Depending on the wire configuration and material properties, as well as the loading, cracks may be routinely neutralized during the wear process until some critical conditions are reached and the crack propagates through the wire. At low design factors this may be when a substantial amount of material has been worn away.

The ultimate tensile strength of the wires in a rope has been used as a measure of the rope's ability to resist bending fatigue. Tests on large-diameter rope have shown that, at the lowest design factors, rope with the highest UTS for the outer wires gave the best fatigue life. At the higher design factors the opposite is true. At the lower design factors the high UTS wires plastically deform less and therefore display better fatigue life. At the higher design factors the lower UTS wires have greater ductility and a tendency toward higher resistance to bending fatigue.

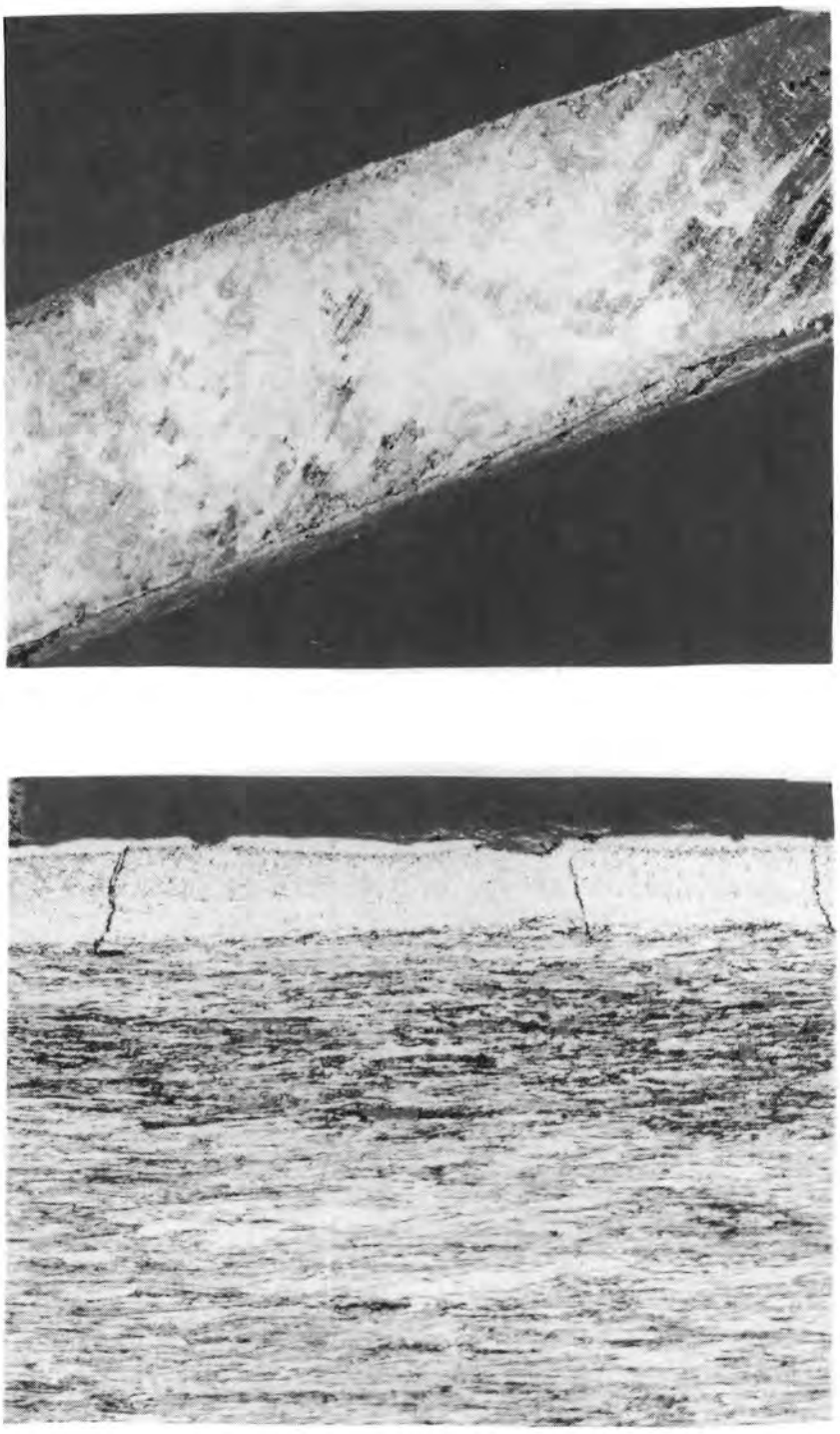

FIGURE 5.2. Martensite Formation on Field Rope Wire

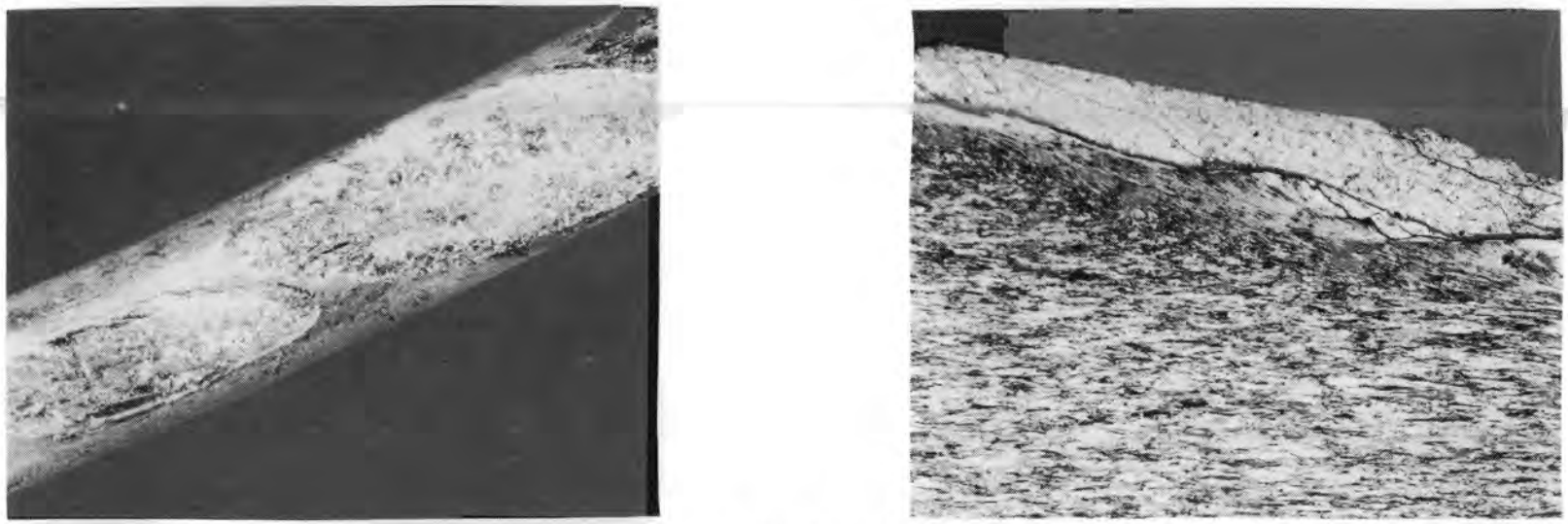

a. Wear Between IWRC and Strand Wire

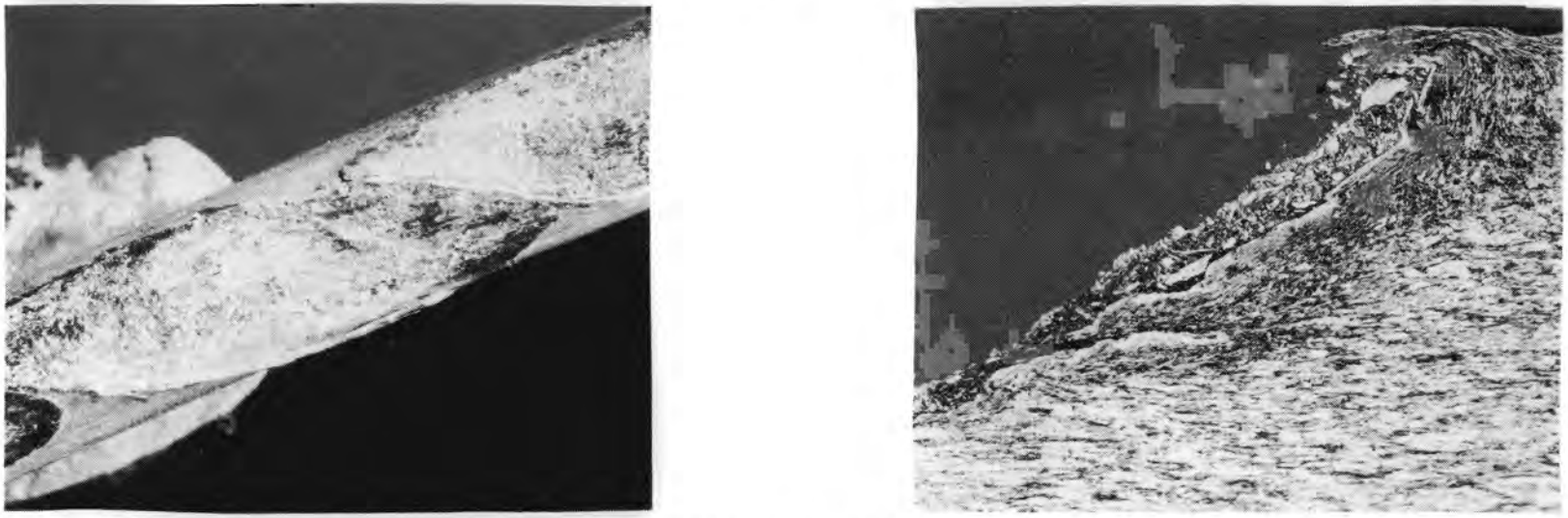

b. Wear Between Adjacent Strand Wires

FIGURE 5.3. Photomicrographs of Wear on Field Rope

Another important wire property is the hardness. The higher hardness wires exhibit better wear resistance and probably increased fatigue life because of less material loss. Figure 5.4 shows the hardness of the strand and IWRC wires in the large-diameter test rope. Figures 5.5, 5.6, and 5.7 show the corresponding values for the small-diameter test ropes.

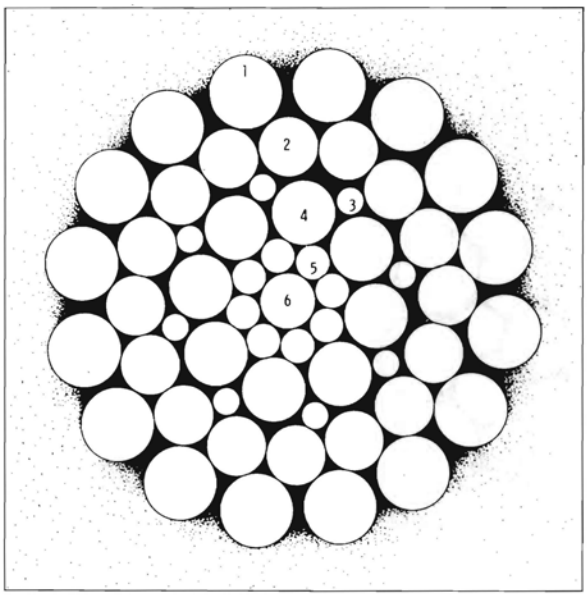

STRAND

INDENT #	DPH
1	440.0
2	526.6
3	495.0
4	500.3
5	536.6
6	482.0

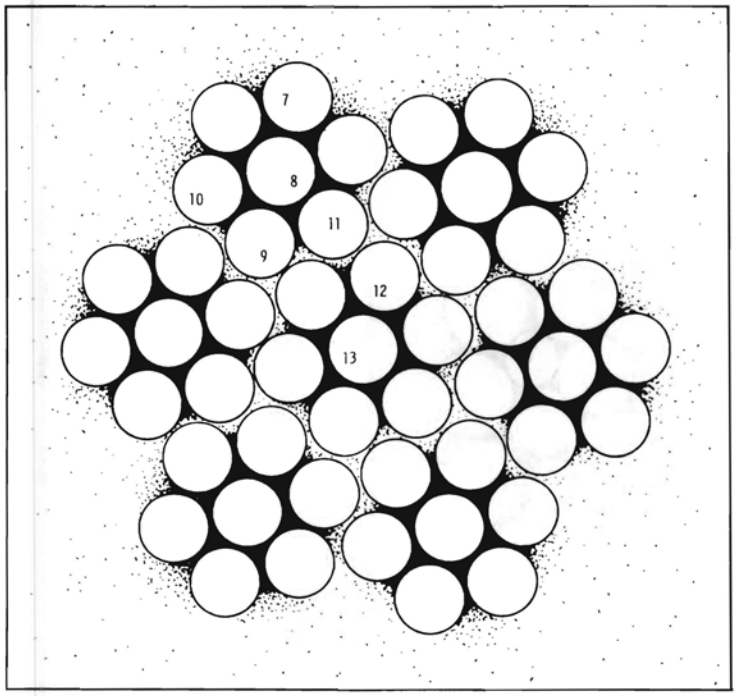

IWRC

INDENT #	DPH
7	339.3
8	330.6
9	439.3
10	336.0
11	354.0
12	321.0
13	384.0

FIGURE 5.4. Microhardness of 3-in. Diameter Test Wire Rope Wires (DPH 1 kg Load)

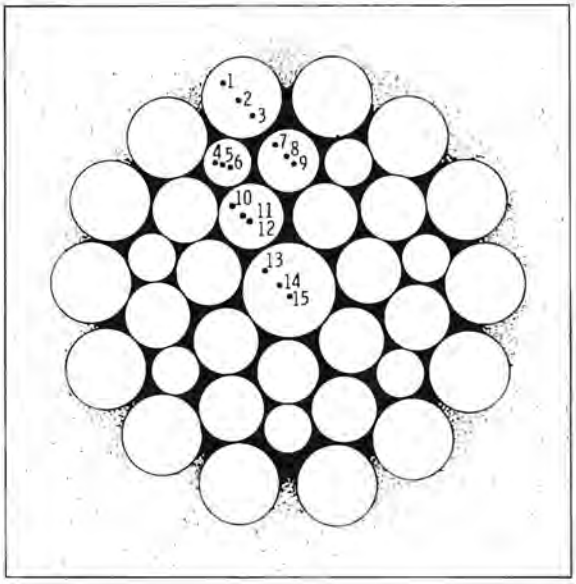

STRAND

INDENT #	DPH
1	481
2	502
3	497
4	569
5	533
6	510
7	498
8	519
9	540
10	538
11	542
12	542
13	544

6 x 36 construction

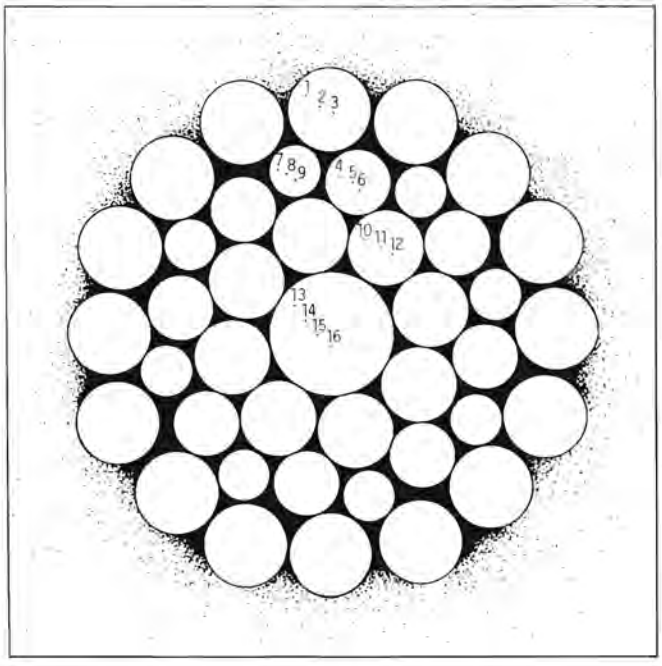

STRAND

INDENT #	DPH
1	529
2	517
3	482
4	527
5	519
6	481
7	604
8	587
9	555
10	529
11	510
12	470
13	498
14	495
15	466

6 x 41 construction

FIGURE 5.5. Microhardness of 3/4-in. Diameter Wire Rope Wires

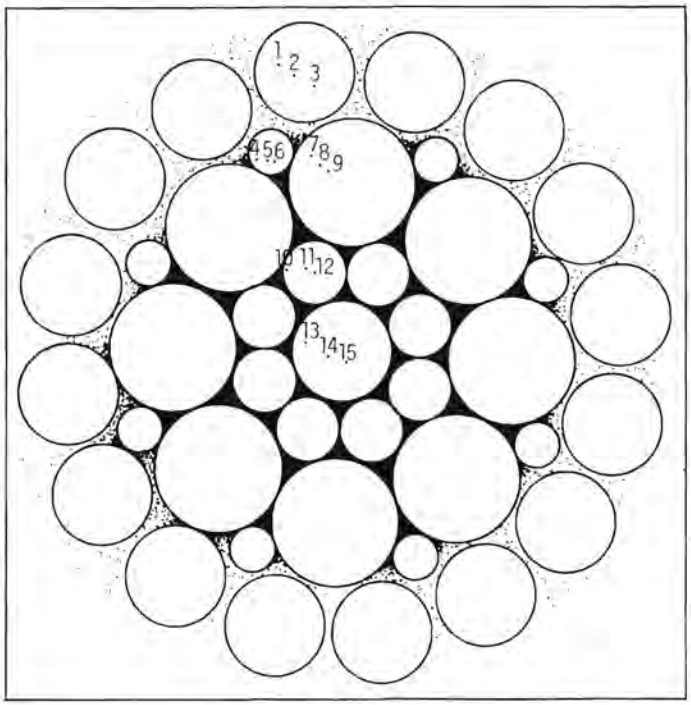

STRAND

INDENT #	DPH
1	540
2	527
3	498
4	613
5	613
6	583
7	573
8	557
9	553
10	563
11	565
12	567
13	519
14	505
15	469

6 x 41 construction

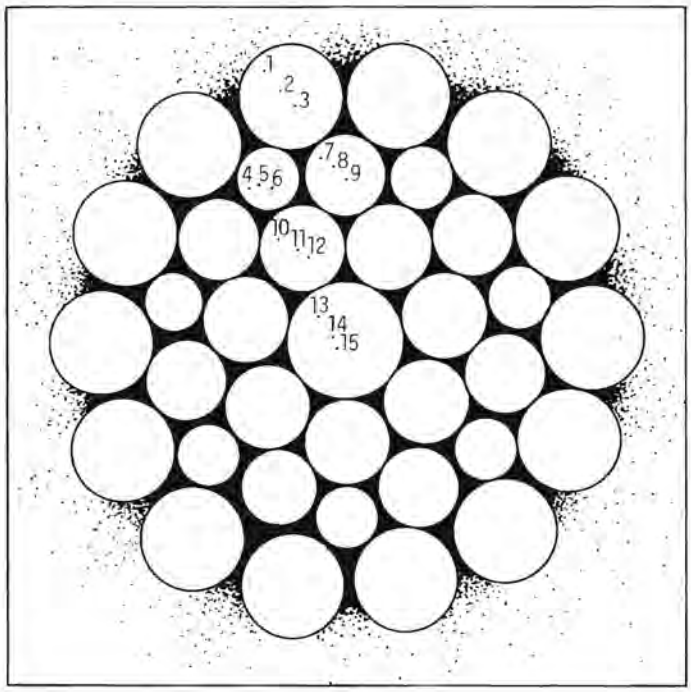

STRAND

INDENT #	DPH
1	540
2	538
3	495
4	573
5	546
6	561
7	507
8	490
9	492
10	476
11	487
12	490
13	476
14	464
15	478

6 x 41 construction

FIGURE 5.6. Microhardness of 1-1/2-in. Diameter Wire Rope Wires

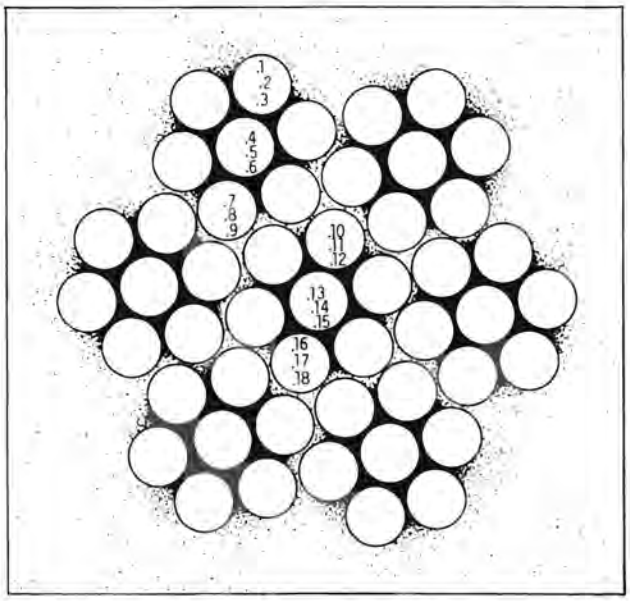

INDENT #	DPH
1	542
2	540
3	549
4	573
5	540
6	546
7	557
8	553
9	569
10	661
11	573
12	549
13	589
14	563
11	531
16	565
17	533
18	527

FIGURE 5.7. Typical Microhardness of Small-Diameter Wire Rope IWRC (DPH 1 kg Load)

6.0 LOAD SENSOR DEVELOPMENT

As part of the initial Wire Rope Improvement Program, a number of large-diameter wire ropes with IWRCs were tested in bend-over-sheave fatigue at loads approaching 50% of catalog breaking strength. The post-mortem examination of these ropes showed that the failure modes associated with very high loads were similar to failures noted in field ropes examined under the same program. This finding suggested that the loads, particularly for the drag ropes on operating draglines, were much higher than anticipated.

Rope loads on operating draglines are now estimated by measuring the drum winding motor current. This technique can be tuned to accurately indicate static rope loads but it is doubtful that it can respond to impulse loads caused by rope dynamics. These impulse loads are felt to be quite high and could account for the apparent high load failures and relatively short service lives of drag ropes.

6.1 OBJECTIVE

This task was undertaken to address the lack of data necessary to evaluate drag rope performance. The primary objective was to develop a load sensor capable of measuring impulse loads on an operating dragline.

6.2 SYSTEM TRADEOFFS

The data requirements were defined in discussions with the program manager, task leaders, and others interested in the load sensor data. The information required was judged to be a load/time history of the digging cycle of an operating dragline compiled over 4 to 6 hours during a typical work day. After the data requirements were established, a literature search was initiated to provide input to the evaluation of data acquisition methods. The available literature revealed nothing directly applicable to a dragline load sensor but contains a wealth of information concerning telemetry that could be useful in a general way.

Load sensor system requirements were established with several key considerations:

- Because the requirement is to measure in-service loads, the sensor must not alter the normal digging cycle of the dragline.
- To prevent attenuation of impulse signals, the response time of the complete unit must be several times that of the drag system.
- The installation, maintenance, operation, and removal of the sensor must have minimal effect on dragline operations.
- The installation must be extremely durable to survive in the dragline environment.

Several methods are available to measure loads in this kind of service. Three were given serious consideration.

- Attach strain gages to an existing piece of hardware to measure strain. This option was considered impractical for two reasons:
  - -- Strain gage installation in the field is time-consuming. Dragline downtime would be excessive.
  - -- The geometry of the existing hardware is complex. Therefore, interpretation would be difficult.
- Acquire a replacement part to be instrumented and calibrated in the laboratory and substituted into the drag system. This option was also rejected as impractical because:
  - -- with the exception of one of the pins, none of the existing pieces of hardware is easily replaceable. Again, dragline downtime would be excessive.
  - -- the mine operators perceive the pins to be the weakest part in the drag system, and expressed reluctance to allow an unknown pin to be used on their draglines.
- Fabricate a link of convenient shape and size and insert it into the drag string.

This latter option offered many advantages and was chosen for the load sensor for four reasons:

- The link could be used on any machine of the same relative size by providing new adapters. This would eliminate the need to fabricate and calibrate a new sensor for each application.
- The link could be designed to provide protection for all the instrumentation required making the load sensor one compact, self-contained unit.
- The installation and removal of a link could be effected very quickly, minimizing dragline downtime.
- A link can be of any size or shape and can, therefore, be made very durable to ensure survival.

Data transmission was addressed by proposing to use radio telemetry while searching for a viable alternative. To date, several methods have been given serious consideration.

The hardwired system was preferred because of its reliability and economy. It was judged unacceptable in this case because its installation would require machine downtime. Further, the probability of survival was very low without drastic modification of the digging cycle.

Several onboard data storage techniques were considered and subsequently rejected. Mechanical scratch gages were rejected due to lack of resolution and frequency response. Electronic data storage provides insufficient capacity for reasonable resolution. Tape recording systems have very low tolerance for vibration (0.5 g). All onboard storage schemes make correlation of the data and the digging cycle difficult.

Low frequency radio telemetry using the drag ropes as the transmission medium was evaluated. This technique has been used successfully in many applications. Data have been transmitted over power transmission lines for hundreds of miles using very low power levels. Test specimens have been used as part of the data transmission path in many experiments. Abundant evidence suggests that this technique is effective when the proposed transmission medium is electrically isolated. However, no documentation could be found to help predict its usefulness when the transmission medium is effectively a

ground plane as in the drag system of a large dragline. The technique is very attractive but was judged to require development at a mine site, an activity outside the scope of this task.

It was concluded that there is no viable alternative to radio telemetry. Different telemetry techniques (digital and pulse-code-modulated systems) were evaluated and, although there are advantages in terms of accuracy and reliability, PNL researchers determined that the increased cost of these systems was not warranted at this time. The system that was judged to best fit the application was the single-channel FM telemetry system shown in Figure 6.1.

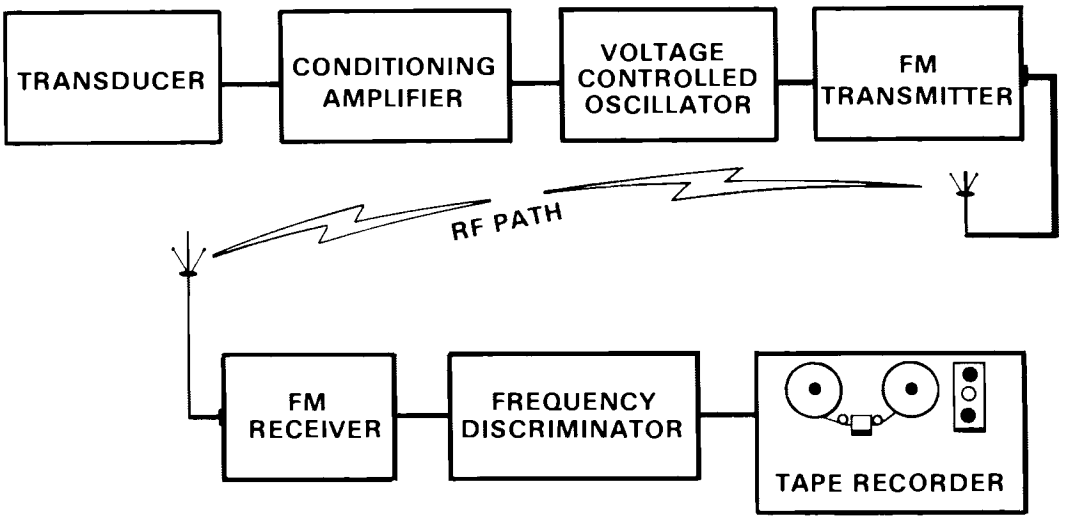

FIGURE 6.1. Single-Channel FM Telemetry System

6.3 FINAL SYSTEM DESIGN AND PROCUREMENT

The overall concept that evolved is shown in Figure 6.2. The elements of the system are a custom load-sensing link with a protected compartment housing a single-channel FM telemetry unit. Adapters are used to interface the link to existing dragline hardware. The remote receiver/discriminator produces an analog waveform that is stored on a data tape recorder.

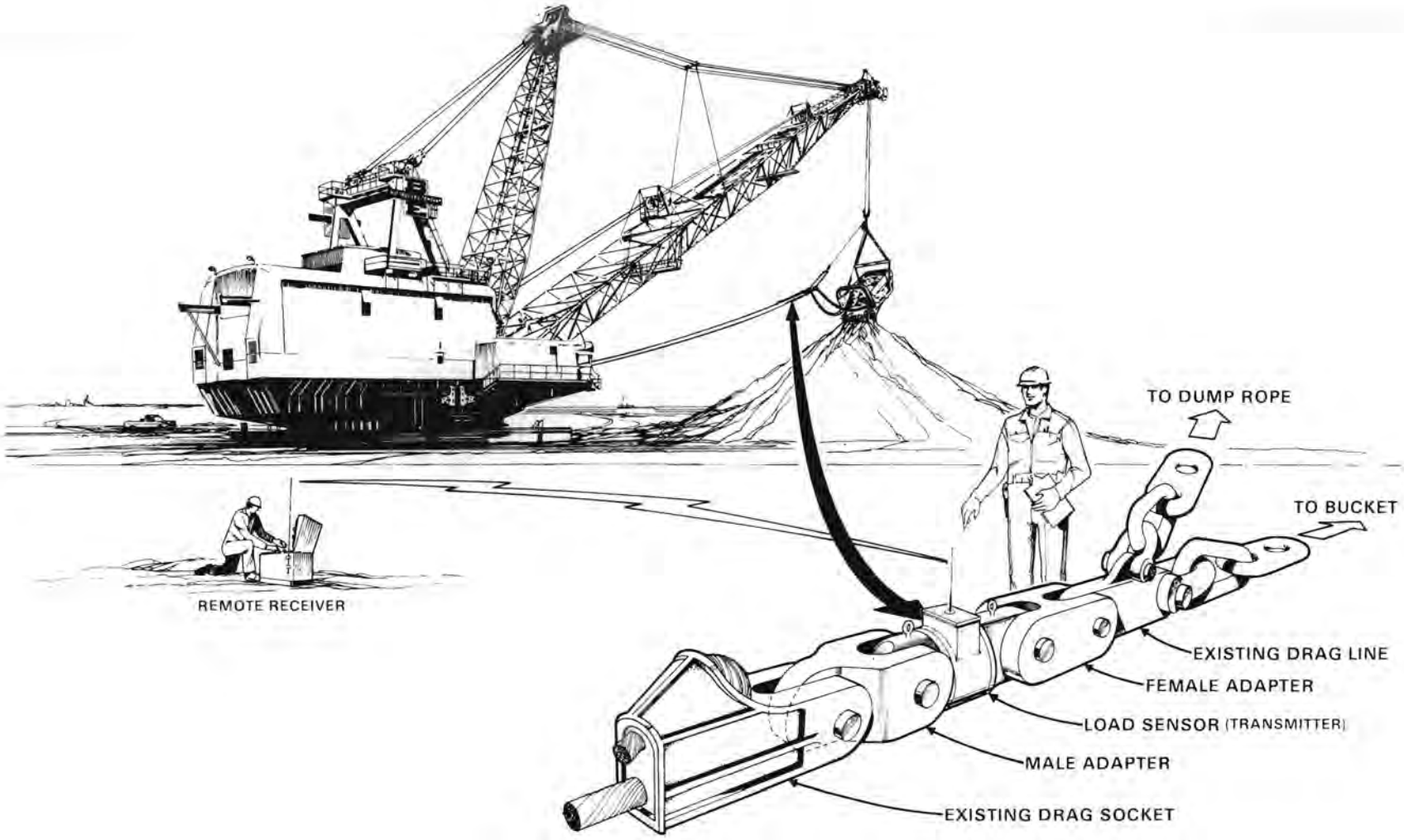

FIGURE 6.2. Dragline Load Sensor

Field verification and initial analysis of the data is performed using a waveform analyzer capable of storing and displaying the analog waveform and its frequency spectrum. This analyzer will provide data such as amplitudes and rise times of load impulses, frequency of their occurrence, and critical frequencies of the drag system.

Requirements for four major pieces of equipment were identified:

- a custom load link
- a telemetry system
- a data tape recorder
- a waveform analyzer.

The effort to write reasonable specifications for the load link and telemetry system was guided by a computer-aided analysis of the drag bucket system. This analysis utilized finite element techniques with the computer code ADINA to investigate the dynamic effect of various load/restraint conditions. This information was used to establish frequency response and optimal load range.

This kind of analysis is a promising tool that can be used to address other aspects of the Wire Rope Improvement Program. The development of the technique is explained in Appendix D.

A technical review of bids received in response to the specifications was used to select a vendor for the load link. After several iterations the configuration was finalized as shown in Figures 6.3 and 6.4. Two of these units were received early in FY80.

Several bids were received in response to the specification for the telemetry system. As expected, the bids included FM and pulse-code-modulated systems. Two transmitters and receivers were received in June 1980.

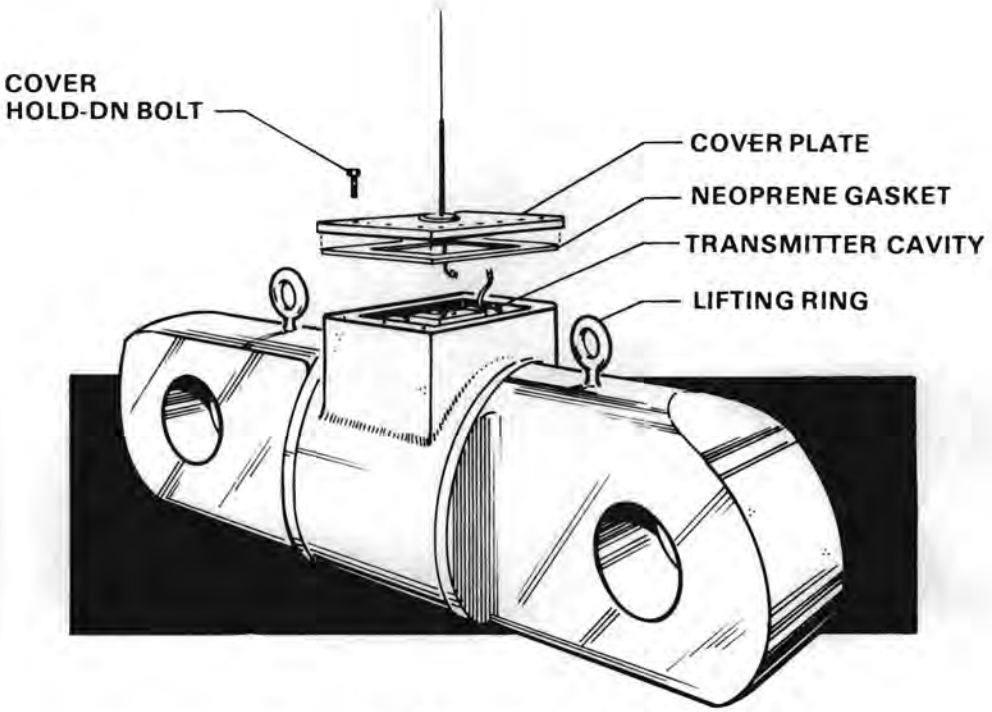

FIGURE 6.3. Load Link Detail

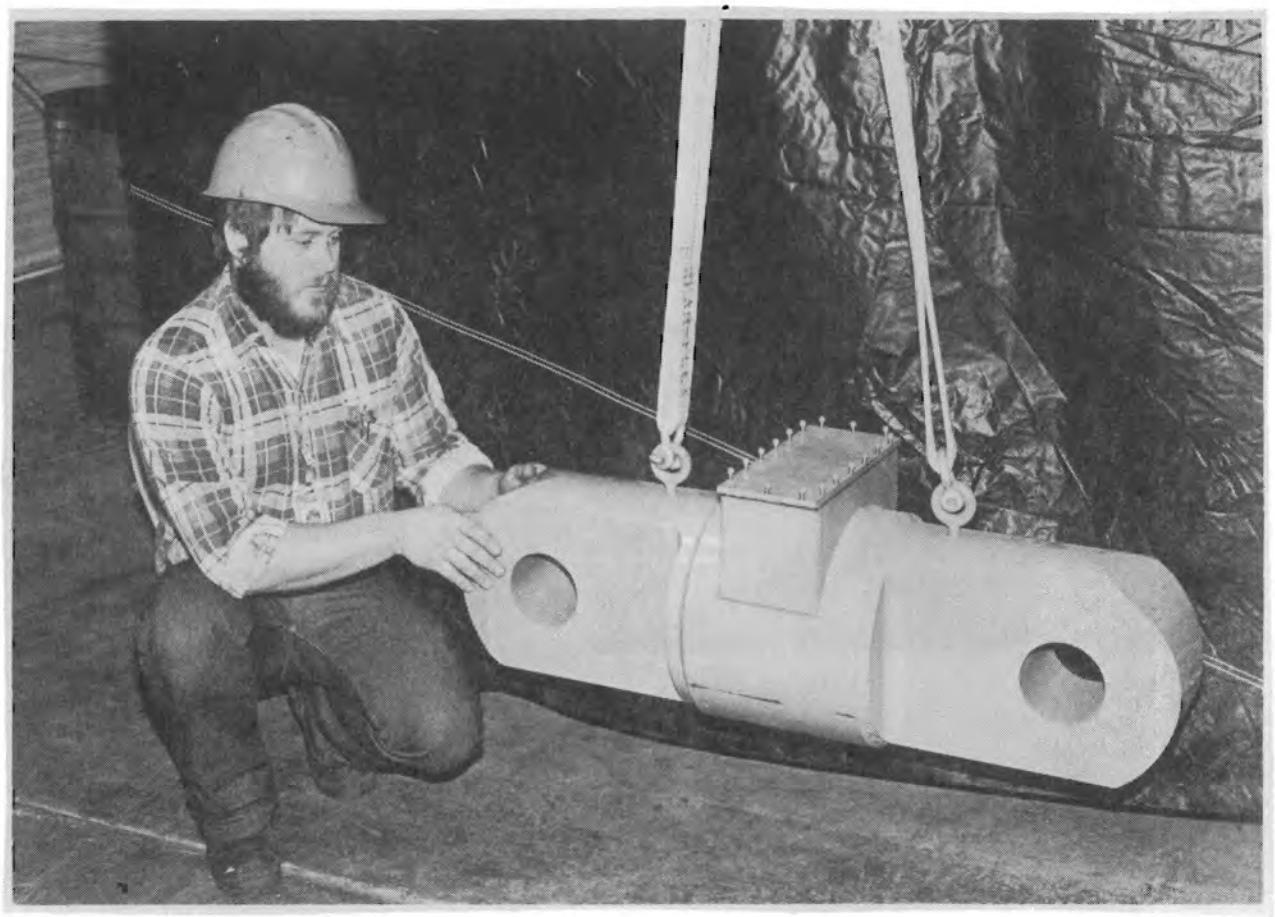

FIGURE 6.4. Load Sensor

7.0 TECHNOLOGY TRANSFER

Several major technology transfer efforts were undertaken as part of the FY79 Wire Rope Improvement Program. These included:

- providing information to the public sector
- writing and distributing technical information stemming from the project
- developing and conducting regional wire rope seminars
- sponsoring and conducting a national wire rope symposium
- producing motion pictures of draglines in operation to show rope dynamics, bucket position factors, and other operational considerations.

Each of these areas is described in this section.

7.1 LITERATURE AND PUBLIC INFORMATION

Throughout the year, requested information was provided to the public sector on a case-by-case basis. Many requests were dealt with by telephone or letter contact. The PNL staff visited a few sites to answer specific questions on wire rope technology. More than 200 copies of the PNL report, Factors Affecting the Service Life of Large Diameter Wire Rope, were disseminated during FY79. Typical requestors included rope manufacturers, mining engineers, industrial sales staff, mine operators, mining associations and college educators.

Early in FY79, a need for broadly documenting the program was identified. A six-page capabilities brochure was developed featuring the history of wire rope R&D needs, previous related research performed at PNL, planned R&D, and a technical explanation of the primary research methodology. Of the 500 brochures printed, approximately 300 were mailed or distributed at seminars to interested parties. The capabilities brochure has been an excellent technology transfer tool.

A six-page technical brief, "Bend-Over-Sheave Fatigue Testing of Large-Diameter Ropes Used in Surface Mining," was issued in April 1979. The brief was designed to present a technical summary of the Wire Rope Improvement Program's past history, R&D conclusions, and planned wire rope testing. The brief has been useful in answering inquiries from the wire rope technical community, especially for those who do not want or need the large report published in FY78 (Beeman 1978). The brief was also disseminated at conferences and seminars.

7.2 REGIONAL WIRE ROPE SEMINARS

Seminar development was a major technology transfer effort in FY79. Approximately 150 technical slides and descriptive narratives were prepared for presentation in 2-day seminars. One day was structured for mining operation personnel; the other day was aimed at the technical manager/supervisor.

For the mining operation personnel (dragline operator), the topics included:

- costs of changing wire ropes (draglines)
- rope properties
- rope construction
- rope classification
- rope design (including lay)
- rope damage
- sheave design
- rope diameter and sheave diameter ratios
- design factors of safety
- example of rope abuse and poor design
- lubrication
- rope R&D from PNL and others
- technology transfer.

Topics for the technical manager or supervisor (plant engineer or mine superintendent) included:

- cost of changing wire rope (draglines)
- brief discussion on construction, design, lay, etc.
- rope research conducted by PNL, BCL, and others
  - -- Drucker-Tachau factors
  - -- bend-over-sheave fatigue
- types of failure
- failure comparisons/rope testing
- rope damage analysis
- rope properties versus rope design
- sheave design
- case studies in rope wear, brittle fracture, etc.
- metallurgical examinations
- technology transfer
- how to reduce load on hoist ropes
- conclusions of PNL R&D and applications to state-of-the-art mining technology.

Four seminars were presented during FY79. Early in the year a training seminar for PNL staff was presented at Richland by PNL subcontractor Dr. Sam Gambrell from the University of Alabama. Dr. Gambrell also presented a mine operators' seminar in September 1979 on the University of Alabama campus.

The third seminar, a cooperative effort of PNL and the South Dakota School of Mines and Technology (SDSM&T), was held at Gillette, Wyoming. Gillette was chosen as an appropriate site because of the extensive local strip mining operations. SDSM&T provided the publicity, meeting plan and other organization tasks and, as cosponsor, lent additional credibility to the technical/mining

content of the seminar. Approximately 30 participants attended the seminar. The majority were from northeastern Wyoming; however, some representatives from North Dakota and Montana mines also participated.

The fourth seminar was presented during the April 1979 COSMET[a] meeting held in Kansas City, Missouri. This seminar was designed primarily for technical managers/supervisors. Special emphasis was placed on dragline hoist ropes and the improvement and/or reductions of hoist loads.

7.3 NATIONAL SYMPOSIUM

Planning, coordinating, and designing a national wire rope symposium began during FY79. The symposium was scheduled for March 1980 at Denver, Colorado. Washington State University (WSU) Engineering Extension Service, Pullman, Washington, was selected as the administrative organizer for the symposium. The university has a national reputation for such activities, with years of experience in symposium/conference management.

During FY79, abstracts were solicited, and the sessions and agenda were selected. Two publicity flyers were released and the meeting site/dates were arranged. Speakers, session chairmen, and a keynote speaker were also selected. The symposium sessions were to cover four general areas:

- simulated service and field experience
- stress analysis
- nondestructive examination and failure analysis
- rope design and manufacturing.

Approximately four presentations and/or papers were expected for each session; symposium proceedings will be published.

Washington State University reported that interest in the symposium was high. Registration fees covered all expenses associated with presenting the symposium. The symposium was conducted as scheduled and was attended by 160 people representing a good cross section of the mining industry, researchers,

---

(a) "Common Surface Mining Equipment Troubleshooting," a mining industry group that meets on a quarterly basis to share problems and solutions connected with excavation machinery, principally draglines.

and government agencies. The symposium was written up as a five-page feature article in Coal Mining and Processing (Sprouls 1980).

7.4 INFORMATION AND RESEARCH FILM

A motion picture of typical dragline coal mining operations was taken during the summer of 1979. Footage covered bucket operation under various conditions such as hard and soft overburden, wet overburden, varied rope load, varied drag and hoist distances, and bucket positions.

The film will be used to design a 15-minute general information film, a 30-minute or longer operator training film, and a 30-minute research film. The research film will be used to correlate, if possible, the operators' dragline workmanship with the dynamic loads caused by good or bad operating techniques. The footage has been recorded on video tape and shown to the host mine. It will be edited for use in future seminars.

8.0 RECOMMENDATIONS

Recommended actions for FY81 are described below for each major research area.

8.1 EXPERIMENTAL WORK

To further define the correlation of large- and small-diameter wire rope fatigue behavior, it is recommended that

- the investigation of the effects of sheave-groove hardness and size be continued
- the fatigue performance of rope wires be evaluated under controlled load and strain conditions
- the cumulative damage process in a wire rope be experimentally evaluated
- the long-life fatigue behavior of surface mining rope constructions be evaluated (on both small and large ropes)
- alternative rope constructions with small outer wires, such as 8 x 41, be investigated for superior fatigue resistance.

8.2 ANALYTICAL WORK

To further enhance abilities to correlate field and laboratory rope behavior, it is recommended that

- a dynamic analysis of drag rope loads be carried out
- the issue of a bucket position factor and its influence on hoist rope loads be studied further in conjunction with careful reviews of field films
- the overall stress analysis of wire ropes be continued
- the effects of wire fatigue properties and failure modes be incorporated into the bearing pressure ratio factor or a new damage parameter.

8.3 WEAR AND FAILURE ANALYSIS

To better understand the causes of failure in ropes subjected to severe wear, abrasion, and dynamic loads, it is recommended that a substantially expanded effort be undertaken in this area to define the role of wear and deformation in rope failures. Specifically, it is recommended that

- the detailed, destructive examination of laboratory and field ropes be continued, including optical and electron microscopy, metallographic examinations, and wear debris analyses, at an increased level of effort
- a preliminary model be formulated, relating the combined effects of wear, deformation, and fatigue on the ultimate retirement life of a wire rope
- the evaluation and development of nondestructive techniques be continued at an increased level of effort.

8.4 LOAD SENSOR

In regard to the load sensor development, it is recommended that

- additional sensors be procured
- sensors be installed on drag, hoist, and dump ropes on a working dragline(s)
- applicability of the system be investigated for operational use and development of an operational system begun if warranted.
- the system be employed in the field to obtain data on specific operational parameters.

8.5 TECHNOLOGY TRANSFER

Technology transfer activities should be continued and expanded in FY81. Specifically, it is recommended that

- a series of seminars be presented to mine operators in both the eastern and western U.S.

- the project sponsor a wire rope symposium in FY81. Presentations and papers would be solicited from three groups: rope manufacturers, equipment manufacturers, and mine operators. A call for papers would also be issued, with priority given to those dealing with operations and maintenance problem-solving.
- other activities, such as distributing literature, presenting films, and responding to written and verbal requests for information, be continued.

REFERENCES

Beeman, G. H. 1978. Factors Affecting the Service Life of Large-Diameter Wire Rope. PNL-2659, Pacific Northwest Laboratory, Richland, Washington.

Drucker, D. C., and H. Tachau. 1944. "A New Design Criteria for Wire Rope." Jour. Appl. Mech. A33-A38.

Gambrell, S. C. 1969. "Study of Low-Cycle Fatigue of Wire Rope." Wire and Wire Products. 127-130.

Gibson, P. T., et al. 1971. The Continuation of Analytical and Experimental Investigation of Aircraft Arresting Gear Purchase Cable. Battelle Columbus Laboratories, Columbus, Ohio.

Gibson, P. T., et al. 1974. A Study of Parameters that Influence Wire Rope Fatigue Life. Battelle Columbus Laboratories, Columbus, Ohio.

Hruska, F. H. 1951. "Calculation of Stresses in Wire Ropes." Wire.

Learmont, T. 1975. "Productivity Improvement in Large Stripping Machines." Transactions of the Society of Mining Engineers. 258:239-246.

Quinn, T. F. J. 1962. British Journal of Applied Physics. I:3,33.

Ramberg, W., and W. R. Osgood. 1943. "Description of Stress-Strain Curves by Three Parameters." NACA TN 902.

Sprouls, M. 1980. "Wire Rope: A Complex Machine." Coal Mining and Processing. 17(6):52-56.

VDI. 1968. VDI Guidelines for Lifting and Hauling. VDI 2358, published in Germany, English translation in NAVSHIPS Translation 1417.

Wire Rope Technical Board. 1979. Wire Rope Users Manual. Published jointly by the Committee of Wire Rope Producers and the Wire Rope Technical Board.

APPENDIX A

TENSILE TEST RESULTS ON ROPE WIRES

APPENDIX A

TENSILE TEST RESULTS ON ROPE WIRES

The results of tensile tests on rope wires are illustrated by Figures A.1 through A.5. The figures illustrate the typical log-linear strain-hardening behavior that most materials exhibit when subjected to a monotonically increasing load beyond the proportional limit. The slope of this log-linear curve is the Ramberg-Osgood value; the strain intercept at a stress of 1 ksi is the plastic strain coefficient. Part a. of each figure shows the standard stress-strain curve. In Part b., a logarithmic plot of stress versus plastic strain is given.

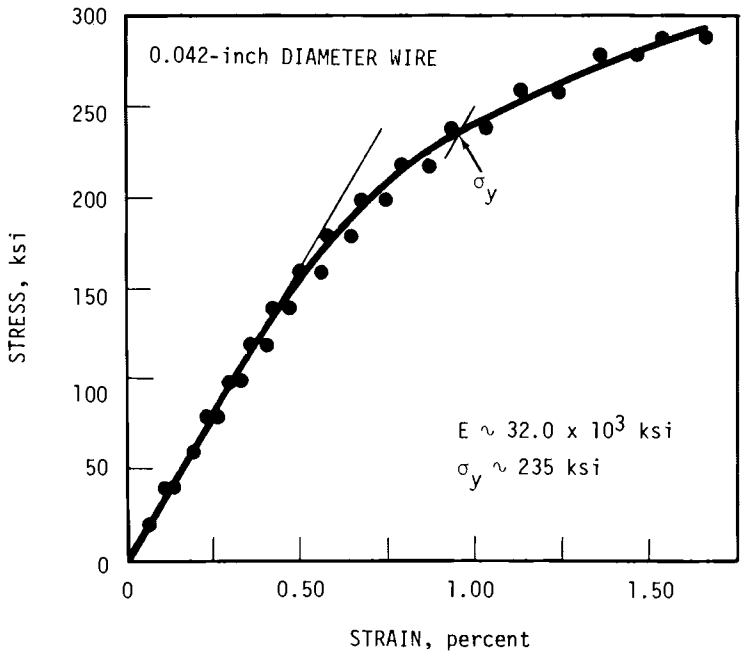

a. Stress-Strain Curve

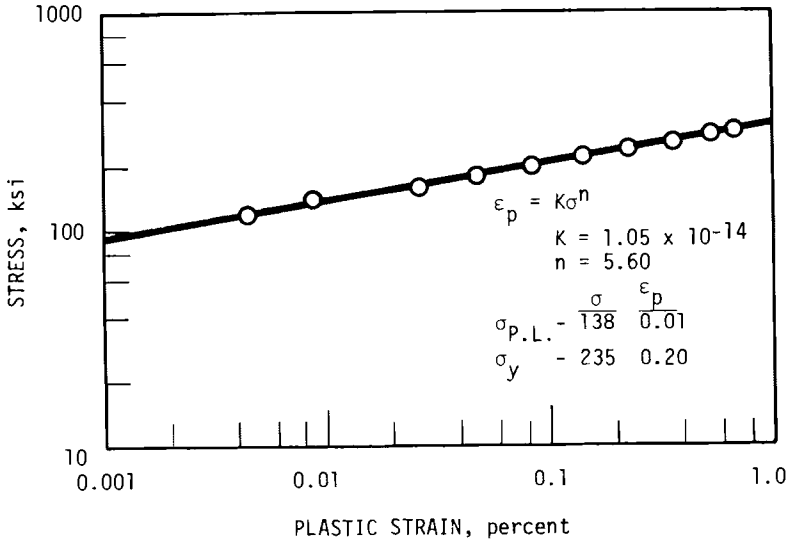

b. Stress-Plastic Strain Curve

FIGURE A.1. Wire Tensile Test Results for 0.042-in. Diameter Wire from 3/4-in. 6 x 36 WS Rope

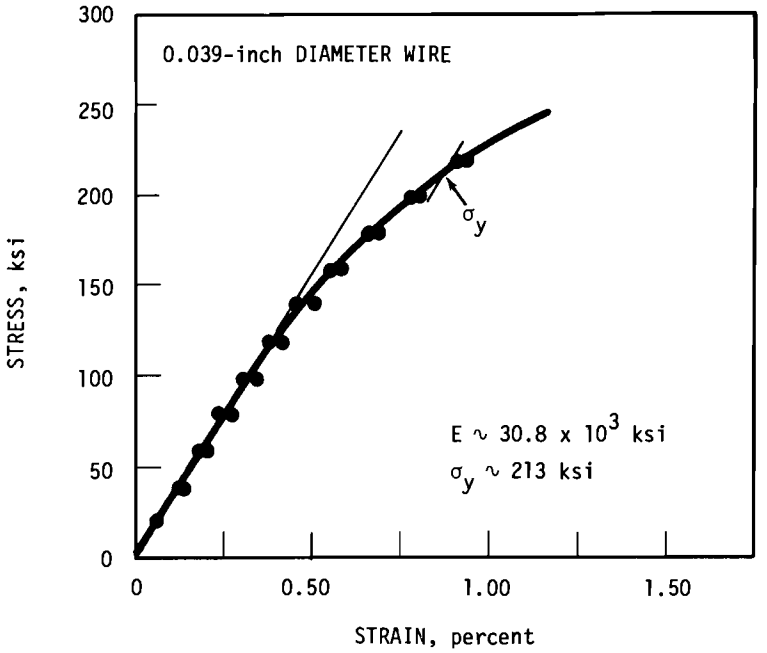

a. Stress-Strain Curve

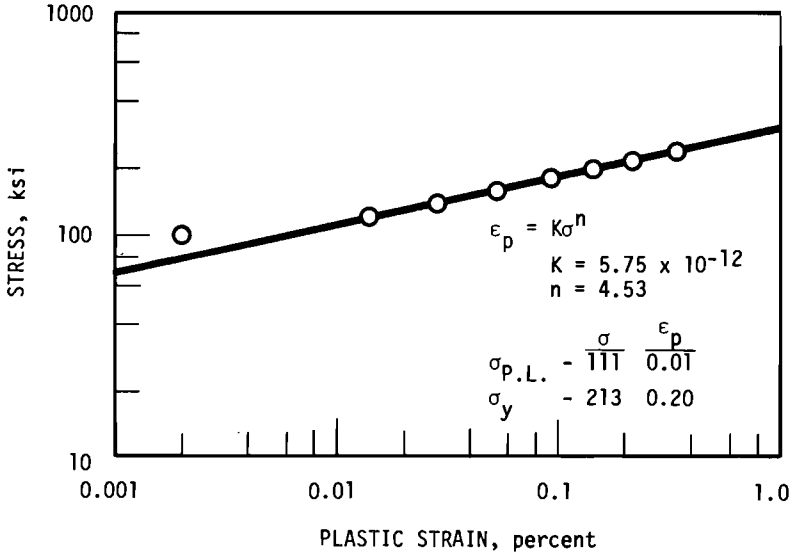

b. Stress-Plastic Strain Curve

FIGURE A.2. Wire Tensile Test Results for 0.039-in. Diameter Wire from 3/4-in. 6 x 41 FWS Rope

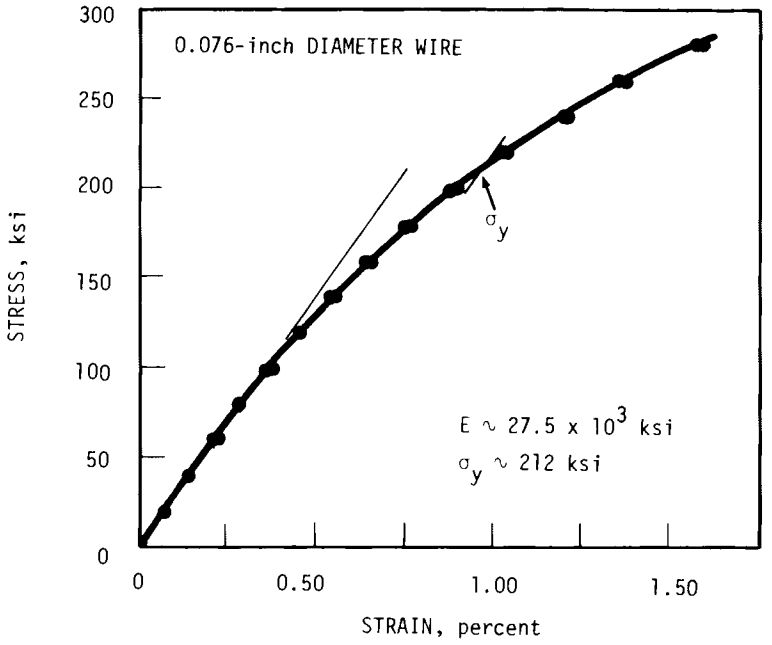

a. Stress-Strain Curve

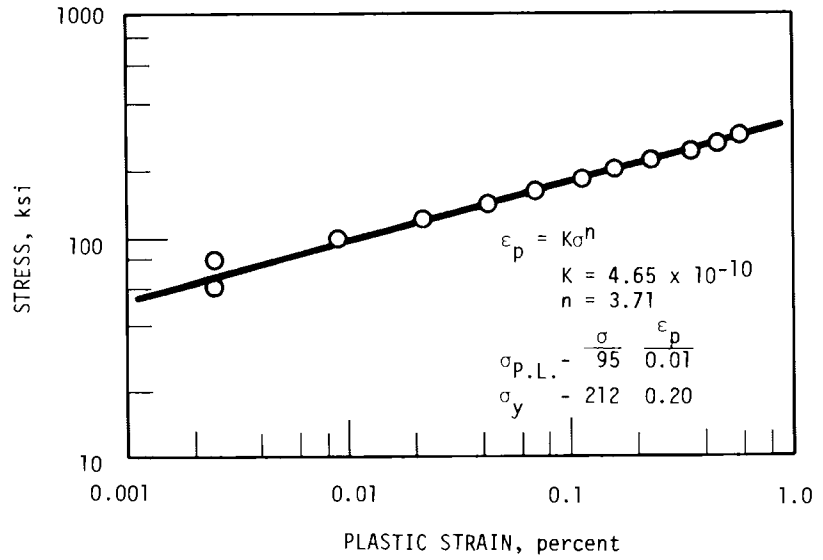

b. Stress-Plastic Strain Curve

FIGURE A.3. Wire Tensile Test Results for 0.076-in. Diameter Wire from 1-1/2-in. 6 x 41 WS Rope

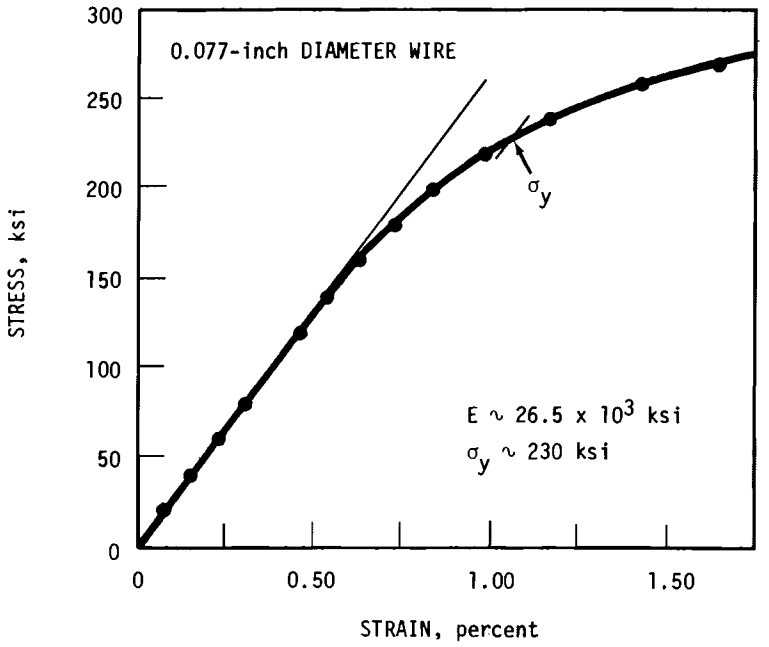

a. Stress-Strain Curve

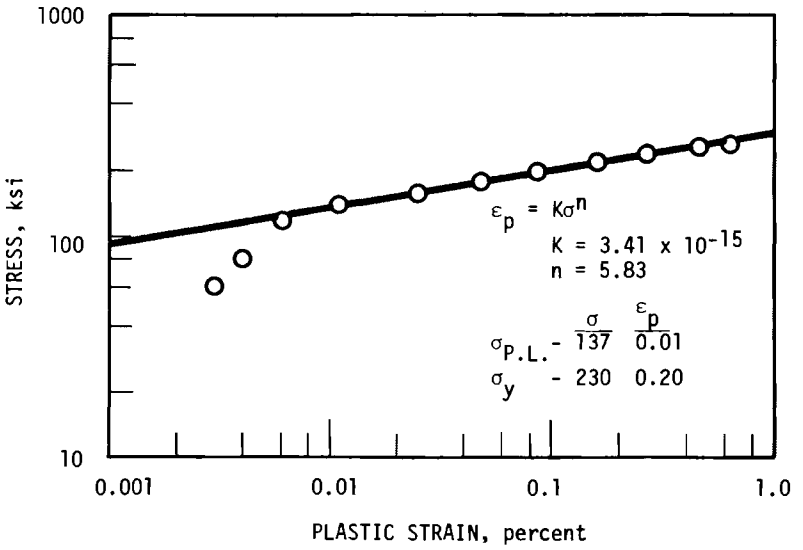

b. Stress-Plastic Strain Curve

FIGURE A.4. Wire Tensile Test Results for 0.077-in. Diameter Wire from 1-1/2-in. 6 x 41 FWS Rope

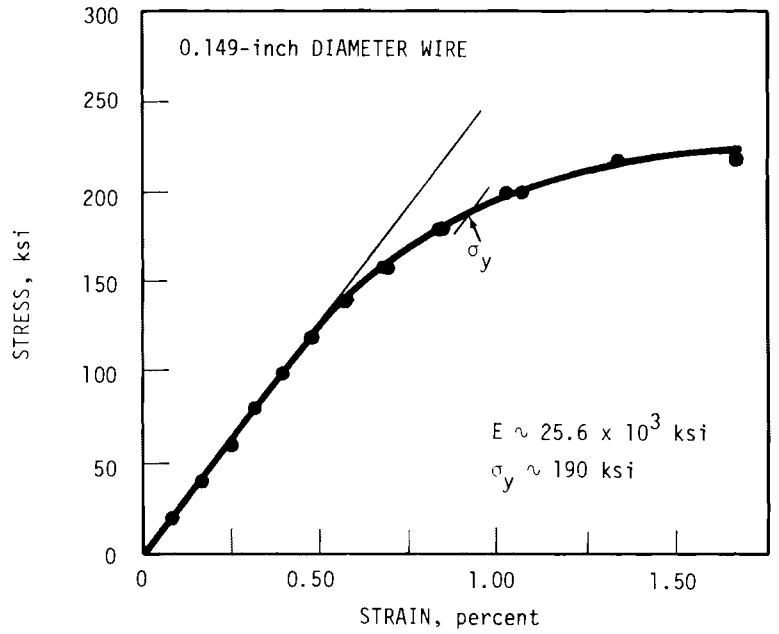

a. Stress-Strain Curve

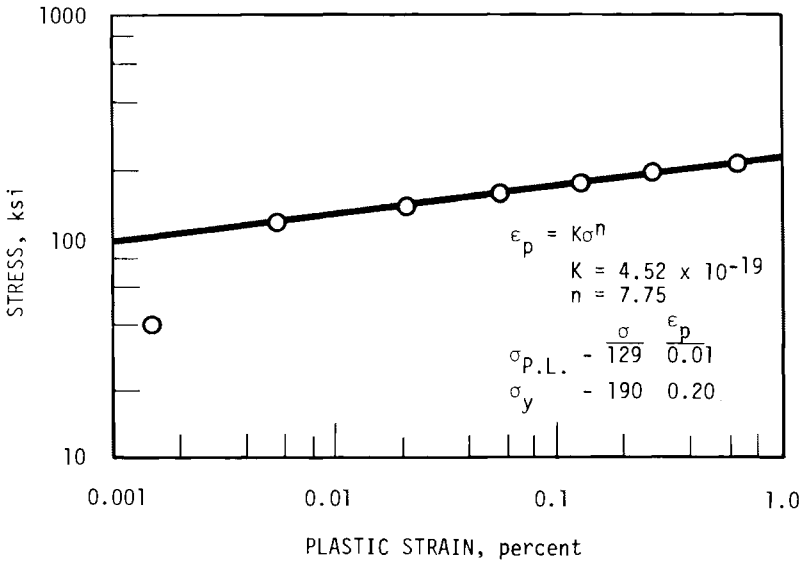

b. Stress-Plastic Strain Curve

FIGURE A.5. Wire Tensile Test Results for 0.149-in. Diameter Wire from 3-in. 6 x 57 FWS Rope

APPENDIX B

LIMITATIONS OF THE BEARING PRESSURE RATIO FACTOR

APPENDIX B

LIMITATIONS OF THE BEARING PRESSURE RATIO FACTOR

The use of the bearing pressure ratio concept for correlating large- and small-diameter wire ropes has been shown to have value for a limited range of fatigue lives and corresponding rope tensions and D/d ratios. The limitations of the bearing pressure ratio concept are illustrated in Figure B.1, where a plot of rope tension versus D/d is presented along with lines radiating from the origin. These lines represent lines of constant bearing pressure ratio and, therefore, should represent constant life lines. Obviously, however, there are physical limitations to the range of usefulness of B for a given rope size and strength. As tension increases toward the breaking strength of the rope, it does not matter how large a sheave is used, the rope will fail in a relatively few cycles. This is shown in Figure B.2 for a 3/4-in. rope construction (solid lines). The dashed lines were approximated from a German publication[(a)] where data for an extensive range of D/d and load levels were presented. It is obvious from Figure B.2 that the constant life lines predicted by B do not correspond with reality for very high and low loads. It must be remembered that this breakdown in the usefulness of B occurred for a single rope diameter, looking only at rope tension and D/d as variables. The range of applicability of B for different rope diameters (as it is now defined) may be even more limited.

(a) VDI. 1968. VDI Guidelines for Lifting and Hauling, VDI 2358, trans. NAVSHIPS Translation 1417.

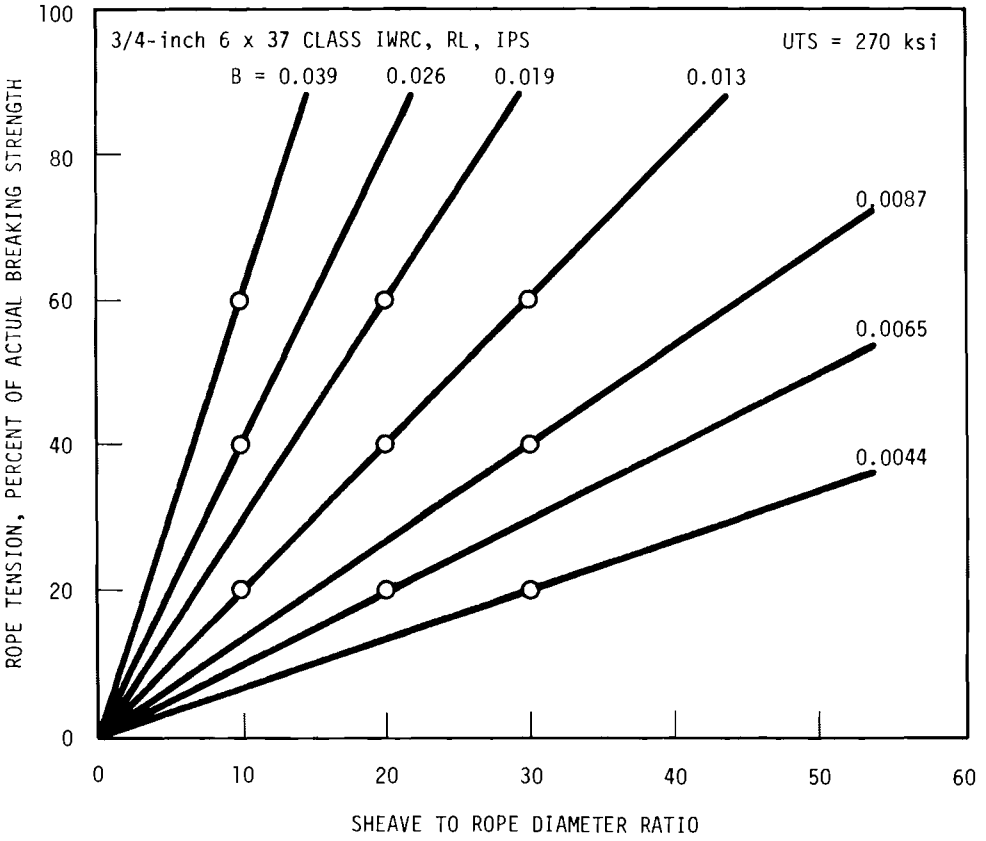

FIGURE B.1. Constant Life Lines Predicted According to the Bearing Pressure Ratio Concept

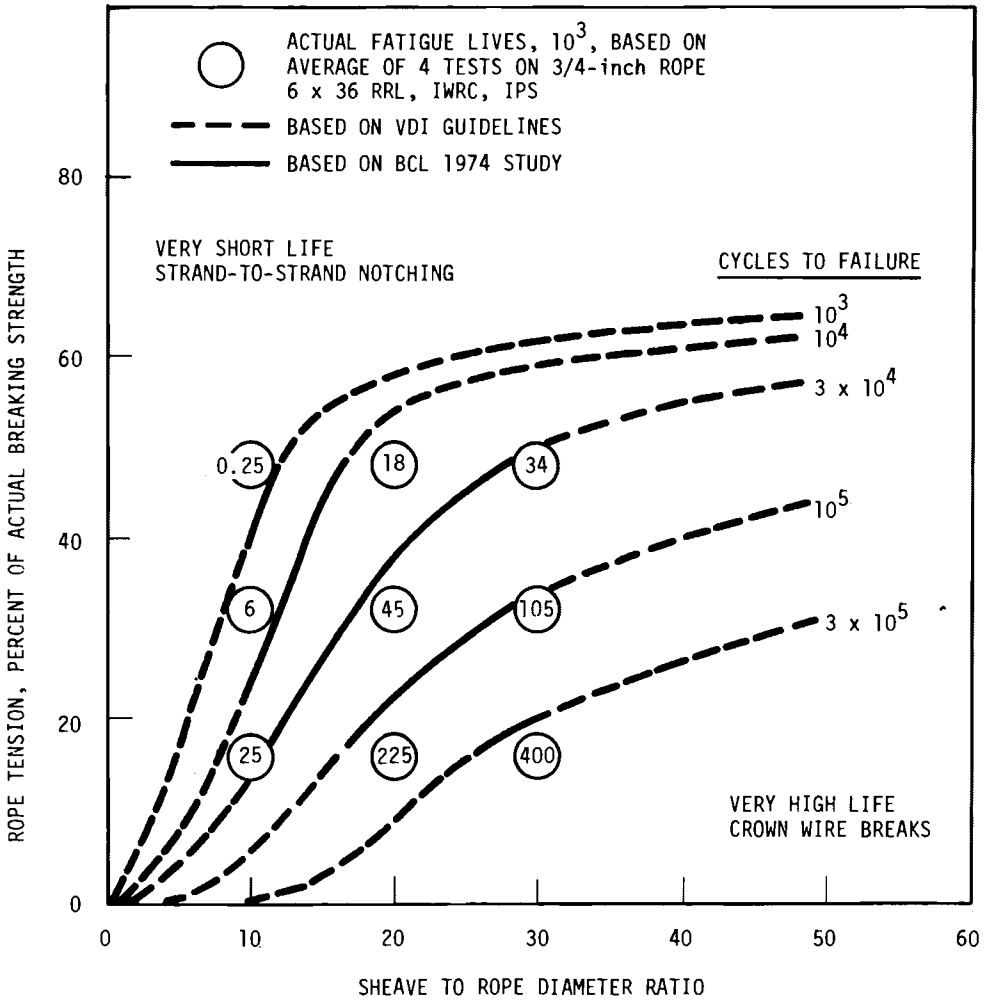

FIGURE B.2. Life Trends for a 3/4-in. Diameter Regular Lay Wire Rope

APPENDIX C

THE BUCKET POSITION FACTOR FOR SURFACE MINING DRAGLINES

APPENDIX C

THE BUCKET POSITION FACTOR FOR SURFACE MINING DRAGLINES

Some very interesting work has recently been initiated[a] on the concept of a bucket position, or load magnification, factor for surface mining draglines. The concept is illustrated in Figure C.1. A dragline bucket is pulled by a set of drag ropes and lifted by a set of hoist ropes. A static analysis of forces indicates that the weight of the suspended bucket must be counteracted by the combined vertical components of forces in the drag and hoist ropes. The horizontal components of force between the drag and hoist ropes must also be balanced in a static analysis. Using these known conditions, it is possible to compute the ratio of hoist rope tension to bucket weight as a function of drag rope angle and hoist rope angle. (The computation ignores rope weight and rope deviation from a straight line.) This ratio has been termed the bucket position factor or the load magnification factor. Figure C.2[b] illustrates the combinations of hoist and drag rope angles which lead to a variety of load magnification factors.

(a) This work was described by W.E. Anderson in his presentation, "Fatigue of Running Ropes," given at a COSMET Meeting, Kansas City, Missouri, April 19, 1979.

(b) Figure C.2 is based on a similar diagram received from Trevor Davidson of Bucyrus Erie, Milwaukee, Wisconsin on May 23, 1979.

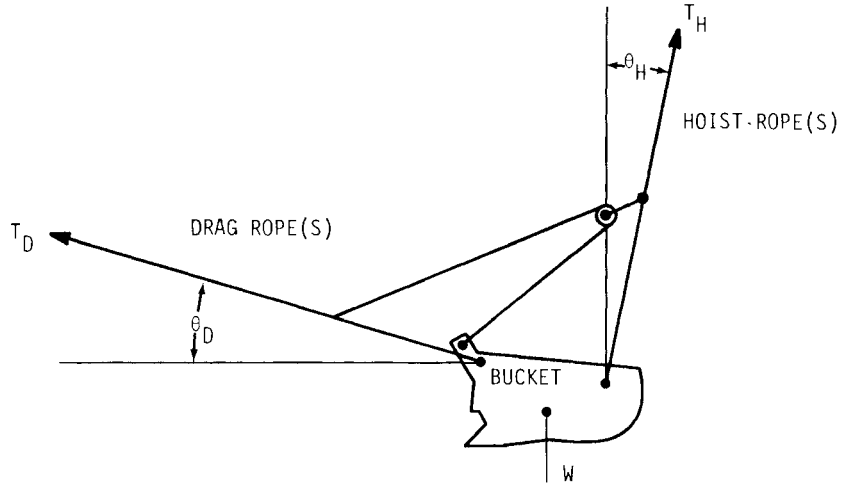

Σ OF HORIZONTAL FORCES: $T_D \cos \theta_D = T_D \sin \theta_H$

Σ OF VERTICAL FORCES: $W = T_H \cos \theta_H + T_D \sin \theta_D$

$$T_H = \frac{W - T_D \sin \theta_D}{\cos \theta_H} \quad \text{AND} \quad \frac{T_H}{W} = \frac{1}{\cos \theta_H - \sin \theta_H \tan \theta_D}$$

T_H/W = BUCKET POSITION FACTOR

FIGURE C.1. Free Body Diagram of Forces in Dragline Hoist and Drag Ropes

T_H/W = LOAD MAGNIFICATION FACTOR ON HOIST ROPE

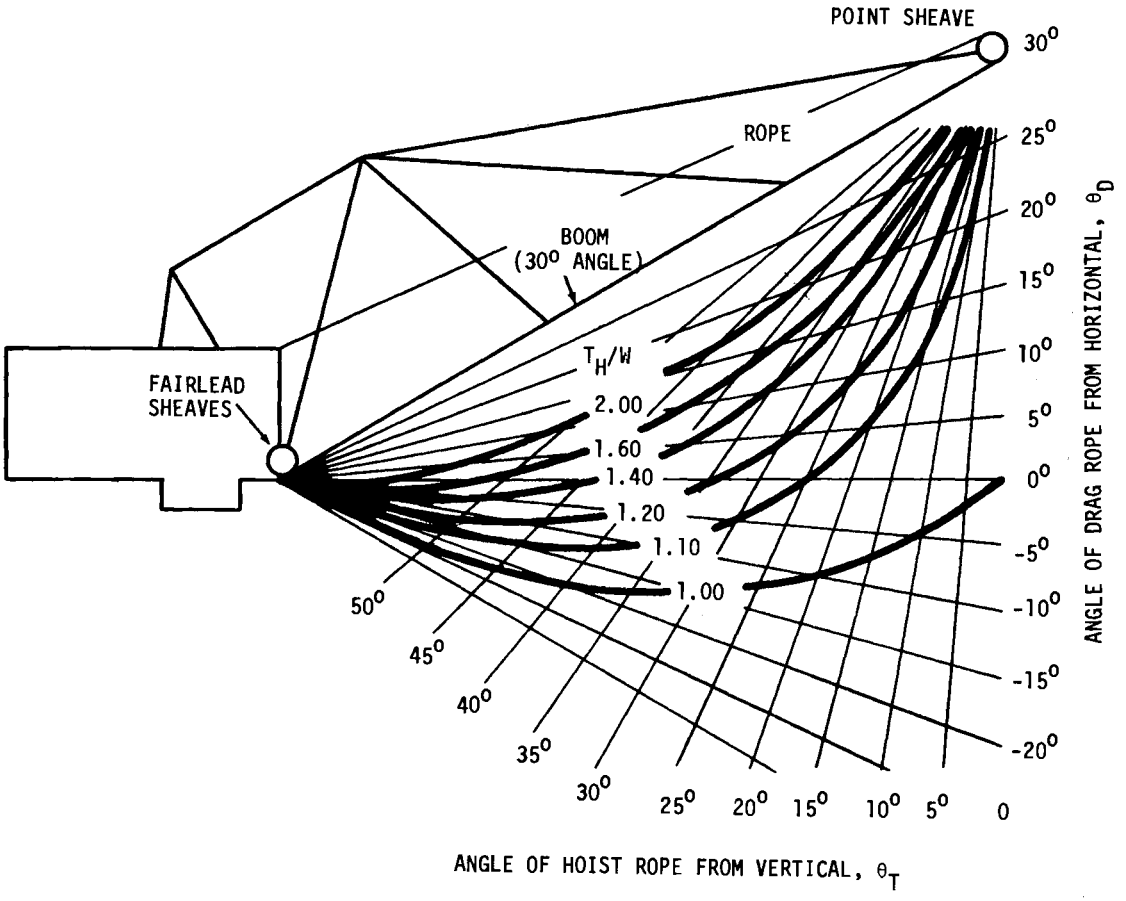

FIGURE C.2. The Effect of Bucket Position on Hoist Rope Tension

APPENDIX D

COMPUTER ANALYSIS

APPENDIX D

COMPUTER ANALYSIS

To analyze the failure of the large diameter wire ropes used in the draglines, the stresses in the ropes due to operational loadings must be known. To be meaningful, the calculation of the stresses must take into account the dynamic behavior of the system. Therefore, to complement the load sensor experimental work, a finite element analysis of the dynamic behavior of the dragline ropes was proposed. During FY79, to prove the validity of using large displacement, dynamic finite element techniques for analyzing wire rope behavior, several models were run. This study showed that good agreement could be obtained between the finite element models and theory for both static and dynamic problems.

SELECTION OF COMPUTER CODE

It was decided that the best approach would be to use an existing finite element code to perform the analyses. Of several general purpose finite element programs capable of modeling large displacement, dynamic behavior of cable-like structures, ADINA (Bathe 1976) was selected after an initial screening because of its efficiency and usability. However, because ADINA is a general purpose nonlinear finite element program, not written specifically for cable type problems, it was necessary to investigate its capabilities along these lines. Therefore, a series of benchmark problems was selected to establish its capabilities. A discussion of these benchmark problems follows.

Nonlinear Static Stiffness of a Catenary Cable

Two aspects of static catenary cable phenomena were studied. First, the classical catenary solution for the static position of a cable loaded under both tension and its weight was duplicated by an ADINA finite element model. Two methods were used. When the initial nodal locations were input at the approximate catenary solution under weight and tension, convergence of the ADINA solution followed readily. However, when a straight cable under tension

was started with zero loading and loaded incrementally with its weight, extremely small increments in loading were required, i.e., it was prohibitively expensive. In all subsequent models, the approximate catenary position was input initially to start the problem and convergence was much quicker.

The second aspect concerns the stiffness of a catenary cable to changes in horizontal end load. Felippa (1974) and Campbell (1970) have presented theoretical approaches to modeling cable responses in which the force-deflection relation is a function of the geometry, elasticity, and axial load. To evaluate the behavior of the nonlinear ADINA truss element, an eight-element single-cable model was loaded horizontally in incremental stages (ΔH) and the corresponding changes in horizontal displacement (ΔL) and sag (d_0-d_1) were noted. Figure D.1 depicts the geometry where L_o is the original length, d_0 the original sag, and H_o the initial horizontal tension. The response is shown in Figure D.2. Convergence required that the maximum incremental nodal displacement not exceed 0.65% of the element length.

The stiffness of the cable is highly nonlinear. Several asymptotic relationships are noted. First, for low tension and large sag, the cable stiffness approaches zero. For high tension and low sag the cable stiffness approaches that of an axial member in tension. The ADINA model results agree within 1.6% with the analytic results of Campbell (1970).

Mode Shapes and Natural Frequencies of Single Catenary Cables

Smith and Vincent (1950), Shears (1968), and Irvine and Caughey (1974) developed similar nondimensional transcendental equations for the vibrational eigenvalues of cables that use a nondimensional parameter as a measure of the tautness and elasticity of a given cable. In exploring the influence of this cable parameter upon the equations of motion, Irvine resolved a 300% discrepancy between the solutions to two very similar problems.

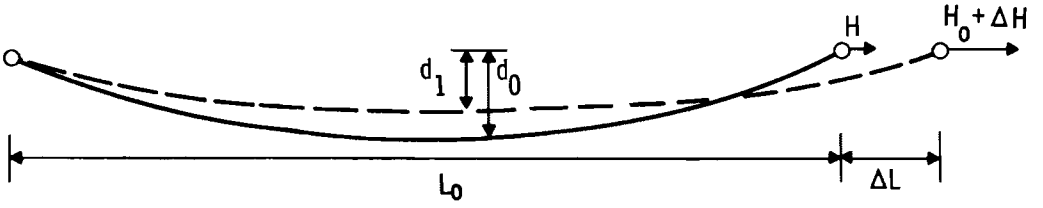

FIGURE D.1. Static Catenary Geometry

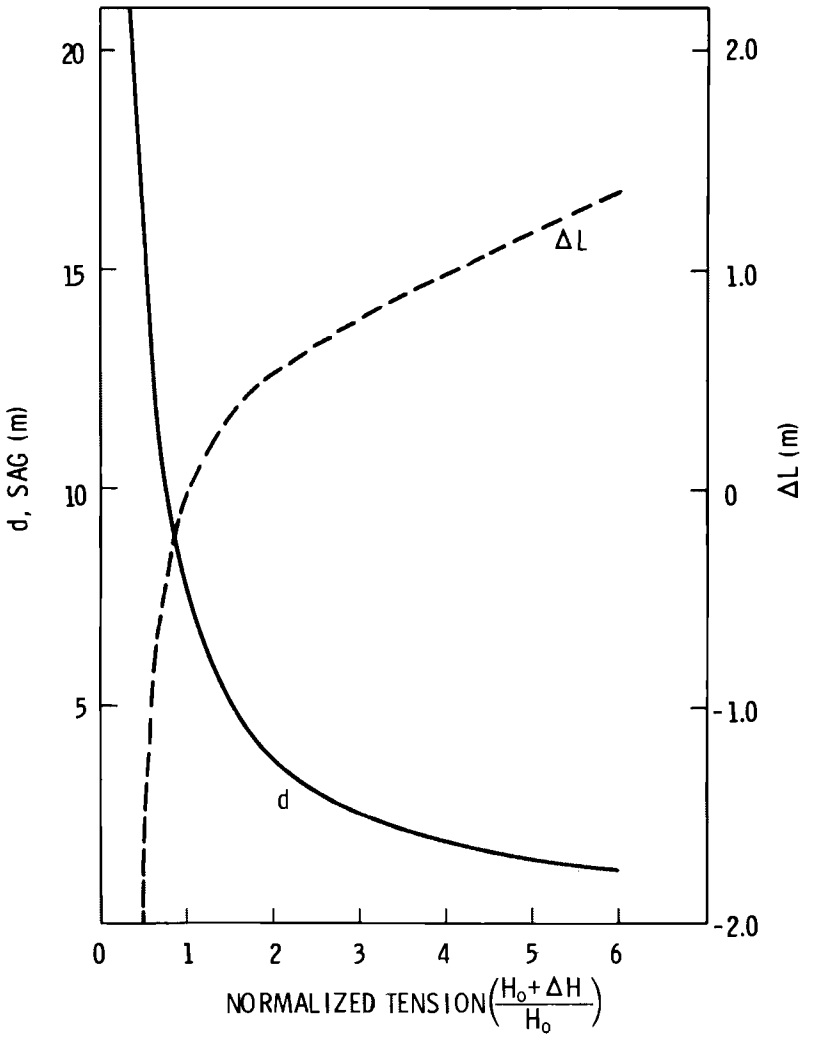

FIGURE D.2. Static Catenary Response

1. For an inextensible string of very small sag-to-span ratio, the lowest symmetric in-plane mode natural frequency is given by the first root of

$$\tan (1/2\ \beta L) = 1/2\ \beta L$$

$$\beta L \cong 2.86\pi$$

2. For an inextensible straight string, the lowest symmetric in-plane mode natural frequency is given by the first root of

$$\cos (1/2\ \beta L) = 0$$

or

$$\beta L = \pi$$

where

$\beta = (m\ w^2/H)^{1/2}$

m = mass per unit length

w = natural circular frequency

H = horizontal tension

L = span.

The conclusion is that the correct merging of solutions to the two problems can occur only by disposing of the assumption of inextensibility and recognizing elastic effects.

Irvine and Caughey (1974) and Smith and Vincent (1950) presented theoretical solutions for the frequencies and mode shapes of horizontal chord cables whose sag-to-span ratio was about 10% or less. This permitted use of the standard assumption that the shape of the cable between horizontally equal supports was parabolic. Shears (1968) included inclination of cables in his formulation. To test the nonlinear finite element program as a means of analyzing conductors, a single cable was modeled in vibration and the results compared with theory. The same cable data were used as in the static stiffness analysis. This line has a sag-to-span ratio of 2.45% and a value for Irvine's cable parameter

$$\lambda^2 = 64\left(\frac{d}{L}\right)^2 \left(\frac{L}{L_e}\right)\left(\frac{AE}{H}\right) = 66$$

where

$L_e = L\left[1 + 8\left(\frac{d}{L}\right)^2\right]$, the approximate arc length of the catenary.

Two finite element models of the cable with horizontal chord were constructed using 8 and 18 truss elements with all three translational degrees of freedom available at nodes between the supports. The elements were slightly shorter at the ends than in the center for the 18-element model. Figure D.3 portrays two of the mode shapes for the 18-element model; they match the shapes presented by Irvine. Note that, for a taut cable, longitudinal displacements are an order of magnitude smaller than transverse displacements. Table D.1 shows the correlation between Irvine's theory and the computed frequencies.

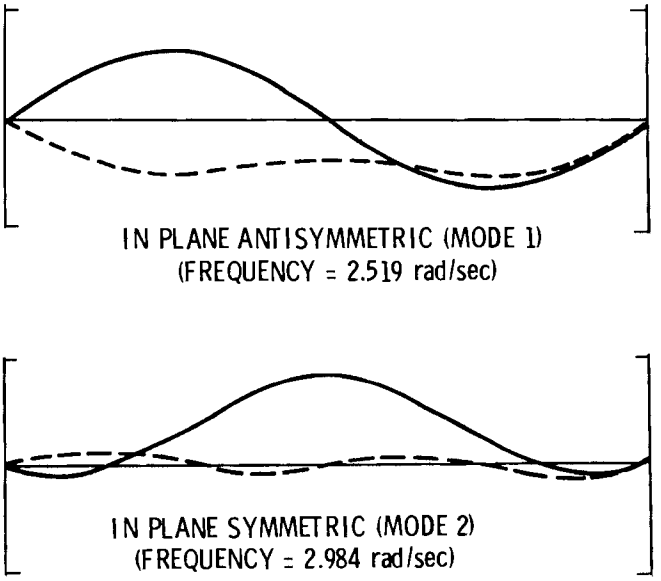

FIGURE D.3. Typical Catenary Mode Shape

TABLE D.1. Theoretical and Computed Frequencies, Single-Cable 304-m Span

Mode	Theoretical Frequency (rad/sec)	8-Element Finite Element Model Frequency (rad/sec)	18-Element Finite Element Model Frequency (rad/sec)
Transverse 1	1.273	1.284	1.273
Antisymmetric In-Plane 1	2.546	2.610	2.519
Transverse 2	2.546	2.617	2.525
Symmetric In-Plane 1	3.001	3.772	2.984
Transverse 3	3.819	4.049	3.730

The transverse modes may be likened to a swinging motion. As Irvine shows, to first order, the transverse modes cause no stretching of the cable and thus are completely uncoupled from the in-plane modes. The sequencing and frequencies of the symmetric and antisymmetric modes are functions of the elasticity-geometry parameter for the conductor. For $\lambda^2 = 66$, Irvine's theory predicts that the lowest frequency in-plane mode shape has antisymmetric transverse displacements and symmetric longitudinal displacements.

To ascertain the effects of varying the cable parameter, a larger sag cable ($\lambda^2 = 3925$) model and a smaller sag cable ($\lambda^2 = 2.43$) were studied using eight elements. The parameters of the cable are the same except that the horizontal tension has been reduced to 6210N to provide a sag of 9.8% of the chord length for the larger sag cable and increased to 74500N to provide a sag of 0.81% of the chord length for the smaller sag cable. The predicted frequencies for these two models are shown in Table D.2. Mode shapes are similar to those of the original cable ($\lambda^2 = 66$) except that the longitudinal displacements are now of a similar order of magnitude as the transverse

TABLE D.2. Computed Frequencies, Single-Cable 304-m Span

Large Sag (λ^2 = 3925)			Small Sag (λ^2 = 2.43)		
Mode	Computed Frequency (rad/sec)	Theoretical Frequency (rad/sec)	Mode	Computed Frequency (rad/sec)	Theoretical Frequency (rad/sec)
Transverse 1	0.639	0.638	Transverse 1	2.225	2.210
Antisymmetric In-Plane 1	1.247	1.276	Symmetric In-Plane 1	2.971	2.950
Transverse 2	1.295	1.276	Antisymmetric In-Plane 1	4.534	4.420
Symmetric In-Plane 1	1.899	1.826	Transverse 2	4.535	4.420
Transverse 3	2.002	1.914	Transverse 3	7.081	6.630

displacements for the larger sag cable. For the smaller sag cable, there is a change in the ordering of the mode shape versus frequency. This effect was predicted by Irvine (1974).

Displacement Pulse Propagation

Another cable behavior of interest is the traveling wave (pulse). Theoretically, a traveling wave of arbitrary shape travels along a cable without changing its shape, provided internal frictional losses are sufficiently small and local changes in tension are neglected. For a cable with constant tension (H) and mass per unit length (m), the transverse wave velocity is given as

$$C = \sqrt{H/m}$$

Modeling traveling waves using discrete truss elements requires that the pulse shape be approximated by a series of straight lines, which may affect pulse shape. To test how well ADINA could predict the traveling wave phenomenon, a finite element model was constructed using 30 axial elements with constant initial tension. A triangular pulse wave was generated by forcing a time-dependent transverse displacement at one end. As shown in Figure D.4, the general shape of the pulse is maintained as the wave translates along the

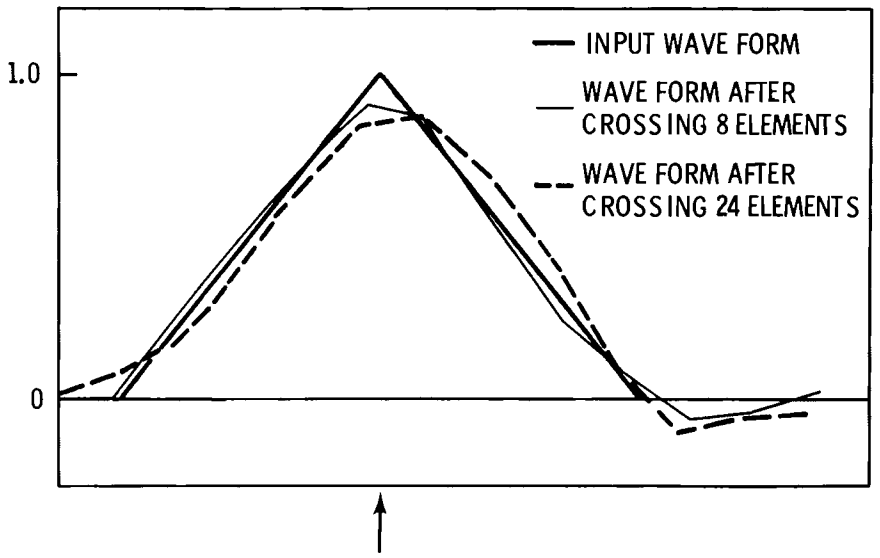

FIGURE D.4. Pulse Shape History

cable. The maximum value of pulse is reduced by 13% after crossing 24 elements. The model pulse velocity agreed with the theoretical velocity within 2%.

Falling Cable

A single-cable model was used to analyze the motion of a cable that had snapped at one of its support ends and was falling freely. The sudden release of tension at one end of the cable travels to the other end at the speed of sound for the conductor material. During this release period, the cable experiences recoil (motion toward the remaining support) in addition to a response to the effect of gravity.

Ideally, one would like to model the truss elements as having low capacity to resist compression. It was decided to use a non-zero compression modulus for the truss elements to maintain a positive definite stiffness matrix. Therefore, a compression modulus of two orders less than the tension modulus was used. This worked satisfactorily with the selected element sizes and a time step of 0.0025 seconds. The analysis results just prior to contact with the ground are illustrated in Figure D.5. The initial geometry was a 20-m support height and a 7.47-m sag. Breakage was assumed to occur at the right-hand support.

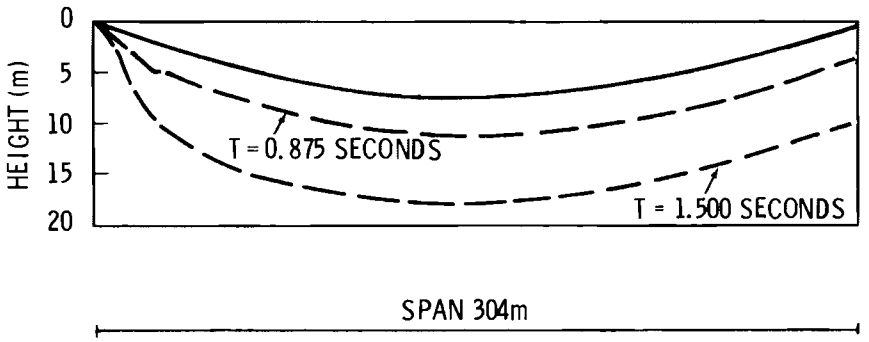

FIGURE D.5. Falling Cable History

The motions computed by the ADINA finite element model indicate a longitudinal springback of approximately 3-m for the 304-m span in 1.5 seconds. An irregularity appears on the cable shape near the remaining support. This could be due to the prevailing compression and is a function of the element size in that region. The computed falling distance of the free end of the conductor at 1.5 seconds is within 5% of that expected from free fall under gravity.

To give some feel for the transient effects, a plot of the cable load at the support point is given in Figure D.6. This clearly shows the time taken for the initial compression stress wave to reach the attached end of the conductor. The implied velocity correlates very well with the sonic velocity of the cable material.

The small compression loading that persists after the initial tension is released is a consequence of the assumed non-zero compression modulus. At about 0.7 seconds after breakage, a sharp increase in tension at the attached cable end is noted. This is due to the undamped stress waves propagating in the cable. The time between tensile loads corresponds to the time required to traverse the cable length at the lower sonic velocity associated with the assumed compression modulus. Following this period is a sequence of further tensile pulses, which are due to interaction between the stress waves and the tension induced by the falling motion.

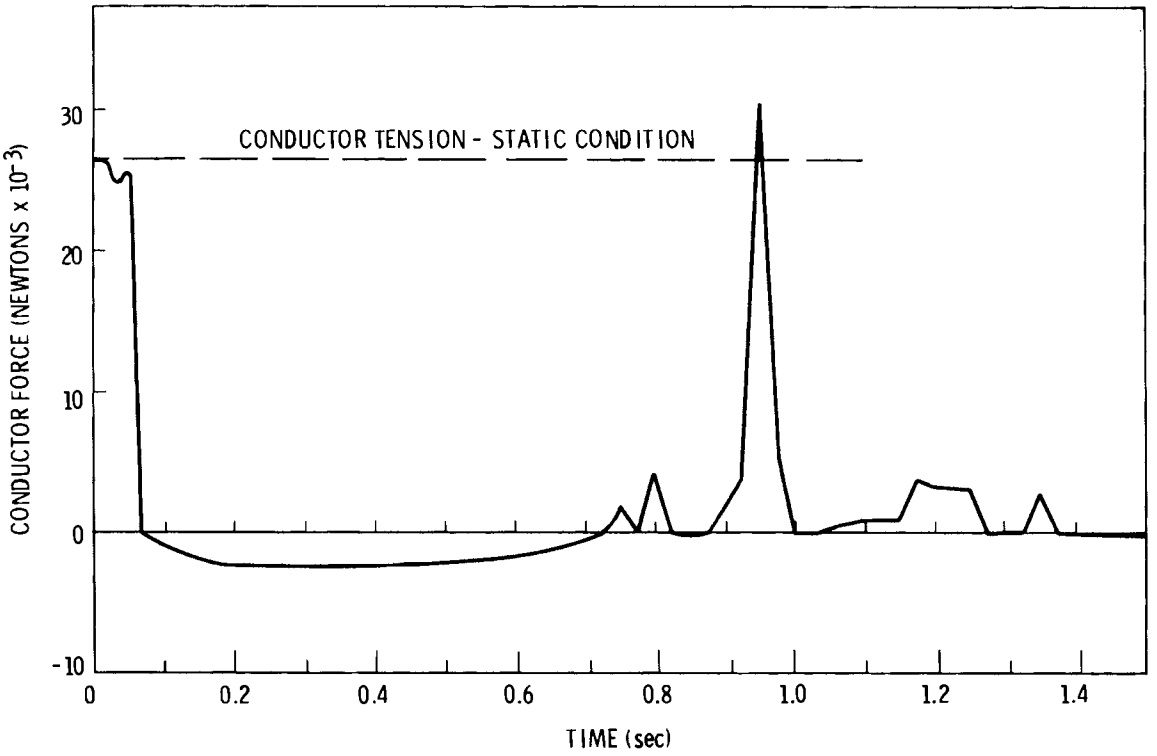

FIGURE D.6. Falling Cable Fixed End Load History

Dragline Rope Response Simulation

Little is known about the actual tensile loads imposed on wire rope during the operating cycle of a dragline. Most load data to date have been developed from records of current flow variations in the electric drum motors. Because of the elasticity of the rope and inertia of the system, transient loads of high amplitude can go undetected using this technique. These dynamic loads are considered to be quite high and are, therefore, a significant factor in rope wear.

By using finite element techniques to predict dragline rope response, the possibility to improve wire rope usage and dragline design exists. To show the feasibility of predicting dragline rope behavior, a model of a drag rope and bucket-connecting hardware was developed. The system was modeled by 35 truss elements. The drag rope was 150 ft long with a sag-to-span ratio of 7%. The drag rope was moving uniformly to the left at 10 ft/sec to

simulate bucket uptake. The right end of the rope was suddenly stopped to simulate bucket stoppage. The tension in the rope 0.01 sec after bucket stoppage is shown in Figure D.7. The maximum tension in the rope is over 700% higher than before the bucket stoppage. The tension near the bucket end is starting to fall off as the rope rebounds. The ripple effect in the high tension region is probably due to stress waves reflecting at individual nodal points and would not be expected in an actual wire rope.

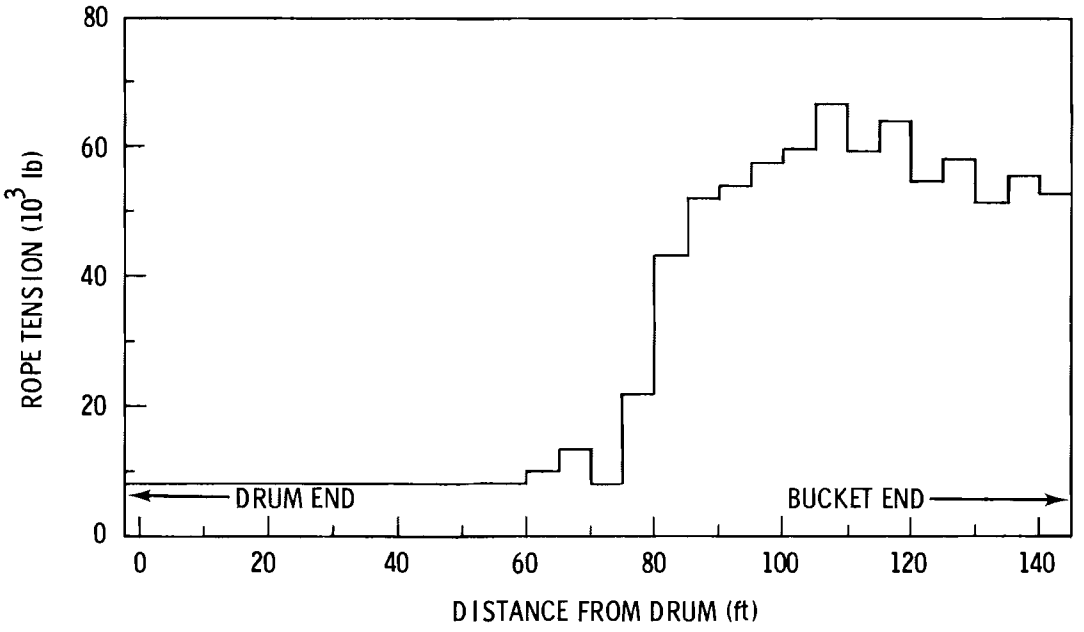

FIGURE D.7. Tension Distribution in Suddenly Stopped Drag Rope

CONCLUSIONS

Two conclusions based on this computer analysis are offered. First, the ability of ADINA truss elements with large displacement capabilities to model static and dynamic behavior of wire ropes has been clearly shown. The nonlinear static stiffness of catenary cables was modeled precisely. Significant dynamic phenomena such as mode shapes and frequencies, pulse propagation, and freely falling cables were also well represented by ADINA models.

Second, care must be taken to ensure that sufficiently small load increments (i.e., time steps) are used to obtain convergence. The nonlinear truss element behavior is quite sensitive to load increment size.

REFERENCES

Bathe, K. J. 1976. ADINA, A Finite Element Program for Automatic Dynamic Incremental Nonlinear Analysis. Report 82448-1.

Campbell, D. G. 1970. "Unbalanced Tensions in Transmission Lines." ASCE Journal of the Structural Division. 96 (ST10): 2189-2207.

Felippa, C. A. 1974. "Finite Element Analysis of Three-dimensional Cable Structures." In Proceedings of the International Conference on Computational Methods in Nonlinear Mechanics. University of Texas, Austin, Texas.

Irvine, H. M., and T. K. Caughey. 1974. "The Linear Theory of Free Vibrations of a Suspended Cable." In Proceedings of the Royal Society of London, London, ENGLAND.

Shears, M. 1968. Static and Dynamic Analysis of Guyed Masts. SESM Report No. 68-6, Department of Civil Engineering, University of California, Berkeley, California.

Smith, F. C., and G. S. Vincent. 1950. Aerodynamic Stability of Suspension Bridges; Part II - Mathematical Analyses. Engineering Experiment Station Bulletin No. 116, University of Washington, Seattle, Washington.

DISTRIBUTION

No. of Copies

OFFSITE

A. A. Churm
DOE Patent Division
9800 S. Cass Avenue
Argonne, IL 60439

H. Reese
DOE Division of Fossil Fuel Extraction
Mail Sta. D-107
Washington, DC 20545

166 DOE Technical Information Center

S. C. Gambrell, Jr.
P.O. Box 6129
University, AL 35486

L. T. Hansson
Bucyrus-Erie Co.
1100 Milwaukee Ave. So.
Milwaukee, WI 53172

ONSITE

DOE Richland Operations Office

H. E. Ransom

No. of Copies

95 Pacific Northwest Laboratory

J. M. Alzheimer
W. E. Anderson
G. H. Beeman
A. J. Currie
G. B. Dudder
W. I. Enderlin
W. S. Kelly
J. A. Merrill
M. H. Morgenstern (2)
L. T. Pedersen
D. E. Rasmussen
L. R. Shotwell
L. A. Strope
E. V. Werry (74)
Technical Information (5)
Publishing Coordination (2)(PG)